JOURNAL OF
GEOPHYSICAL RESEARCH

The continuation of

ERRESTRIAL MAGNETISM AND ATMOSPHERIC ELECTRICITY
(1896-1948)

An International Quarterly

OLUME 57 September, 1952 NUMBER 3

CONTENTS

(Contents concluded on outside back cover)

PUBLISHED BY
THE WILLIAM BYRD PRESS, INC.
P. O. Box 2-W—Sherwood Ave. and Durham St., Richmond 5, Virginia
FOR THE JOHNS HOPKINS PRESS, BALTIMORE 18, MARYLAND

EDITORIAL OFFICE:
5241 Broad Branch Road, Northwest, Washington 15, D.C., U.S.A.

THREE DOLLARS AND FIFTY CENTS A YEAR SINGLE NUMBERS, ONE DOLLAR

JOURNAL OF GEOPHYSICAL RESEARCH

The continuation of

Terrestrial Magnetism and Atmospheric Electricity

(1896-1948)

An International Quarterly

Founded 1896 by L. A. BAUER *Continued 1928–1948 by* J. A. FLEMING

Fields of Interest

Terrestrial Magnetism
Atmospheric Electricity
The Ionosphere
Solar and Terrestrial Relationships
Aurora, Night Sky, and Zodiacal Light
The Ozone Layer
Meteorology of Highest Atmospheric Levels
The Constitution and Physical States of the Upper Atmosphere
Special Investigations of the Earth's Crust and Interior, including experimental seismic waves, physics of the deep ocean and ocean bottom, physics in geology
And similar topics

This Journal serves the interests of investigators concerned with terrestrial magnetism and electricity, the upper atmosphere, the earth's crust and interior by presenting papers of new analysis and interpretation or new experimental or observational approach, and contributions to international collaboration. It is not in a position to print, primarily for archive purposes, extensive tables of data from observatories or surveys, the significance of which has not been analyzed.

Forward *manuscripts* to the editorial office of the Journal at 5241 Broad Branch Road, Northwest, Washington 15, D. C., U.S.A., or to one of the Associate Editors. It is preferred that manuscripts be submitted in English, but communications in French, German, Italian, or Spanish are also acceptable. A brief abstract, preferably in English, must accompany each manuscript. A *publication charge* of $4 per page will be billed by the Editor to the institution which sponsors the work of any author; private individuals are not assessed page charges. Manuscripts from outside the United States are invited, and should not be withheld or delayed because of currency restrictions or other special difficulties relating to page charges. Costs of publication are roughly twice the total income from page charges and subscriptions, and are met by subsidies from the Carnegie Institution of Washington and international and private sources.

Back issues and *reprints* are handled by the Editorial Office, 5241 Broad Branch Road, N.W., Washington 15, D.C., U.S.A.

Subscriptions are handled by The Johns Hopkins Press, Baltimore 18, Maryland, U.S.A.

THE JOHNS HOPKINS PRESS

Baltimore 18, Maryland

Entered as second-class matter at the Post Office at Richmond, Virginia, under the act of March 3, 1879.

Journal of

GEOPHYSICAL RESEARCH

The continuation of

Terrestrial Magnetism and Atmospheric Electricity

VOLUME 57 SEPTEMBER, 1952 No. 3

WAVE SOLUTIONS, INCLUDING COUPLING, OF IONOSPHERICALLY REFLECTED LONG RADIO WAVES FOR A PARTICULAR *E*-REGION MODEL*

BY J. J. GIBBONS AND R. J. NERTNEY

Ionosphere Research Laboratory, The Pennsylvania State College, State College, Pennsylvania

(Received January 25, 1952)

ABSTRACT

This paper is concerned with the solution of the coupled wave equations which arise in the application of the wave theory to the problem of ionospheric wave propagation. It concerns an extension of previous work [see 1 of "References" at end of paper], which will henceforth be referred to as [1]. The method of "variation of parameters" is used to obtain approximate solutions to the coupled equation from the uncoupled solutions obtained in [1].

A diurnal and seasonal model representing the *E*-region of the ionosphere above State College, Pennsylvania, is considered. This model, as in [1], consists of a Chapman-like *E*-region whose maximum in electron density is at a constant height. Approximate 150 kc/sec wave solutions including coupling are obtained for this model. These wave solutions, of course, exhibit the well-known reflection condition corresponding to an electron density of around 3,000 electrons/cm^3.

It is shown that the effect of the coupling is to cause a wave traversing a coupling region to excite a new wave propagated in the direction of propagation of the incident wave and also a back-

*The research reported in this paper has been sponsored by the Geophysics Research Division of Air Force Cambridge Research Center under Contract AF19(122)-44.

scattered wave propagated in the reverse direction. As indicated below, these coupling effects become important in our model below the "reflection" level. The back-scattered wave due to the initial upgoing wave will thus appear as a reflected wave originating in the coupling region. The forward-scattered wave due to the downgoing wave from the upper "reflection" level also must be considered, particularly in calculating the polarization of ionospherically reflected waves.

It is shown that, in the case of 150 kc/sec waves, the coupling effects occur in the neighborhood of $N = 300$ electrons/cm^3, which corresponds to the "classical reflection" level for the "ordinary" wave. The coupling effects become greater as the collisional frequency, ν, associated with the coupling N value decreased toward the critical collisional frequency, ν_c [2], for the night-time models due to the increase in heights of the "bottom" of the layer at these times. This results in stronger split echoes and greater departure from circularity in the polarization ellipses.

The results of computations utilizing the theory, in comparison with experimental results, indicate that the stratification observed in the height records may be explained as outlined above. The absorption and polarization experimental results, however, cannot be accounted for by the E-region model utilized alone. The consideration of an electronic D-region, however, readily accounts for all three experimental factors, as will be discussed in detail in a later paper.

Introduction

In a previous paper [1], approximate solutions were obtained for the uncoupled wave equations which arise in the course of the application of the wave theory to the problem of 150 kc/sec radio waves vertically incident on the ionosphere over the northeastern United States. These solutions were obtained for an E-region model consisting of an electron distribution of Chapman-like shape which differed from a true Chapman in that the height of the maximum ionization was fixed at 115 km absolute height. Collisions were introduced through an exponentially-decreasing collisional frequency with a "fix point" determined by Huxley [3]. A scale height of 10 km was assumed. The earth's magnetic field is that for State College, Pennsylvania, evaluated at 100 km. This model is shown in Figure 1 of [1].

For comparison with experimental results, the model is completed on a seasonal-diurnal basis through the E-layer critical frequency, f_c , *vs* time curves as shown in Figure 1. This involves an implicit assumption that the specification of the critical frequency determines the model uniquely regardless of the seasonal or diurnal time when this critical frequency occurs. This affords an experimental link between the experimental results and our theory which has no means for predicting the particular model to be chosen for a particular time. These values of f_c for $f_c > 1$ Mc/sec were obtained from CRPL-F bulletins [4] and are valid

for Washington, D. C. The night-time portion of the curves for $f_c < 1$ Mc/sec was obtained from a limited amount of data available at our own Laboratory.

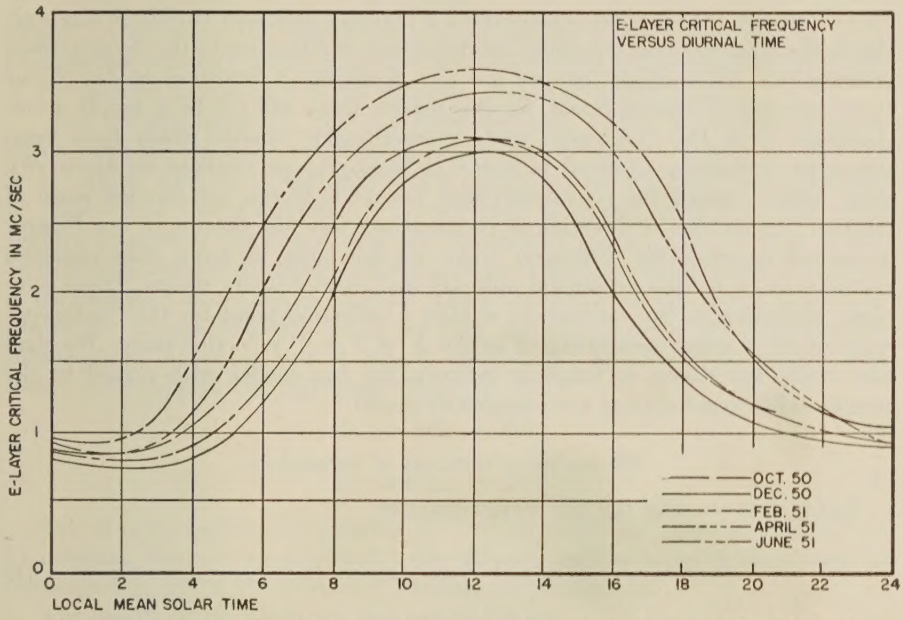

FIG. 1—THE ASSUMED VARIATION FOR THE E-LAYER CRITICAL FREQUENCY

In [1] it was found that, neglecting coupling, these models showed a single reflection level for one of the magneto-ionic components in the neighborhood of the electron density corresponding to the $X = 1 + Y$ level (using the notation of Ratcliffe [5]). The $X = 1$ reflection level disappeared due to the effects of the relatively high collisional frequency in the neighborhood of this level. The height of reflection was in quite good agreement with certain of the experimental data. It was obtained that, for all models, the absorption experienced by the reflected component was on the order of one neper. Unless some "limiting polarization" phenomenon is assumed, the polarization of the return wave predicted by this theory is circular.

On the basis of experimental results, three facts become immediately evident. In the first place, a single 150 kc/sec echo is not always returned from the E-layer and, in fact, night-time splitting of the "first-hop" echo is the rule rather than the exception; secondly, the experimental absorption is not constant diurnally or seasonally, on the order of one neper; and, finally, the observed polarizations are not, in general, circular. It becomes necessary, then, to reinvestigate our theory and/or our model.

In this paper attention is confined to attempting to improve our theory by including the effects of coupling. In order to give names to the two characteristic modes of propagation in the ionosphere, we shall accept the convention of naming

one mode the "ordinary" and the other the "extraordinary." We shall differ from certain other conventions, however, in that a mode will be defined as a wave solution having continuous indices of refraction and characteristic polarizations. This continuity is to be maintained even if it becomes necessary to change algebraic sign in the magneto-ionic equations for the indices of refraction or the characteristic polarizations. This means that we are now speaking of *structural* modes of our entire ionospheric structure and, for this reason, there will not be a unique correspondence with the "ordinary" and "extraordinary" modes which have been somewhat arbitrarily assigned in terms of homogeneous medium solutions. We shall, further, adopt the convention that the mode having left-handed sense of rotation (viewed in the direction of propagation) near the bottom of our E-layer model will be called the "ordinary" wave. On this basis, we have, then, obtained solutions in [1] for the uncoupled ordinary and extraordinary waves. These solutions, according to our convention, exhibit a reflection point for the "ordinary" wave at an N value corresponding to the $X = 1 + Y$ reflection point. We shall now study the effects of coupling between the two modes with regard to the results to be expected from our ionospheric model.

The method of variation of parameters

Let us first consider the differential equation

$$\frac{d^2y}{dx^2} + \epsilon(x)\frac{dy}{dx} + g(x)y = S(x) \quad \ldots\ldots\ldots\ldots\ldots\ldots (1)$$

Let us further suppose that we have two independent solutions of the equation for $S(x) = 0$. In this case, the general solution of the equation for $S(x) = 0$ is $y = Ay_1 + By_2$, where A and B are determined appropriately to the boundary conditions of the problem.

It may be shown that the general solution to the differential equation (1) for arbitrary $S(x)$ may be expressed in the form

$$y(x) = y_1(x)\int \frac{Sy_2}{y_1'y_2 - y_2'y_1}\,dx - y_2(x)\int \frac{Sy_1}{y_1'y_2 - y_2'y_1}\,dx \quad \ldots\ldots\ldots (2)$$

where the arbitrary constants are now included in the limits of integration and again are selected to fit the boundary conditions of the problem.

The application of variation of parameters to the ionospheric problem

In order to eliminate a triple or quadruple subscript system, let us write the coupled wave equations [6] symbolically as

$$O'' + (K_0^2\epsilon_0^2 + M^2)O = -XM' - 2X'M \quad \ldots\ldots\ldots\ldots\ldots (3)$$

$$X'' + (K_0^2\epsilon_x^2 + M^2)X = -OM' - 2O'M \quad \ldots\ldots\ldots\ldots\ldots (4)$$

Here O and X indicate the "x" component of the ordinary and "y" component of the extraordinary waves, respectively, and M indicates the coupling factor

$$\frac{\frac{du_{1,2}}{dh}}{(1 - u_{1,2}^2)} \equiv M$$

where $u_{1,2}$ represent the characteristic polarizations of the two waves. K_0 is the propagation constant of free space and the ϵ's are the complex dielectric constants of the medium for the two waves which are functions of the height, h.

Now assume, from [1], that we have solutions to the uncoupled equations which form the left-hand members of equations (3) and (4), neglecting the term in M^2 which appears on this side of the equations. As discussed later, this may be done, since the p solutions, [1], associated with the index $K_0^2\epsilon^2$ differ only slightly from those associated with the "equivalent index" $(K_0^2\epsilon^2 + M^2)$. It may be shown that this slight difference will produce negligible change in the magnitude of the scattered waves due to coupling. There will, however, be certain "reflection" effects due to this deviation which we shall also discuss later. We shall use zero subscripts to indicate a pair of linearly independent solutions. Our general solutions to the unperturbed equations, then, are

$$O_0 = AC_{02} + BO_{01} \quad \ldots\ldots\ldots\ldots\ldots\ldots\ldots\ldots\ldots\ldots (5)$$

$$X_0 = CX_{01} + DX_{02} \quad \ldots\ldots\ldots\ldots\ldots\ldots\ldots\ldots\ldots\ldots (6)$$

Let us next consider these waves as "driving forces" in equations (3) and (4) by inserting them in the right-hand side of these equations and determining new coefficients by use of the method of variation of parameters.

The equations for which we desire solutions are

$$O'' + K_0^2\epsilon_0^2 O = -M'[CX_{01} + DX_{02}] - 2M[CX_{01} + DX_{02}]' \quad \ldots\ldots (7)$$

$$X'' + K_0^2\epsilon_x^2 X = -M'[BO_{01} + AO_{02}] - 2M[AO_{02} + BO_{01}]' \quad \ldots\ldots (8)$$

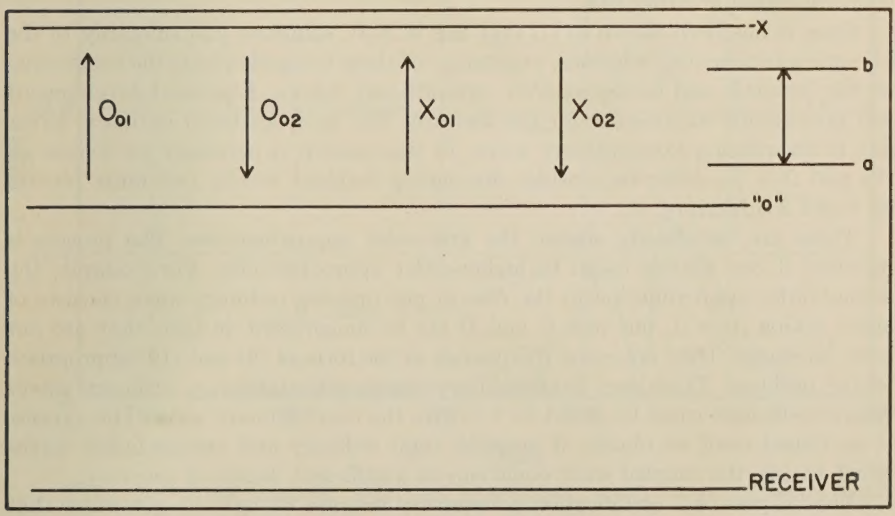

FIG. 2—THE SUBSCRIPT SYSTEM

Let us consider an isolated coupling region such that ϵ_o and $\epsilon_x \simeq 1 + jO$ and $(\epsilon'/\epsilon)^2$, $(\epsilon''/\epsilon) \ll 1$ everywhere; that is, a region in which our solutions reduce to W.K.B. solutions. In such a region, the linearly independent W.K.B. solutions have the ray optical significance of "upgoing" and "downgoing" waves at the upper and lower surfaces of the coupling region. The direction of propagation, indicated by the subscript number, is illustrated in Figure 2 for the unperturbed waves.

For simplicity let $B = C = D = O$ and $A = 1$. Then, if we assume solutions of the W.K.B. form, we find the expressions for the first-order scattered waves X_1 (upgoing) and X_2 (downgoing)

$$X_2 = \frac{X_{02}}{2j} \int_{-b}^{-a} M\left(\sqrt{\frac{\epsilon_x}{\epsilon_o}} + \sqrt{\frac{\epsilon_o}{\epsilon_x}}\right) \exp\left\{-jK_0 \int_a^b (\epsilon_x - \epsilon_o)\, dx\right\} \quad \ldots\ldots\ldots (9)$$

and

$$X_1 = \frac{X_{01}}{2j} \int_{-b}^{-a} M\left(\sqrt{\frac{\epsilon_x}{\epsilon_o}} + \sqrt{\frac{\epsilon_o}{\epsilon_x}}\right) \exp\left\{jK_0 \int_a^b (\epsilon_x - \epsilon_o)\, dx\right\} \quad \ldots\ldots\ldots (10)$$

with similar expressions for the O waves.

The above indicate that, to first order, our downgoing ordinary wave excites a forward- and a back-scattered extraordinary wave and we have evaluated the coefficients of these waves through the limits of integration. In this problem, this is done in such a manner that the upgoing extraordinary wave is zero at the lower face of the coupling region, since there is no extraordinary wave approaching the region from below with $B = C = D = 0$. Similarly, the limits of integration are adjusted so that there is no downgoing extraordinary wave approaching the region from above. The effect of this adjustment is to determine the algebraic sign to be affixed to the integral, since the limits of integration are the boundaries of the coupling region in either case.

Since it has been shown in [1] that the W.K.B. solutions join smoothly to the free-space exponential solutions, evaluation of these integrals yields the coefficients on the forward- and back-scattered extraordinary waves. A parallel development will give similar expressions for the forward- and back-scattered ordinary waves due to an upgoing extraordinary wave. In this case, it is necessary to reverse all O's and X's. In order to consider downgoing incident waves, one must reverse all 1 and 2 subscripts.

These are, as already stated, the first-order approximations. The process is repeated if one desires to go to higher-order approximations. For example, the second-order approximation in the case of our upgoing ordinary wave consists of again taking $A = 1$, but now C and D are no longer zero, in fact, they are not even constants. They are equal to integrals of the form of (9) and (10) appropriate to the problem. These new extraordinary waves will excite new ordinary waves whose coefficients must be added to A to give the total ordinary wave. This process is continued until we obtain, if possible, total ordinary and extraordinary waves which satisfy the coupled wave equations to a sufficient degree of accuracy.

The "if possible" qualification is necessary because we have no guarantee that this process is convergent. Divergence of the process, however, does not necessarily

mean that our method is completely useless and, in fact, if we can find *a step* in the successive approximations where the total ordinary and extraordinary waves are sufficiently good approximations, we may stop the process and be in as good a position as if the process were convergent. This will be discussed again later when we apply the method to our ionospheric problem.

A question might be raised regarding our treating the upgoing and downgoing waves separately, but there is no problem here, since in each case we obtain wave solutions satisfying the wave equation and the boundary conditions. If we simply add all these waves together, we obtain a new wave solution satisfying the wave equation and the boundary conditions. If this solution is not unique, the problem is meaningless. There *is* difficulty, however, in considering these waves as upgoing and downgoing *pulses*. This phase of the problem is not considered in this paper.

Application—Now let us proceed to the ionospheric problem. As in the case of the uncoupled equations considered in [1], we are again forced to obtain our results in terms of c.w. solutions because of our inability to handle the variation of the coupling with frequency at this time. This poses a new difficulty since the c.w. solutions, in the case of multiple coupling or reflection levels, result in complex standing wave patterns which are very difficult to interpret in terms of our experimental pulsed results.

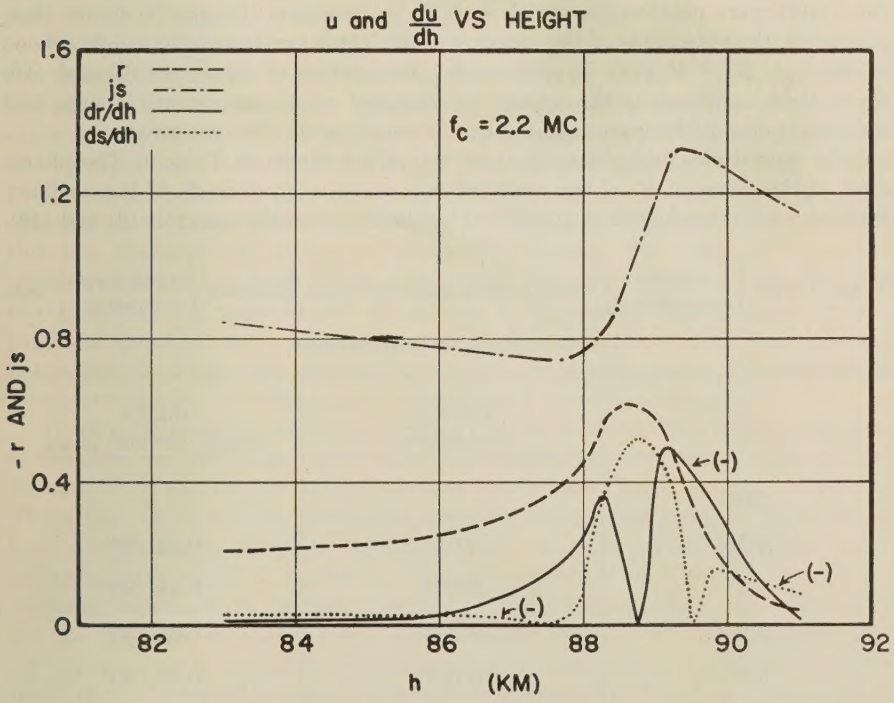

FIG. 3—THE WAVE POLARIZATION AND ITS DERIVATIVE AS A FUNCTION OF HEIGHT (ORDINARY COMPONENT)

We solve this problem by considering the effects of isolated coupling regions on infinite monochromatic wave trains. In this manner, we may isolate our "upgoing" and "downgoing" waves and later reassemble the entire picture with the various waves labeled as "upgoing" and "downgoing" from each reflection level. This is not difficult in our case since, as we shall see, we have regions of ϵ_o , $\epsilon_x \simeq 1 + jO$ and $(\epsilon'/\epsilon)^2$, $(\epsilon''/\epsilon) \ll 1$ immediately above and below the region where the coupling is important. As stated before, this means that the W.K.B. solutions have the significance of upgoing and downgoing waves. We shall refer to the back-scattered wave due to an upgoing wave as u.g.b.s. and the forward-scattered wave due to a downgoing wave as d.g.f.s. We shall, then, consider the forward- and back-scattered waves due to coupling regions of the type which occur in our ionospheric model.

The first problem which arises is the evaluation of the coupling term M. If we plot the "u" values as functions of height [7] for our model, we obtain curves of the type shown in Figure 3. The result of numerically differentiating the "u" curve is also shown in this Figure. Once having this result, we may evaluate the integrands of equations (9) and (10) for the first-order u.g.b.s. and d.g.f.s. waves. These quantities are related to the coefficients on the d.g.f.s. and u.g.b.s. waves through integrals (9) and (10), respectively.

In the case of both the u.g.b.s. and d.g.f.s. waves, we find that the effects of the coupling are greatest for our $f_c = 0.55$ Mc/sec layer. It may be shown that, in general, the magnitude of the coupling coefficient is greatest in the neighborhood of the $1 - X = 0$ point in each model. Integration of equations (9) and (10) shows that the phase of the infinity of scattered wave components is such that the amplitudes of the waves excited by the coupling also become greater.

The amplitudes and phases of these waves are shown in Table 1. The phases refer to the phase of E_y of the extraordinary wave referred to E_x of the ordinary wave at a reference level $x = a$ selected by the limits on the integrals (9) and (10).

TABLE 1—*The* $\left\{\begin{matrix}\text{ordinary}\\\text{extraordinary}\end{matrix}\right\}$ *scattered waves excited by a unit amplitude* $\left\{\begin{matrix}\text{extraordinary}\\\text{ordinary}\end{matrix}\right\}$ *wave while traversing the coupling region*

f_c	u.g.b.s. amplitude	d.g.f.s. amplitude and phase
Mc		*a*
0.55	0.01	0.52 /98°
1.1	0.001	0.48 /88°
2.2	0.001	0.39 /96°
3.0	0.001	0.37 /90°
4.4	0.001	0.30 /90°

For this work, the reference level has been selected as 83 km; see Figure 1 of [1]. It should be noted that, while a steeper N gradient will result in an increased coupling by increasing the derivative du/dx, this is not the case here. It is actually the decreasing value of ν associated with $1 - X = 0$ point which causes the increase in the effect of the coupling and, in fact, Figure 1 of [1] shows that the N gradient actually becomes less as we consider the models corresponding to lower critical frequency (and stronger coupling).

It should further be noted that the ordinary and extraordinary waves, below the coupling level, will be propagated with phase velocities determined by the real part of the refractive indices μ_o and μ_x, resulting in an additional phase shift of $K_0 \int_a^c (\mu_o - \mu_x)\, dx$, where $x = a = 83$ km is the reference level at the bottom of E-layer and c represents the level of our receiver. There will also be a change in relative amplitude of these waves $K_0 \int_a^c (\chi_o - \chi_x)\, dx$, involving the difference between the imaginary part of the refractive indices, in addition to the absolute absorption. This means that the effect of any "D-region" which might be postulated below "E-region" will be threefold. The absolute absorption will be changed, as is well known. The angle of tilt of the polarization ellipse will be changed due to the difference in phase path for the two modes, and, finally, the angle of ellipticity θ will be changed through differential absorption. (These terms are defined later in connection with Figure 4.) This means that we now have a three-parameter hold on any "D-region" which we may desire to construct.

We see from the above, then, that we must make some assumption regarding the constitution of the region between the reference level "a" and the ground. We must calculate the *relative* phase delay and absorption on the ordinary and extraordinary waves, and we must also make a decision as to whether our magneto-ionic components retain their significance in regions of very low electron density.

Let us first assume that our magneto-ionic components do retain their significance as they travel from our E-layer to a region of sufficiently high collisions that the characteristic waves are essentially circular. The existence of such a region will depend on both N and ν, of course, but for N small, say less than 100 electrons/cm^3, a ν value of 10^7 will suffice. In our model, this corresponds to a height of about 65 km. Let us also assume that the electron densities are so small below this level that the relative phases and amplitudes of the X and O waves are not modified appreciably in traveling from E-layer to the ground.

If we make these assumptions, we find that, in order to obtain the polarization of the main or "reflection" echo which we would observe at the ground, all that we need do is add two circularly-polarized waves with opposite senses of rotation. These two waves are the downgoing ordinary wave which resulted from the selective reflection at the true "reflection level" and the forward-scattered extraordinary wave which is excited by this ordinary wave as it passes through the coupling region. Since we have assumed a coefficient of unity with zero phase for the ordinary wave, we have (remembering that the O wave represents an "x" component O_x, and X wave represents a "y" component X_y) that ψ, the angle of tilt of the ellipse with respect to the x-axis, is one-half of the phase angle between the O and X waves; that is, one-half of the phase angle of the X wave referred to zero phase. The angle θ which describes the ellipticity of the ellipse is exactly

$\theta = \tan^{-1}[(1 - a)/(1 + a)]$, where a is the *magnitude* of the coefficient of the extraordinary wave. These relations are shown diagrammatically in Figure 4. We may note that the direction of rotation will be that of the larger of the two circularly-polarized waves, that is, $a < 1$ corresponds to left-handed sense of rotation, so the wave will *appear* to be ordinary. (The polarization to be expected on the coupling level echo will be discussed later.)

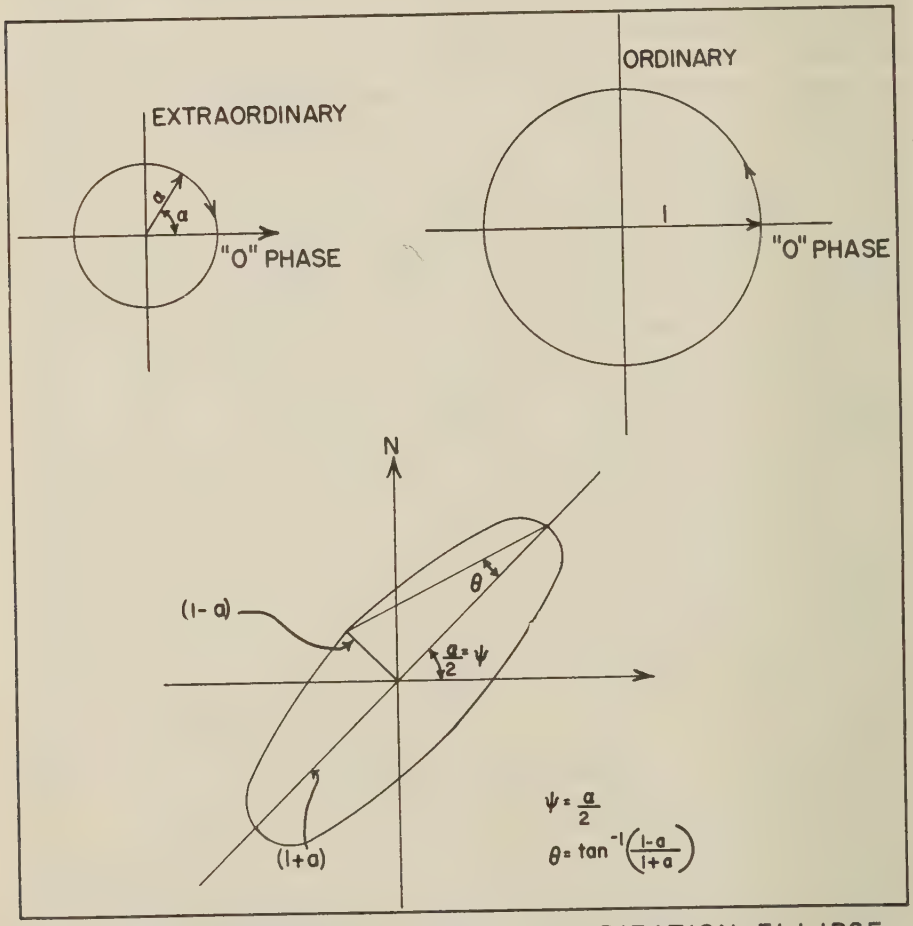

FIG. 4—THE SYNTHESIS OF THE POLARIZATION ELLIPSE FROM ORDINARY AND EXTRAORDINARY COMPONENTS IN A REGION OF LOW ELECTRON DENSITY AND HIGH COLLISIONAL FREQUENCY

It must be emphasized that we may not obtain the total wave polarization, in general, by adding two circularly-polarized waves. When we are within the ionized medium, we must add waves of the two characteristic polarizations in the proper amplitude and phase. An analogue computer for this purpose has been

constructed [8] and the polarization of the *entire* downgoing wave *within* our ionosphere model has been calculated. We find that, if the total wave polarization of the downgoing wave is tracked through the coupling region, the polarization of the total wave shows a strong tendency to "limit" and the total wave polarization changes very little. The situation is that the wave has been resolved within the ionosphere into two elliptically-polarized components, each of which is varying rapidly in the coupling region, but the *coefficients* on each of these waves vary in such a manner as to hold the polarization of the entire wave relatively constant. This verifies a fact of which we were already aware, namely, that our choice of the "characteristic" homogeneous medium modes was unfortunate *in* the coupling region and these modes are not necessarily "characteristic" of an inhomogeneous region in which the characteristic wave polarizations are rapidly varying.

Numerical results

The numerical values of the coefficients of the u.g.b.s. and the d.g.f.s. waves are shown in Table 1. These are relative values referred to an upgoing ordinary wave of unit amplitude. It may be noted that the amplitude of the back-scattered wave is very small for the models having large f_c , but increases by a factor of 10 as we go from the $f_c = 1.1$ Mc/sec model to the $f_c = 0.55$ Mc/sec model. This is consistent with the results of Rydbeck [9], which predict that this back-scattered wave will be negligible for $\nu > \nu_c$.

There is, however, one further effect which must be considered. It was stated

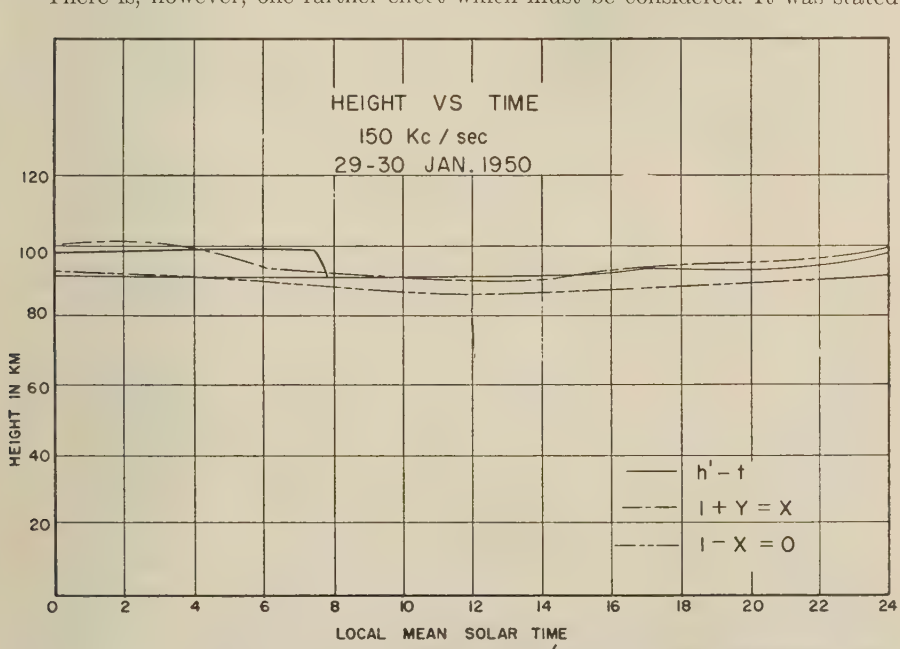

FIG. 5—A TYPICAL RECORD OF 150 KC/SEC VIRTUAL HEIGHT VS TIME COMPARED WITH THE HEIGHT OF THE "CRITICAL LEVELS" OF OUR E-LAYER MODEL

earlier that the modification of the wave solution by the M^2 term which appears with $K_0^2\epsilon^2$ was slight as far as the coupled wave results are concerned. We do find, however, that this slight deviation in the form of the solution is important when we consider the "reflection" condition at the $X = 1$ level and, in fact, we find that there is a back-scattered wave of the "reflection" type on both the ordinary and extraordinary modes. By "reflection-type" echo, we refer to the fact that the reflection condition [see 1] appears in the uncoupled equations (including the M^2 term), and an ordinary wave is reflected as an ordinary and an extraordinary wave is reflected as extraordinary. The magnitude of this wave is such that this coupling level echo will be of appreciable magnitude, on the order of 0.8 of the main reflection amplitude, for the $f_c = 0.55$ Mc/sec model.

This is an extremely critical point and the appearance of this echo should give a rather sensitive method of determining the collisional frequency associated with the $1 - X = 0$ level and at the same time yield the height of this level. It may

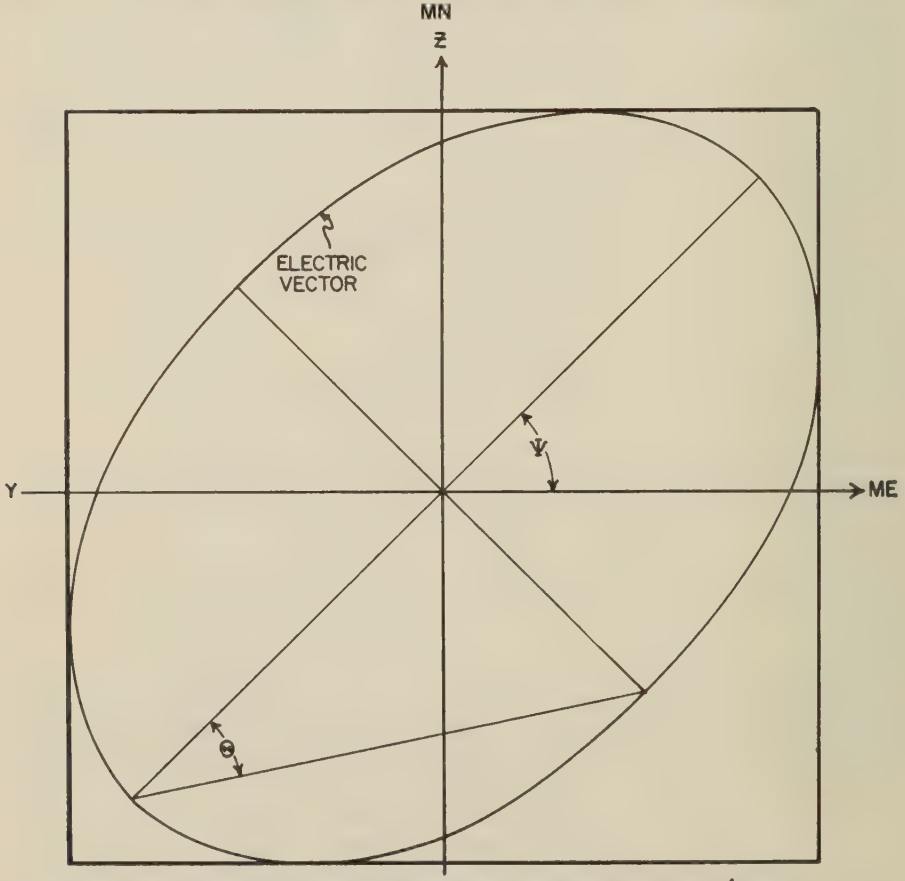

FIG. 6—THE POLARIZATION COORDINATES (WAVE ELECTRIC VECTOR)

be noted that an amplitude of, say, 0.01 on this back-scattered wave referred to unity-amplitude upgoing ordinary wave will correspond to a ratio of approximately 0.05 in echo amplitudes for the upper and lower (reflection and coupling level) echoes because of the fact that (1) the upper echo experiences greater absorption and (2) the coupling level echo is excited by both the ordinary and extraordinary components of the transmitted pulse, whereas *only* the *ordinary* wave excites the upper echo.

Let us now consider the effects of introducing coupling on the theoretical results derived in [1] and again compare our results briefly with experiment. As before, attention is confined to E-region.

Height of reflection—Our phase heights of reflection are not modified by the coupling (to first order). The coupling and inclusion of the M^2 term in the "equivalent index" does have the effect, however, of introducing an apparent second height of reflection at the coupling level, particularly during the night hours when f_c is small, which is in good qualitative agreement with experiment. This is illustrated in Figure 5, where the "critical" levels for the model of Figure 1 of [1] are determined via Figure 1 of this paper and the experimental *group* heights are plotted throughout the day of interest.

The absorption—The coupling produces no change in the true dissipative absorption and, in the absence of strong splitting, the only effect of the coupling on the experimental absorptions is to introduce certain second-order effects depending on the polarization of the reflected wave. As shown in Table 1 of [1], the theoretical E-layer absorption is relatively constant, having a value of about one neper for all the models.

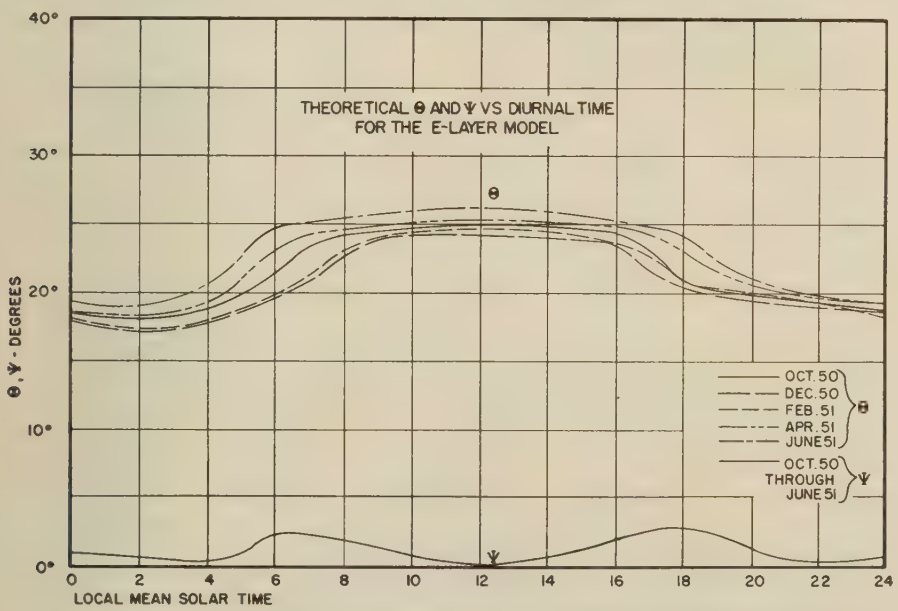

FIG. 7—THEORETICAL Θ AND Ψ VS DIURNAL TIME FOR THE E-LAYER MODEL

The polarization—The polarization of the main or reflection level echo is given in terms of the parameters ψ and θ, as shown in Figure 6. If we desire to compare the theoretical values with the experimental data, we must again assume values

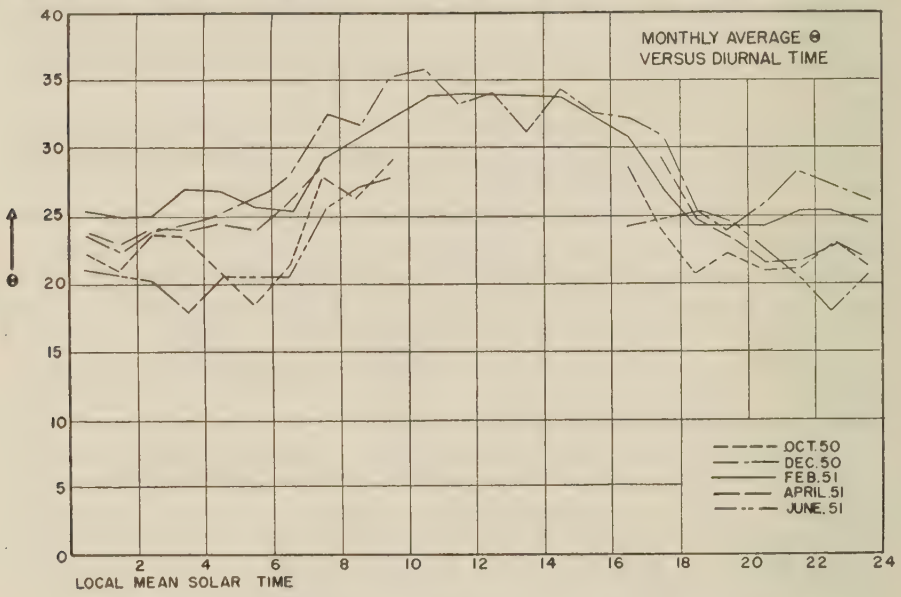

FIG. 8—MONTHLY AVERAGE Θ VS DIURNAL TIME

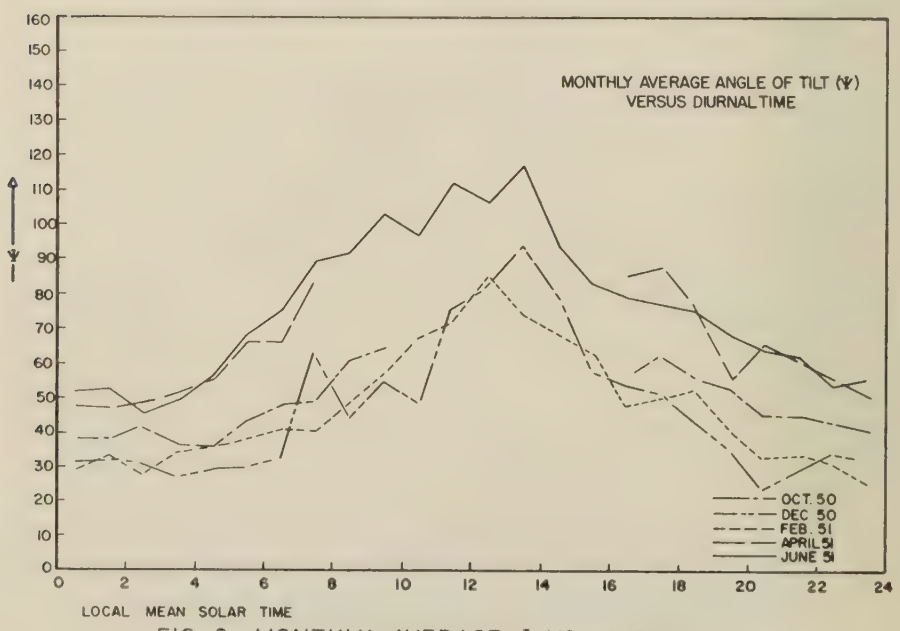

FIG. 9—MONTHLY AVERAGE Ψ VS DIURNAL TIME

for E-layer critical frequencies. Let us consider the f_c mean monthly diurnal variations shown in Figure 1. These yield the theoretical curves shown in Figure 7. We see now, referring to Figures 8 and 9 of experimental data, that our theoretical θ values are slightly too small and the theoretical ψ values, which are very nearly constant around zero degrees, are much too small. We do have now, however, a mechanism which will explain the departure from circularity in the polarization ellipses for the upper echo.

We may now also consider the polarization to be expected on the "coupling" reflection. We see from the symmetry of the coupling mechanism and the transmission problem that the magnitudes of the back-scattered ordinary and extraordinary waves should be nearly equal. This means that, in general, the ellipticity of the back-scattered ellipse should be very nearly that of the upgoing wave. The relative phases, however, are not necessarily the same, which means that, in general, the angle of tilt may be changed. The question of polarization is discussed in greater detail in another paper [10].

Conclusions

It has been shown that the method of "variation of parameters" may be used to obtain approximate solutions to the coupled wave equations for our E-layer model. Consideration of the coupling terms introduces the possibility of obtaining "reflection" from a level lower than, and in addition to, the "reflection" level determined from the equations when coupling is neglected.

Of great importance, in this connection, is the fact that the apparent stratification of the echo, under this condition, occurs for monotonically varying $N - \nu$ distributions as a function of height. Hence, the physically undesirable stratification of the ionosphere in a relatively small range of height is not required to explain the observed phenomenon.

Within the limitations of the c.w. solutions obtained, it is indicated that the model may probably be satisfactory as regards group heights and the return of at least two echoes for a single incident pulse. This is shown not to be the case as regards absoprtion and polarization. As implied in the body of the report, it appears that the latter two factors may be suitably accounted for by consideration of an electronic D-region below E. This has been studied in some detail and is considered elsewhere.

It should, perhaps, be reiterated that only c.w. solutions have been obtained in this paper, in that the dispersive characteristics of the medium have not been considered. The pulse solutions are now being studied for a limited number of models. The results of this work will be reported shortly and currently appear to support the conclusions reached in this paper.

References

[1] J. J. Gibbons and R. J. Nertney, A method for obtaining the solutions of ionospherically reflected long waves, J. Geophys. Res., **56**, 355–371 (1951).

[2] S. K. Mitra, The upper atmosphere, Calcutta, Royal Asiatic Society of Bengal (1949).

[3] L. G. H. Huxley, Ionospheric cross-modulation at oblique incidence, Proc. R. Soc., **200**, 486–511 (1950).

[4] Ionospheric data, CRPL-F, Reports Central Radio Propagation Laboratory, Nation. Bur. Stan., Washington, D. C.
[5] J. A. Ratcliffe, Magneto-ionic theory, Wireless Eng., **10**, 354–363 (1933).
[6] O. E. H. Rydbeck, On the propagation of radio waves, Gothenburg, Trans. Chalmers Univ. Tech., No. 34 (1944).
[7] J. M. Kelso, Magneto-ionic calculations for 150 kilocycles/sec, Tech. Rep. No. 24, Pennsylvania State College, Ionosphere Research Laboratory, Tech. Rep. No. 24 (1951).
[8] G. H. Friedman, An elliptical polarization synthesizer, submitted for publication in Rev. Sci. Instr.
[9] O. E. H. Rydbeck, Magneto-ionic triple splitting of ionospheric waves, J. App. Phys., **21**, 1205–1214 (1950); also Trans. Chalmers Univ. Tech., No. 101 (1951).
[10] J. M. Kelso, H. J. Nearhoof, R. J. Nertney, and A. H. Waynick, The polarization of vertically incident long radio waves, Ann. Geophys., **7**, 215–244 (1951).

SECULAR VARIATION OF THE MAGNETIC FIELD AT COLABA AND ALIBAG

By S. K. Pramanik

Meteorological Office, Poona 5, India

(Received March 5, 1952)

ABSTRACT

We have data of magnetic observations at Colaba, Bombay, from 1846 to 1905, and at Alibag, 18 miles to the south, from 1904 onward, with two years of comparative observations during 1904 and 1905. Moos had studied in 1910 the secular variations of the magnetic field with data up to 1905. In view of the changes in the magnetic field and the very large amount of data collected since, a further study was undertaken.

The value of H has been increasing continuously since 1916, and it is likely that the increase will continue at least for some more years. The westward drift of declination commenced from 1879 and is still continuing. The rate of drift, however, has decreased during the last five years, and within the next few years it may begin to return eastward or move westward at an increased rate. The vertical force had been continuously increasing from 1853 and it reached its maximum value in 1937, after which there was a fall for some years, but the falling tendency appears to have been arrested and the vertical force may again begin to increase. During the first six solar cycles, the average values of H, ΔH, and $\Delta' H$ are greater during sunspot minimum years than during sunspot maximum years, but this does not hold during the last three cycles. No periodicity of about 11 years was apparent in the curves representing the differences between the observed and calculated values of H, D, and V or in the curves representing ΔH, $\Delta' H$, ΔD, $\Delta' D$, ΔV, and $\Delta' V$, and no parallelism was noticeable between these curves and the sunspot curve.

(1) Magnetic observations were started in 1840 at Colaba, Bombay (lat. 18° 53′ 45″ north, long. 72° 48′ 56″ east), but they were not regular and not properly recorded. Observations were taken regularly and properly recorded from 1846. Till 1871, eye-reading instruments were used, and in 1872 photographic magnetographs were installed. In 1900, it was decided by the city of Bombay that electric traction would be introduced, and in order to avoid vitiation of the magnetic observations, a site at Alibag (lat. 18° 38′ 18″ north, long. 72° 52′ 24″

east), about 18 miles to the south of Colaba, was selected, and comparative observations at Colaba and Alibag were made during 1904 and 1905. The observations were stopped at Colaba in March 1906, but have been continued at Alibag since 1904. From the comparative observations of two years, differences in the values of the magnetic elements at the two places were determined, and we thus have a continuous record of the values of the magnetic elements for about a century.

(2) The secular variation of the magnetic field at Colaba was studied by Moos [see 1 of "References" at end of paper] in 1910, taking into account data of H (the mean annual horizontal force) from 1872 to 1905, of D (the mean annual declination) from 1871 to 1905, and of V (the mean annual vertical force) from 1888 to 1905, though for the sake of comparison he also used some data of previous years which he considered were not so reliable. Changes in the secular trends of the magnetic elements have occurred since, and meanwhile a very considerable amount of data has also been collected. A further study of the subject was therefore undertaken. In this note, the Colaba data have been reduced to Alibag by applying the corrections determined from the two years of comparative observations. The corrections applied to Colaba data are as follows:

H	-510γ
D (easterly)	$+53'.5$
V	$+600\gamma$

Vestine, *et al.* [2, 3], have given the main magnetic field over the world and its secular changes, together with an estimate of the geomagnetic variation with sunspot cycle for the period 1905-1945. In this note, the details of the secular changes of the magnetic elements at Colaba and Alibag for about a century are examined.

(3) It should be mentioned that the data for 1947 and 1949 are those of absolute instruments, while those for other years are from magnetographs, and hence the values of annual changes indicated in the magnetic elements from 1946 to 1949 are not strictly comparable with those of previous years.

Horizontal force

(4) The values of the mean annual horizontal force are given in column 2 of Table 1. Data for years previous to 1890 are given in Table 8. Moos after an examination concluded in 1910 that the data from 1872 to 1905 based on magnetograph and the Kew unifilar were practically free from errors, and he fitted the curve $H = a + bt + ct^2$, where $a = 37237.1\,\gamma$, $b = 16.75\,\gamma$, and $c = -0.35\,\gamma$, t being reckoned from 1871.5 to these data. He stated that the curve should be depended upon for parallelism just for the period considered, but it was interesting to note that this theoretical curve was parallel to the absolute values derived from Grubb's magnetometer for the whole period of 1846 to 1905. The parallelism of the theoretical curve, however, was not maintained in later years, and the difference between observed and calculated values increased with time, as will be seen from Table 2. (The value of a in the formula has been decreased by $510\,\gamma$ to make it applicable to Alibag.)

TABLE 1—*Annual mean values of horizontal force*
(Unit = 1γ = 0.00001 CGS)

Year	Observed	Calculated	Diff., col. 3 minus col. 2	ΔH	$\Delta' H$
(1)	(2)	(3)	(4)	(5)	(6)
	γ	γ	γ	γ	γ
1890	36924	37360	436	5	1
1891	36914	37323	409	−10	−8
1892	36895	37268	373	−19	−5
1893	36909	37225	316	14	−5
1894	36898	37185	287	−11	7
1895	36917	37147	230	19	8
1896	36934	37110	176	17	14
1897	36939	37076	137	5	3
1898	36927	37044	117	−12	−1
1899	36931	37016	85	4	−2
1900	36932	36989	57	1	1
1901	36929	36965	36	−3	−4
1902	36918	36942	24	−11	−10
1903	36902	36923	21	−16	−16
1904	36881	36905	24	−21	−15
1905	36872	36890	18	−9	−9
1906	36874	36877	3	2	−6
1907	36862	36866	4	−12	−5
1908	36857	36858	1	−5	−10
1909	36844	36852	8	−13	−6
1910	36845	36848	3	1	0
1911	36856	36847	−9	11	10
1912	36874	36848	−26	18	12
1913	36880	36851	−29	6	8
1914	36881	36856	−25	1	−1
1915	36870	36864	−6	−11	−4
1916	36867	36874	7	−3	−2
1917	36875	36886	11	8	5
1918	36886	36901	15	11	11
1919	36900	36918	18	14	16
1920	36922	36937	15	22	16
1921	36935	36959	24	13	15
1922	36946	36983	37	11	21
1923	36985	37009	24	39	31
1924	37029	37037	8	44	40
1925	37065	37068	3	36	31
1926	37079	37101	22	14	30
1927	37119	37136	17	40	29
1928	37152	37174	22	33	43
1929	37209	37214	5	57	45

Table 1—*Annual mean values of horizontal force*—Concluded
(Unit = 1γ = 0.00001 CGS)

Year	Observed	Calculated	Diff., col. 3 minus col. 2	ΔH	$\Delta' H$
(1)	(2)	(3)	(4)	(5)	(6)
	γ	γ	γ	γ	γ
1930	37253	37256	3	44	57
1931	37323	37300	−23	70	52
1932	37364	37347	−17	41	52
1933	37408	37396	−12	44	46
1934	37462	37448	−14	54	53
1935	37524	37501	−23	62	62
1936	37593	37557	−36	69	63
1937	37652	37616	−36	59	60
1938	37705	37676	−29	53	62
1939	37779	37739	−40	74	58
1940	37826	37805	−21	47	54
1941	37867	37872	5	41	55
1942	37944	37942	−2	77	58
1943	37999	38014	15	55	61
1944	38051	38088	37	52	54
1945	38107	38165	58	56	51
1946	38152	38244	92	45	75
1947*	38275	38325	50	123	70
1948	38317	38409	92	42	84
1949*	38405	38495	90	88	....

*Absolute observations.

Table 2—*Horizontal force*

Year	Observed	Calculated from Moos curve	Diff.
	γ	γ	γ
1906	36874	36887	13
1910	36845	36848	3
1915	36870	36788	−82
1920	36922	36716	−206

(5) As Moos' curve did not fit the observed data after 1915, another curve of the same type, $H = A + Bt + Ct^2$, was fitted to the data from 1911 to 1945, in which $A = 37173.75\ \gamma$, $B = 38.77\ \gamma$, and $C = 1.15\ \gamma$, counting t from 1928. The calculated values from this curve and the differences between these and the observed values are given in columns 3 and 4 of Table 1. Although the curve has been calculated to fit observed values between 1911 and 1945, it will be seen that

it fits well the observations from 1896 to 1949. From an examination of the trend of secular variation of H and the curve (Fig. 1), it appears likely that the curve will continue to fit the mean annual values at least for some more years.

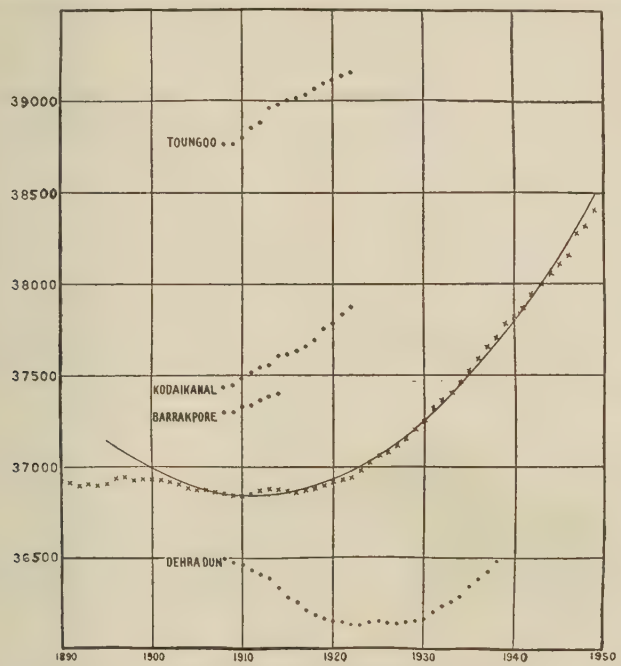

FIG. 1. ANNUAL MEAN HORIZONTAL FORCE (H)

(6) Moos found that there was a good parallelism between the mean annual sunspot-figure curve and the curve representing the variations of observed values from the curve fitted to these values, and further that the force values were on the average lower during maximum sunspot years than during minimum sunspot years. This latter effect has been noticed also by some other writers [4, 5], and this has been attributed to the greater incidence in the number of magnetic storms near sunspot maximum. The annual sunspot values and the differences of the observed values from the calculated values given in column 4 of Table 1, have been plotted (curves *a* and *b*) in Figure 4. It will be seen that no parallelism is apparent between the two curves. It is also found that there is no periodicity of about 11 years in curve *b*. Regarding mean annual H, it is found that during the first and second three sunspot cycles the average values (36673 γ and 36909 γ) for the sunspot minimum years are greater than those (36647 γ and 36885 γ) for the sunspot maximum years, but during the last three cycles the value (37481 γ) for the sunspot minimum years (1923, 1933, and 1944) is less than that (37693 γ) for the sunspot maximum years (1928, 1937, and 1947). However, it should be mentioned that during the last three cycles H has been continuously increasing at a rapid rate and the value for any year is greater than those of previous years irrespective of its position in the solar cycle, and the sunspot effect might have

been masked by the large secular change. To consider the question further, the gradient ΔH and the smoothed gradient (mean for three years) $\Delta' H$ were calculated and are given in columns 5 and 6 of Table 1. The average value of ΔH (15 γ) during the first six cycles for the sunspot minimum years is a little greater than that (13 γ) for the sunspot maximum years, but during the last three cycles the value of ΔH (45 γ) for the sunspot minimum years is, as in the case of H, less than that (72 γ) for the sunspot maximum years. The average value of $\Delta' H$ also is greater for the sunspot minimum years than that for the sunspot maximum years during the first six sunspot cycles, but is less during the last three cycles. The values of ΔH and $\Delta' H$ have also been plotted in curves *c* and *d* in Figure 4. There is apparently no periodicity of about 11 years in the two curves, nor is there any apparent parallelism between these and the sunspot curve (*a*, Fig. 4).

(7) Magnetic observations were taken for some years at Dehra Dun, Kodaikanal, Toungoo, and Barrakpore. In Figure 1, the available observed values of the mean annual horizontal force at these places have been plotted. It will be seen that the general trends of secular variation of the horizontal force at these places, except between 1910 and 1927 at Dehra Dun, are similar. The values of H for Dehra Dun were between 33300 γ and 32900 γ, and in the curve for this place in Figure 1 please read 33300 γ in place of 36500 γ.

(8) Taking data from 1948 into account, it is seen that the value of H has been generally increasing, the increase to 1949 being about 2360 γ or about 7 per cent of its value in 1848. The minimum value in this century occurred in 1909-1910, and it has been continuously increasing since 1916, the increase in the last 33 years being about 1540 γ, with an average rate per year of about 47 γ.

Declination

(9) The values of D are available from the records of the magnetograph which was installed in 1871. Values from eye observations are available from 1846, but the values before 1862 are less reliable. The mean annual values of declination from 1884 are given in column 2 of Table 3, values for earlier years being given

Table 3—*Annual mean values of declination*
(Unit = 1 minute, east positive)

Year	Observed	Calculated	Diff., col. 3 minus col. 2	ΔD	$\Delta' D$
(1)	(2)	(3)	(4)	(5)	(6)
	′	′	′	′	′
1884	109.0	123.6	14.6	1.6	0.6
1885	108.5	120.8	12.3	0.5	1.2
1886	107.0	118.0	11.0	1.5	1.0
1887	105.9	115.2	9.3	1.1	1.2
1888	104.8	112.4	7.6	1.1	1.4
1889	102.9	109.6	6.7	1.9	1.7
1890	100.9	106.8	5.9	2.0	1.8
1891	99.3	104.0	4.7	1.6	1.8

TABLE 3—*Annual mean values of declination*—Continued
(Unit = 1 minute, east positive)

Year	Observed	Calculated	Diff., col. 3 minus col. 2	ΔD	$\Delta' D$
(1)	(2)	(3)	(4)	(5)	(6)
	′	′	′	′	′
1892	97.4	101.2	3.8	1.9	1.9
1893	95.2	98.4	3.2	2.3	2.1
1894	93.0	95.6	2.6	2.1	2.3
1895	90.6	92.8	2.2	2.4	2.2
1896	88.4	90.0	1.6	2.2	2.3
1897	86.2	87.2	1.0	2.2	2.5
1898	83.2	84.4	1.2	3.0	2.3
1899	80.0	81.6	1.6	3.1	2.7
1900	78.0	78.8	0.8	2.1	2.6
1901	75.4	76.0	0.6	2.6	2.4
1902	72.9	73.2	0.3	2.5	2.3
1903	71.1	70.4	−0.7	1.8	2.1
1904	69.0	67.6	−1.4	2.1	1.8
1905	67.5	64.8	−2.7	1.5	1.9
1906	65.5	62.0	−3.5	2.0	1.7
1907	63.8	59.1	−4.7	1.7	1.8
1908	62.2	56.3	−5.9	1.6	1.7
1909	60.3	53.5	−6.8	1.9	2.0
1910	57.7	50.7	−7.0	2.6	2.5
1911	54.7	47.9	−6.8	3.0	3.0
1912	51.2	45.1	−6.1	3.5	3.4
1913	47.6	42.3	−5.3	3.6	3.5
1914	44.2	39.5	−4.7	3.4	3.5
1915	40.7	36.7	−4.0	3.5	3.6
1916	36.8	33.9	−2.9	3.9	3.9
1917	32.5	31.1	−1.4	4.3	4.2
1918	28.2	28.3	0.1	4.3	4.1
1919	24.5	25.5	1.0	3.7	4.1
1920	20.3	22.7	2.4	4.2	4.1
1921	15.9	19.9	4.0	4.4	4.0
1922	12.6	17.1	4.5	3.3	3.8
1923	8.9	14.3	5.4	3.7	3.4
1924	5.6	11.4	5.8	3.3	3.2
1925	3.4	8.6	5.2	2.2	2.7
1926	−0.8	5.8	6.6	2.6	2.5
1927	−1.9	3.0	4.9	2.7	2.4
1928	−3.8	0.2	4.0	1.9	2.2
1929	−5.9	−2.6	3.3	2.1	2.0

Table 3—*Annual mean values of declination*—Concluded
(Unit = 1 minute, east positive)

Year	Observed	Calculated	Diff., col. 3 minus col. 2	ΔD	$\Delta' D$
(1)	(2)	(3)	(4)	(5)	(6)
	′	′	′	′	′
1930	−8.0	−5.4	2.6	2.1	2.2
1931	−10.5	−8.2	2.3	2.5	2.3
1932	−12.7	−11.0	1.7	2.2	2.2
1933	−14.5	−13.8	0.7	1.8	1.9
1934	−16.2	−16.6	−0.4	1.7	1.7
1935	−17.7	−19.4	−1.7	1.5	1.8
1936	−19.9	−22.2	−2.3	2.2	1.9
1937	−21.8	−25.0	−3.2	1.9	2.2
1938	−24.4	−27.8	−3.4	2.6	2.5
1939	−27.5	−30.7	−3.2	3.1	2.8
1940	−30.3	−33.5	−3.2	2.8	2.8
1941	−32.8	−36.3	−3.5	2.5	2.8
1942	−36.0	−39.1	−3.1	3.2	2.6
1943	−38.0	−41.9	−3.9	2.0	2.3
1944	−39.8	−44.7	−4.9	1.8	1.6
1945	−40.7	−47.5	−6.8	0.9	1.1
1946	−41.2	−50.3	−9.1	0.5	0.6
1947*	−41.7	−53.1	−11.4	0.5	0.4
1948	−42.0	−55.9	−13.9	0.3	0.8
1949*	−43.6	−58.7	−15.1	1.6	....

*Absolute observations.

in Table 8. Moos fitted the curve $D = At + B - \sqrt{Ct^2 + Ft + E}$, where $A = 1.060944$, $B = 123.12$, $C = 13.53812$, $F = -255.7413$, and $E = 11807.2912$ (unit = 100 seconds), to the mean annual observed values of declination for the years 1862-1894, and found that the curve ran practically concurrently with the values for the period 1859-1905. He expected the curve to represent the observed values satisfactorily at least for the next five years.

(10) The observed values and those calculated from the curve for some years are given in Table 4. (53′.5 have been added to the values obtained from the formula to make them applicable to Alibag.)

(11) It will be seen that Moos' curve does not fit the observed values from 1934. From Figure 2, in which the observed values have been charted, it will be seen that they lie approximately in a straight line. A straight line $D = mt + C$ was fitted to the annual values, where $C = 106'.844$ and $m = -2'.806$, t being counted from 1890. The values calculated from the straight line and the differences between these and observed values are given in columns 3 and 4 of Table 3. The straight line has also been plotted in Figure 2. It will be seen that the fit is satisfactory from 1887 to 1946.

TABLE 4—*Declination*

Year	Observed	Calculated from Moos curve	Diff.
	′	′	′
1909	60.3	60.8	0.5
1914	44.2	44.9	0.7
1919	24.5	28.1	3.6
1924	5.6	10.5	4.9
1929	−5.9	−7.9	−2.0
1934	−16.2	−26.5	−10.3
1939	−27.5	−45.7	−18.2

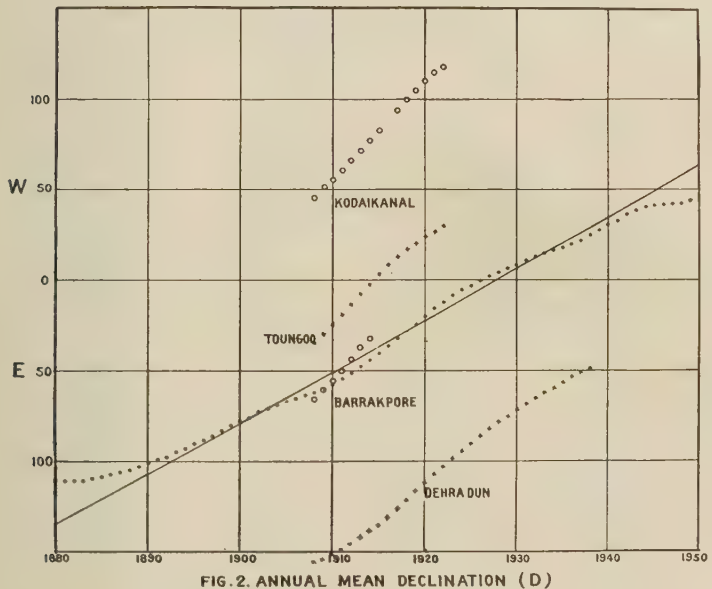

FIG. 2. ANNUAL MEAN DECLINATION (D)

(12) The figures in column 4 of Table 3, giving the differences between observed and calculated values of declination, have been plotted in curve *b* of Figure 5. No periodicity of about 11 years is noticeable in curve *b* and no parallelism is apparent between this curve and the curve of sunspot numbers (curve *a*, Fig. 4). The values of ΔD and $\Delta' D$ mean (average of 3 years) have been plotted in curves *c* and *d* of Figure 5. There is no apparent evidence of a periodicity of about 11 years in the two curves. The mean values of ΔD during the nine sunspot cycles for the sunspot maximum years and the sunspot minimum years are the same, 1′.1.

(13) In Figure 2, the mean annual values of *D* for Dehra Dun, Kodaikanal, Toungoo, and Barrakpore have also been plotted. It will be seen that the general trends of secular variation at these places are similar.

(14) The declination increased from 1° 02′.9 east in 1846 to 1° 50′.9 east in 1879, but has been decreasing since that year and, changing to west in 1927, its value in 1949 was 43′.6 west. The average rate of change since 1879, though it has been variable, is about 2′.21 per year. The rate of increase in westward declination during the last five years, however, has been much less, about 0′.8 per year, and one may expect that within the next few years it will either begin to decrease or to increase rapidly.

Vertical force

(15) Moos examined the values of vertical force up to 1905, and found that those from 1888 onwards and those for the years 1868 to 1873 were reliable. He found that the curve $a + bt + ct^2$, where $a = 13700\,\gamma$, $b = 60.78\,\gamma$, and $c = 0.894\,\gamma$,

TABLE 5—*Annual mean values of vertical force*
(Unit = 1γ = 0.00001 CGS)

Year	Observed	Calculated	Diff., col. 3 minus col. 2	ΔV	$\Delta' V$
(1)	(2)	(3)	(4)	(5)	(6)
	γ	γ	γ	γ	γ
1888	14351	14035	−316	51	70
1889	14451	14158	−293	100	74
1890	14522	14279	−243	71	79
1891	14587	14399	−188	65	61
1892	14635	14516	−119	48	48
1893	14665	14631	−34	30	46
1894	14726	14745	19	61	65
1895	14829	14857	28	103	87
1896	14927	14967	40	98	83
1897	14975	15075	100	48	75
1898	15054	15181	127	79	75
1899	15151	15285	134	97	93
1900	15253	15287	34	102	100
1901	15353	15488	135	100	94
1902	15434	15587	153	81	85
1903	15507	15683	176	73	75
1904	15577	15778	201	70	83
1905	15683	15871	188	106	85
1906	15762	15963	201	79	89
1907	15844	16052	208	82	80
1908	15922	16139	217	78	82
1909	16008	16225	217	86	86
1910	16101	16309	208	93	109
1911	16250	16390	140	149	120
1912	16367	16470	103	117	124

TABLE 5—*Annual mean values of vertical force*—Concluded
(Unit = 1γ = 0.00001 CGS)

Year	Observed	Calculated	Diff., col. 3 minus col. 2	ΔV	$\Delta' V$
(1)	(2)	(3)	(4)	(5)	(6)
	γ	γ	γ	γ	γ
1913	16474	16549	75	107	111
1914	16583	16625	42	109	107
1915	16688	16699	11	105	105
1916	16790	16772	−18	102	99
1917	16880	16842	−38	90	97
1918	16979	16911	−68	99	93
1919	17068	16978	−90	89	89
1920	17147	17043	−104	79	83
1921	17227	17106	−121	80	75
1922	17293	17168	−125	66	75
1923	17372	17227	−145	79	75
1924	17452	17285	−167	80	78
1925	17527	17340	−187	75	73
1926	17590	17394	−196	63	66
1927	17650	17446	−204	60	57
1928	17698	17496	−202	48	49
1929	17736	17545	−191	38	42
1930	17777	17591	−186	41	36
1931	17806	17636	−170	29	31
1932	17830	17678	−152	24	22
1933	17848	17719	−129	14	19
1934	17867	17758	−109	19	19
1935	17892	17795	−97	25	18
1936	17902	17830	−72	10	13
1937	17906	17863	−43	4	−2
1938	17885	17895	10	−21	−2
1939	17897	17925	28	12	−8
1940	17881	17952	71	−16	−10
1941	17855	17978	123	−26	−19
1942	17840	18002	162	−15	−23
1943	17813	18024	211	−27	−21
1944	17791	18044	253	−22	−22
1945	17774	18063	289	−17	−14
1946	17770	18078	308	−4	−12
1947*	17754	18093	339	−16	−7
1948	17754	18106	352	0	−3
1949*	17761	18116	355	7	....

*Absolute observations.

represented the values of V from 1888 to 1906. Moos' curve represented the values of V fairly well till before 1922, as will be seen from Table 6. (The value of a in the formula has been increased by 600 γ to make it applicable to Alibag.)

Table 6—*Vertical force*

Year	Calculated from Moos curve	Observed value	Diff.
	γ	γ	γ
1907	15873	15844	29
1912	16379	16367	12
1917	16929	16880	49
1922	17523	17293	230
1927	18162	17650	512

(16) A new curve $V = A + Bt + Ct^2$, where $A = 16842.4\ \gamma$, $B = 69.722\ \gamma$, and $C = -9335\ \gamma$, counting t from 1917, was fitted to the annual values from 1888 to 1945. The observed and calculated values are given in columns 2 and 3 of

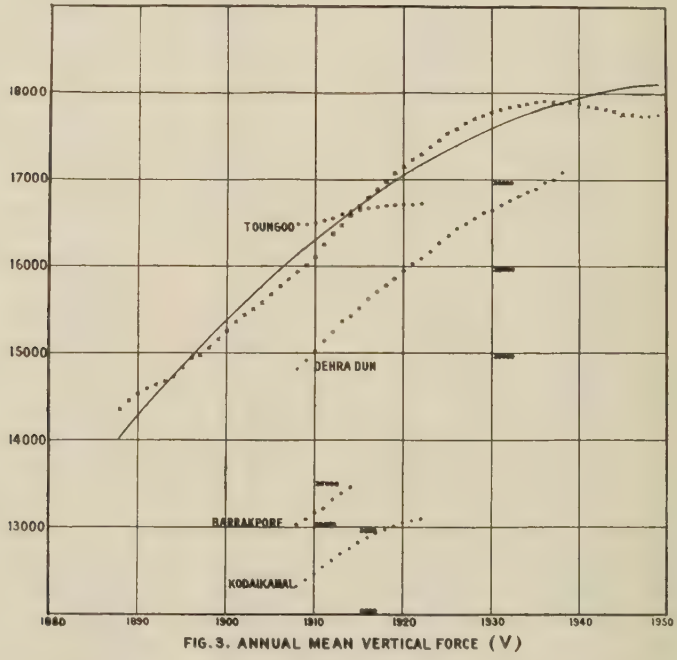

FIG. 3. ANNUAL MEAN VERTICAL FORCE (V)

Table 5 and are charted in Figure 3. The fit, however, is not quite satisfactory, particularly before 1891 and after 1943. Two separate curves, $V = 14136.28 + 89.387\ t$, counting t from 1887, and $V = 17891 + 8.732\ t - 2.350t^2$, counting t from 1935.5, were fitted to the data for the two periods 1888 to 1925 and 1926 to 1945. The values calculated from the two curves and the differences between these and the observed values are given in columns 3 and 4 of Tables 7 (*A*) and (*B*). The fit of these curves to the data is quite satisfactory from 1888 to 1947.

TABLE 7 (*A*)—*Annual mean value of vertical force, 1888–1925*
(Unit = 1γ = 0.00001 CGS)

Year	Observed	Calculated	Diff., col. 3 minus col. 2	Year	Observed	Calculated	Diff., col. 3 minus col. 2
(1)	(2)	(3)	(4)	(1)	(2)	(3)	(4)
	γ	γ	γ		γ	γ	γ
1888	14351	14226	−125	1907	15844	15924	80
1889	14451	14315	−136	1908	15922	16013	91
				1909	16008	16103	95
1890	14522	14404	−118				
1891	14587	14494	−93	1910	16101	16192	91
1892	14635	14584	−51	1911	16250	16282	32
1893	14665	14673	8	1912	16367	16371	4
1894	14726	14762	36	1913	16474	16460	−14
1895	14829	14851	22	1914	16583	16550	−33
1896	14927	14941	14	1915	16688	16639	−49
1897	14975	15030	55	1916	16790	16728	−62
1898	15054	15120	66	1917	16880	16818	−62
1899	15151	15209	58	1918	16979	16907	−72
				1919	17068	16997	−71
1900	15253	15298	45				
1901	15353	15388	35	1920	17147	17086	−61
1902	15434	15477	43	1921	17227	17175	−52
1903	15507	15566	59	1922	17293	17265	−28
1904	15577	15656	79	1923	17372	17354	−18
1905	15683	15745	62	1924	17452	17444	−8
1906	15762	15835	73	1925	17527	17533	6

TABLE 7 (*B*)—*Annual mean value of vertical force, 1926–1949*
(Unit = 1γ = 0.00001 CGS)

Year	Observed	Calculated	Diff., col. 3 minus col. 2	Year	Observed	Calculated	Diff., col. 3 minus col. 2
(1)	(2)	(3)	(4)	(1)	(2)	(3)	(4)
	γ	γ	γ		γ	γ	γ
1926	17590	17596	6	1938	17885	17899	14
1927	17650	17648	−2	1939	17897	17893	−4
1928	17698	17694	−4				
1929	17736	17735	−1	1940	17881	17883	2
				1941	17885	17868	−17
1930	17777	17772	−5	1942	17840	17849	9
1931	17806	17805	−1	1943	17813	17825	12
1932	17830	17832	2	1944	17791	17796	5
1933	17848	17855	7	1945	17774	17762	−12
1934	17867	17873	6	1946	17770	17724	−46
1935	17892	17887	−5	1947	17754	17681	−73
1936	17902	17895	−7	1948	17754	17634	−120
1937	17906	17899	−7	1949	17761	17581	−180

(17) The differences (curve *b*) given in column 4, Table 5, between the observed and calculated values of V have been plotted in Figure 6. No parallelism

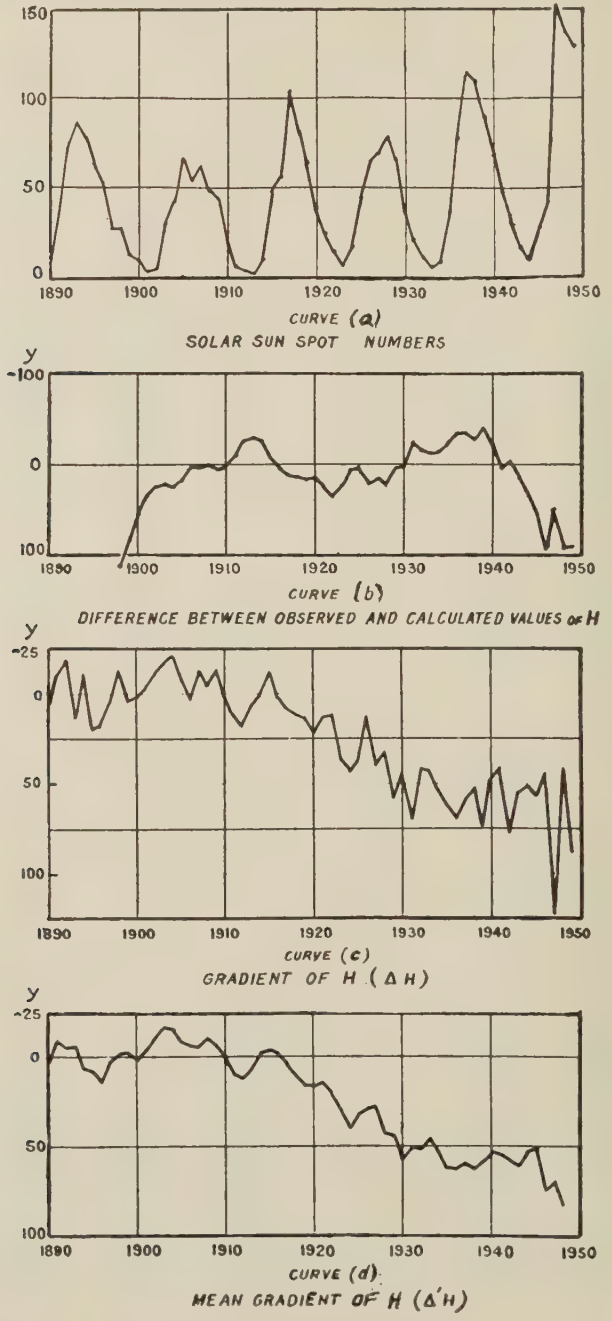

FIG. 4

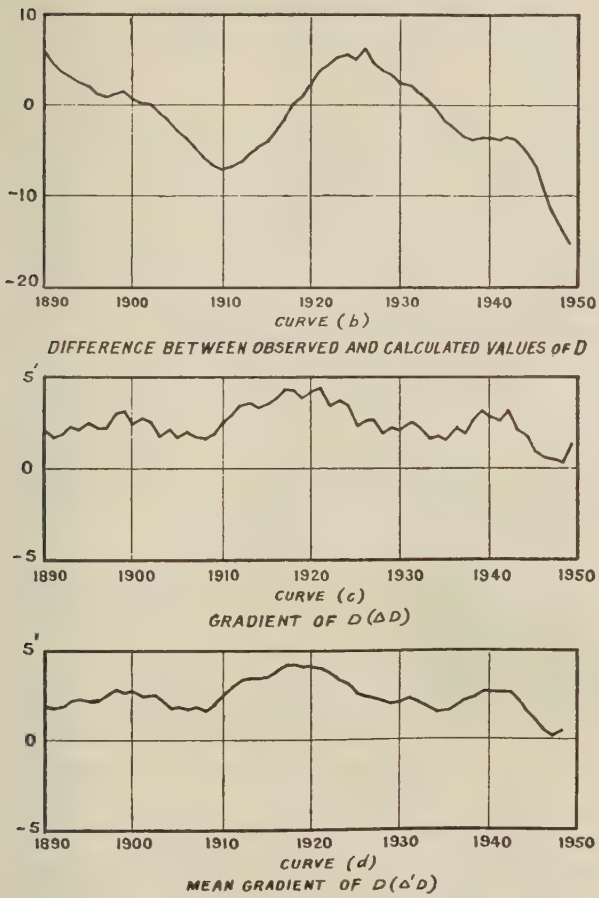

FIG. 5

is seen between this curve and the sunspot curve (curve *a*; Fig.4). The values of ΔV and $\Delta' V$ have been plotted in curves *c* and *d*, Figure 6. There is no evidence of a periodicity of about 11 years in curves *c* and *d*, and there is no parallelism apparent between these and the sunspot curve. The mean value of ΔV for the last nine sunspot minimum years is 52 γ, while that for the nine sunspot maximum years is 37 γ.

(18) The available values of F at Dehra Dun, Kodaikanal, Toungoo, and Barrakpore have been plotted in Figure 3. The trend of secular variation at all these places is similar, except at Toungoo, where the gradient is much less.

(19) The vertical force has increased from 1853 to 1937 about 4640 γ, or about a third of its value in the former year. After 1937, there has been a tendency to decrease, but this tendency appears to have been arrested and the vertical force may begin to increase again.

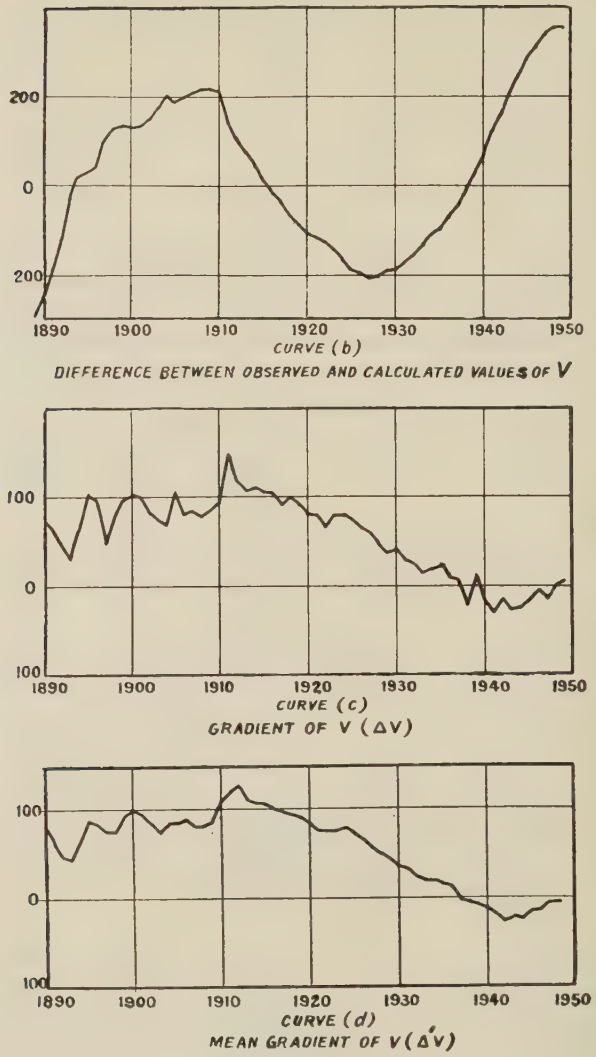

FIG. 6

Conclusion

(20) The value of H has been increasing continuously since 1916, and it is likely that the increase will continue at least for some more years. The westward drift of declination commenced from 1879 and is still continuing. The rate of drift, however, has decreased during the last five years, and within the next few years it may begin to return eastward or move westward at an increased rate. The vertical force had been continuously increasing from 1853 and it reached its maximum value in 1937, after which there was a fall for some years, but the falling tendency appears to have been arrested and the vertical force may again begin to increase.

TABLE 8—*Annual mean values of horizontal force, declination, and vertical force*

Year	H	D	V	Year	H	D	V
	γ	′	γ		γ	′	γ
1846	.....	62.9	.....	1870	36686	103.1	13525
1847	.....	63.7	.....	1871	36693	104.7	13553
1848	36047	64.1	13289	1872	36718	106.6	13590
1849	36112	64.2	13282	1873	36741	107.5	13624
				1874	36771	107.9	13661
1850	36176	65.6	13275	1875	36803	108.9	13699
1851	36208	66.4	13271	1876	36823	109.5	13740
1852	36300	66.4	13269	1877	36833	110.1	13782
1853	36330	67.9	13267	1878	36849	110.4	13825
1854	36375	67.7	13268	1879	36862	110.9	13871
1855	36420	69.0	13271				
1856	36443	68.6	13276	1880	36853	110.7	13918
1857	36444	68.9	13282	1881	36848	110.7	13968
1858	36421	69.5	13289	1882	36830	110.4	14019
1859	36442	71.1	13299	1883	36865	110.6	14071
				1884	36904	109.0	14126
1860	36467	73.6	13311	1885	36901	108.5	14182
1861	36502	76.7	13325	1886	36896	107.0	14240
1862	36521	79.6	13339	1887	36901	105.9	14300
1863	36548	83.3	13356	1888	36912	104.8	14351
1864	36573	85.9	13375	1889	36919	102.9	14451
1865	36609	89.6	13396				
1866	36623	93.7	13418				
1867	36649	96.3	13442				
1868	36667	98.9	13474				
1869	36669	100.7	13503				

(21) During the first six solar cycles, the average values of H, ΔH, and $\Delta' H$ are greater during sunspot minimum years than during sunspot maximum years, but this does not hold during the last three cycles. No periodicity of about 11 years was apparent in the curves representing the differences between the observed and calculated values of H, D, and V, or in the curves representing ΔH, $\Delta' H$, ΔD, $\Delta' D$, ΔV, and $\Delta' V$, and no parallelism was noticeable between these curves and the sunspot curve.

References

[1] N. A. F. Moos, Magnetic observations made at the Government Observatory, Bombay, for the period 1846 to 1905 and their discussion, Bombay, Govt. Central Press (1910).

[2] E. H. Vestine, I. Lange, L. Laporte, and W. E. Scott, The geomagnetic field, its description and analysis, Washington, D. C., Carnegie Inst. Pub. 580 (1947).

[3] E. H. Vestine, L. Laporte, I. Lange, C. Cooper, and W. C. Hendrix, Description of the earth's main magnetic field and its secular change, 1905-1945, Washington, D. C., Carnegie Inst. Pub. 578 (1948).

[4] H. W. Fisk, Magnetic secular variation and solar activity, Internat. Res. Council, Third Rep. Comm. Solar and Terrestrial Relationships (1931).

[5] S. Chapman and J. Bartels, Geomagnetism, Oxford, Clarendon Press (1940).

A PROCEDURE FOR THE DETERMINATION OF THE VERTICAL DISTRIBUTION OF THE ELECTRON DENSITY IN THE IONOSPHERE*

By John M. Kelso

Ionosphere Research Laboratory, The Pennsylvania State College, State College, Pennsylvania

(Received February 13, 1952)

ABSTRACT

A procedure is given for the determination of the "true height of reflection" of a radio wave incident vertically on the ionosphere. Since—for a given operating frequency—the electron density required for reflection is easily found, the present procedure allows the electron density to be determined as a function of height. To find the "true height" at some particular frequency, f_v , it is only necessary to take the average of the values of group height measured at a set of predetermined frequencies. These frequencies depend on f_v and the accuracy desired in the results. In scaling standard experimental curves for this work, it was sufficient to use five values, except near cusps or steps where double that number was found desirable.

The present method is based on the use of the Gauss-Christoffel quadrature formula, which is used for the numerical integration of the well-known integral for "true height" as a function of group height. The restrictions on this integral apply to all of the work contained here and are: (1) The earth's magnetic field is neglected; (2) the effects of collisions are neglected; (3) it is assumed that ray theory may be used; (4) it is assumed that the curve of electron density as a function of height has no maxima or minima in the region considered.

INTRODUCTION

Although the determination of the variation with height of the electron density is one of the major problems in ionospheric research, very little experimental work has been done on this problem because of the great amount of computational labor involved. Theoretical work has been done on this problem by a number of workers, in particular, Pekeris [see 1 of "References" at end of paper], Rydbeck [2], and Manning [3]. All three have given methods to be used in determining the true height of reflection of the signal (simply related to the electron density,

*The research reported in this paper was supported by the Geophysical Research Division of the Air Force Cambridge Research Center.

according to ray theory) when collisions and the earth's magnetic field are neglected; and Rydbeck has also extended these results to consider the extraordinary ray in longitudinal propagation, neglecting collisions.

Kraus [4] has applied the Gauss-Christoffel quadrature formula [5] to the more restricted case above, and thus reduced the computations to a reasonable amount of effort for scaling large numbers of records. The present work makes a particular application of Kraus' method to the determination of the true heights from experimental equivalent height *versus* frequency records. With the method utilized, it is possible to extend these computations to any degree of approximation justified by the data with very little additional preparatory effort.

In order to obtain the "true height" at some particular frequency, f_v, one determines from the experimental h'—f record the equivalent height, h', corresponding to a set of other frequencies—each a definite fraction of f_v—and takes the average of these values of h'. This average is an approximation to the "true height;" the degree of the approximation depends upon the number, n, of frequencies at which the h'—f curve was read. The ratio of these n frequencies to the frequency f_v is completely determined by the value of n. To make the work more rapid, a group of calculations of the set of frequencies has been made for $n = 5$ and for $n = 10$. The values for $n = 5$ were used wherever the experimental curve was smooth, and for $n = 10$ near discontinuities or cusps, or other bad behavior. To determine the true height at a given value of f_v, one obtains first the proper set of frequencies. Then h' is read at each of these frequencies. Adding these values of h' and averaging, the true height is obtained. In practice, the h' values can be added on a calculator as they are read, so that it is necessary to record only the final answer.

The Gauss-Christoffel quadrature formula is quite general, and could be useful in other problems in this field. Much of the information on this subject, and in particular the basis of proof given here, has been obtained from a report by Friedman [5], who applied the Gauss-Christoffel formula to the determination of the group paths in several types of layers for propagation including the earth's magnetic field.

The remainder of this paper contains a brief discussion of the integral which must be evaluated in order to obtain the "true height," and later some typical examples of the results obtained by this procedure.

THE GAUSS-CHRISTOFFEL QUADRATURE FORMULA

This formula is discussed—usually in a somewhat restricted form—in a number of standard references for physicists and engineers, among them Milne [6], Margenau and Murphy [7], and Courant and Hilbert [8].

Let us consider a set of polynomials, of which the one of degree n is

$$p_n(x) = a_0 + a_1x + a_2x^2 + \cdots + a_nx^n = \sum_{k=0}^{n} a_kx^k \quad \ldots\ldots\ldots\ldots (1)$$

where all of the coefficients may be altered if the degree n is changed. Let us suppose that there is some given, non-negative, function, $w(x)$, called a weight function such that over some interval $a \leq x \leq b$, the integral

$$\int_a^b w(x)\,dx \qquad (2)$$

exists. Then the given set of polynomials is said to be orthogonal and normalized over the interval (a, b) with weight function $w(x)$ if, respectively,

$$\int_a^b p_n(x)p_m(x)w(x)\,dx = 0 \qquad (3)$$

for all $m \neq n$ and

$$\int_a^b \{p_n(x)\}^2 w(x)\,dx = 1 \qquad (4)$$

for all values of n. The Legendre polynomials are such an example with $a = -1$, $b = +1$, and $w(x)$ equal to unity.

Let the n numbers, x_j $(j = 1, 2, \cdots, n)$ be the roots of the polynomial $p_n(x)$. Then the Gauss-Christoffel quadrature formula can be stated as follows:

If $g(x)$ is an arbitrary polynomial of degree $2n - 1$, then there exist real numbers $\lambda_1, \lambda_2, \cdots \lambda_n$, such that

$$\int_a^b g(x)w(x)\,dx = \lambda_1 g(x_1) + \lambda_2 g(x_2) + \cdots + \lambda_n g(x_n) \qquad (5)$$

The numbers, λ_j, are uniquely determined by the weight function $w(x)$, the degree n, and the interval (a, b).

If $g(x)$ is not a polynomial of the specified degree, then the right-hand side of equation (5) is an approximation to the integral on the left, and is equivalent to the result obtained by approximating $g(x)$ by a polynomial of degree $2n - 1$. It is in this sense that we may say that our n points, chosen in this way, give almost twice the accuracy as, say, n equally-spaced points.

The constants λ_j in equation (5) are given by

$$\lambda_j = \int_a^b \frac{p_n(x)}{p_n'(x_j)(x - x_j)}\, w(x)\,dx \qquad (6)$$

The polynomials $p_n(x)$ may be determined by solving the $n + 1$ equations

$$\sum_{k=0}^{n} a_k \int_a^b x^{j+k} w(x)\,dx = 0; \qquad j = 0, 1, 2, \cdots, n - 1$$

$$\int_a^b [p_n(x)]^2 w(x)\,dx = 1$$

CALCULATION OF ELECTRON DENSITY

Neglecting the earth's magnetic field and the effects of collisions, the index of refraction for a radio wave incident vertically in an ionosphere layer may be written

$$\mu^2 = 1 - \frac{4\pi N e^2}{mp^2} \qquad (7)$$

where μ = index of refraction, $p/2\pi$ = operating frequency, N = electron density, and e, m = charge and mass of an electron.

It is well known that under the conditions noted above, the group path, P', is given by

$$P' = 2\int_0^{h_T} \frac{ds}{\mu} \quad (8)$$

where the integral is taken along the path of the ray from the bottom of the layer up to the point of reflection, h_T .

It has been shown [1, 3] that equation (8) may be transformed to give an expression for the height of reflection, h_T , for some frequency f_v , in terms of the group height $h' = P'/2$, and the operating frequency f. This expression is

$$h_T(f_v) = \frac{2}{\pi}\int_0^{f_v} \frac{h'(f)\,df}{\sqrt{f_v^2 - f^2}} + h_0 \quad (9)$$

where h_0 is the height from ground level to the bottom of the layer.

If we now make the substitution

$$x = \frac{f}{f_v} \quad (10)$$

then equation (9) can be written

$$h_T(f_v) = \frac{2}{\pi}\int_0^1 \frac{h'(x)\,dx}{\sqrt{1 - x^2}} + h_0 \quad (11)$$

Equation (11) then gives the integral which must be evaluated in order to determine the true height. The group height can be measured as a function of frequency, so that all of the information for the experimental determination of the true height of reflection is available. It is required only to carry out the integration in equation (11). This, however, is somewhat difficult, and is usually done graphically. The use of the Gauss-Christoffel quadrature formula makes the integration much simpler than by other methods, so that large numbers of experimental curves can be readily scaled in this manner.

For the approximate ionosphere conditions defined above, the signal is reflected at a level at which $\mu = 0$. Then, using equation (7), we can solve for the value of N belonging to this level

$$N(h_T) = \frac{mp^2}{4\pi e^2} \quad (12)$$

Thus, for each value of the true height of reflection, determined from equation (11), we can compute from equation (12) the value of electron density existing at that height.

The applicability of the results in equations (11) and (12) is restricted by the assumptions made. These assumptions are: (1) The earth's magnetic field can be neglected; (2) the effects of collisions can be neglected; (3) ray theory (geometrical optics) is valid; and (4) it is assumed that for each electron density there is a unique height. The effects of this last assumption have been discussed in a second paper by Manning [9], while Rydbeck [2] has considered the others. How-

ever, the primary purpose of the present paper is to present the use of the Gauss-Christoffel quadrature formula, so that the extended treatment of the physical problems will not be taken up here.

APPLICATION OF QUADRATURE FORMULA TO ELECTRON DENSITY DETERMINATION

We may now consider the application of the Gauss-Christoffel quadrature formula, equation (5), to the evaluation of the integral in equation (11) for the true height (or the electron density). Thus, following Kraus [4], we wish to evaluate the integral

$$I = \int_0^1 \frac{h'(x)\,dx}{\sqrt{1-x^2}} \qquad (13)$$

that is, we wish to integrate $h'(x)$ over the interval (0, 1) with a weight function $1/\sqrt{1-x^2}$. In our notation, the relation obtained by Kraus [4], using the Gauss-Christoffel formula, is

$$h_T(f_v) = 0.440h'(0.939f_v) + 0.364h'(0.550f_v) + 0.196h'(0.124f_v)$$

However, in the present case, the procedure can be simplified, and the results made much more flexible by the adoption of the following device.

Since the group height is defined only for positive values of x, we are free to define it for negative values of x so that $h'(x)$ is an even function; that is,

$$h'(-x) = h'(x) \qquad (14)$$

Then equation (13) becomes

$$I = \frac{1}{2}\int_{-1}^1 \frac{h'(x)\,dx}{\sqrt{1-x^2}} \qquad (15)$$

Now, write

$$x = \cos\theta \qquad (16)$$

and equation (15) may be written

$$I = \frac{1}{2}\int_0^\pi h'(\cos\theta)\,d\theta \qquad (17)$$

The integral in equation (17) is to be taken over the interval (0, π) with unity weight function. Since the variable is now cos θ, the desired polynomials will be trigonometric polynomials. It is well known that the set of such polynomials orthogonal over the given interval with unity weight function are cos $n\theta$ ($n = 0, 1, 2, \cdots$), which are in fact polynomials of degree n in the variable cos θ. (It might be noted that these polynomials are simply related to the Tschebycheff polynomials [7].) When normalized, the polynomials become

$$\left.\begin{aligned} p_0 &= \frac{1}{\sqrt{\pi}} \\ p_n &= \sqrt{\frac{2}{\pi}}\cos n\theta, \qquad n = 1, 2, \cdots \end{aligned}\right\} \qquad (18)$$

and the n zeros of the nth polynomial are given by

$$\theta_k = \frac{2k - 1}{2n}\pi, \qquad k = 1, 2, \cdots, n \ldots\ldots\ldots\ldots\ldots\ldots (19)$$

In order to apply the Gauss-Christoffel quadrature formula, it remains only to determine the constant multipliers, λ_j, in equation (5). Following a procedure developed by Friedman [5], we may write, for an arbitrary polynomial $g(x)$ of degree $n - 1$,

$$g(x) = c_0 p_0(x_j) + \sum_{1}^{n-1} c_k p_k(x)$$

Hence,

$$g(x_j) = c_0 p_0(x_j) + \sum_{k=1}^{n-1} c_k p_k(x_j) \qquad j = 1, 2, \cdots, n$$

$$= \frac{c_0}{\sqrt{\pi}} + \sqrt{\frac{2}{\pi}} \sum_{k=1}^{n-1} c_k \cos k \frac{(2j - 1)}{2n}\pi$$

Summing $g(x_j)$ over all values of j, that is, from 1 to n,

$$\sum_{j=1}^{n} g(x_j) = \frac{n}{\sqrt{\pi}} c_0 + \sqrt{\frac{2}{\pi}} \sum_{j=1}^{n} \sum_{k=1}^{n-1} c_k \cos k \frac{(2j - 1)}{2n}\pi \ldots\ldots\ldots (20)$$

Interchanging the order of summation and making use of the identity

$$\sum_{j=1}^{n} \cos k \frac{(2j - 1)}{2n}\pi = 0, \qquad k = 1, 2, \cdots, n - 1 \ldots\ldots\ldots (21)$$

equation (20) becomes

$$\sum_{j=1}^{n} g(x_j) = \frac{n}{\sqrt{\pi}} c_0 \ldots\ldots\ldots\ldots\ldots\ldots\ldots\ldots (22)$$

We then have, by the orthogonality relations,

$$\int_0^{\pi} p_k(\theta)\, d\theta = 0,$$

$$\int_{-1}^{1} g(x)w(x)\, dx = \int_0^{\pi} g(\theta)\, d\theta = c_0 \int_0^{\pi} p_0\, d\theta + \sum_{k=1}^{n-1} c_k \int_0^{\pi} p_k(\theta)\, d\theta$$

$$= c_0 \int_0^{\pi} p_0\, d\theta = \sqrt{\pi}\, c_0 = \frac{\pi}{n} \sum_{j=1}^{n} g(x_j)$$

Comparing with equation (5), we then see that the λ_j's are given by

$$\lambda_j = \frac{\pi}{n}, \qquad j = 1, 2, \cdots, n \ldots\ldots\ldots\ldots\ldots\ldots (23)$$

Then, from the Gauss-Christoffel quadrature formula,

$$I = \frac{1}{2}\int_{-1}^{1} \frac{h'(x)\,dx}{\sqrt{1-x^2}} = \frac{1}{2}\int_{0}^{\pi} h'(\cos\theta)\,d\theta$$

$$= \frac{\pi}{2n}\sum_{k=1}^{n} h'(\cos\theta_k)$$

$$I = \frac{\pi}{2n}\sum_{k=1}^{n} h'(x_k), \qquad \text{where} \qquad x_k = \cos\theta_k \ldots\ldots\ldots\ldots (24)$$

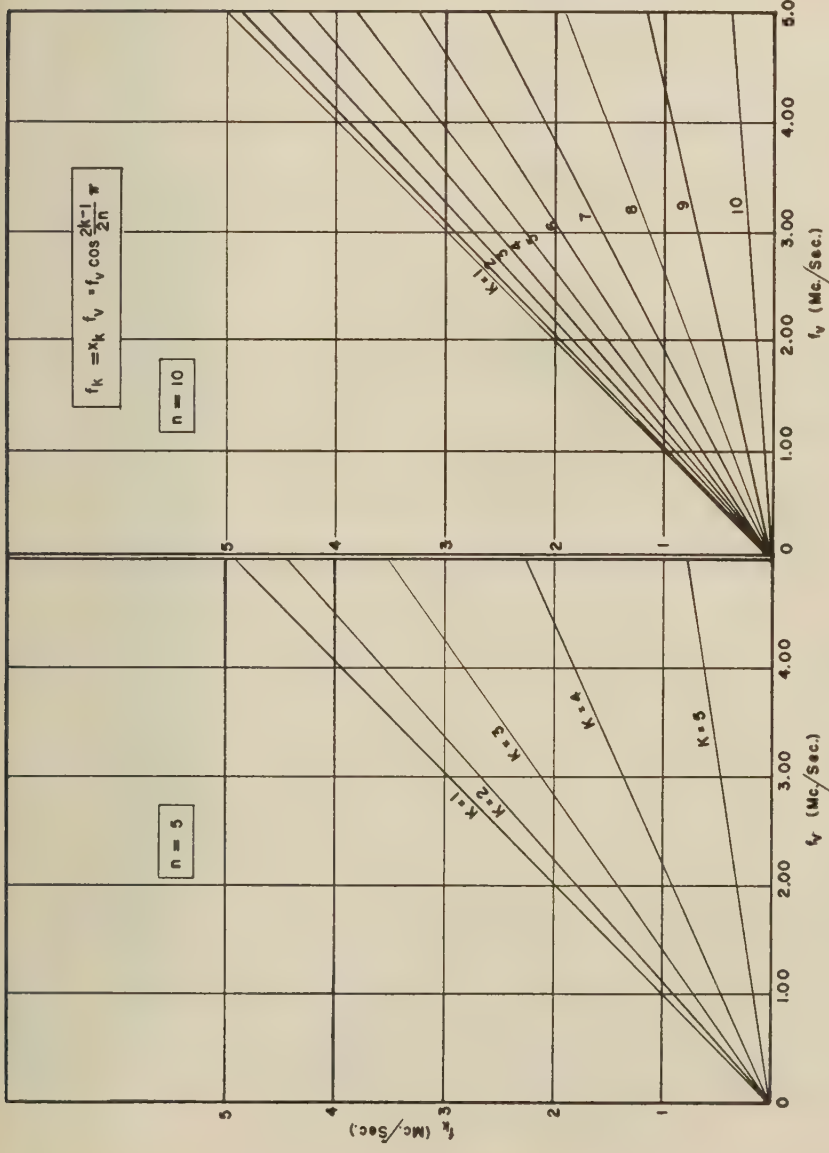

FIG. 1 — f_K VERSUS f_V (IN MC/SEC) FOR PARAMETRIC VALUES OF K (RANGE OF FREQUENCIES SUITABLE FOR E LAYER)

(It might be noted that this result was proved by Mehler [10] in 1864.)
From equation (10)

$$I = \frac{\pi}{2n} \sum_{k=1}^{n} h'(f_k), \qquad \text{where} \qquad f_k = x_k f_v \ldots\ldots\ldots\ldots\ldots\ldots (25)$$

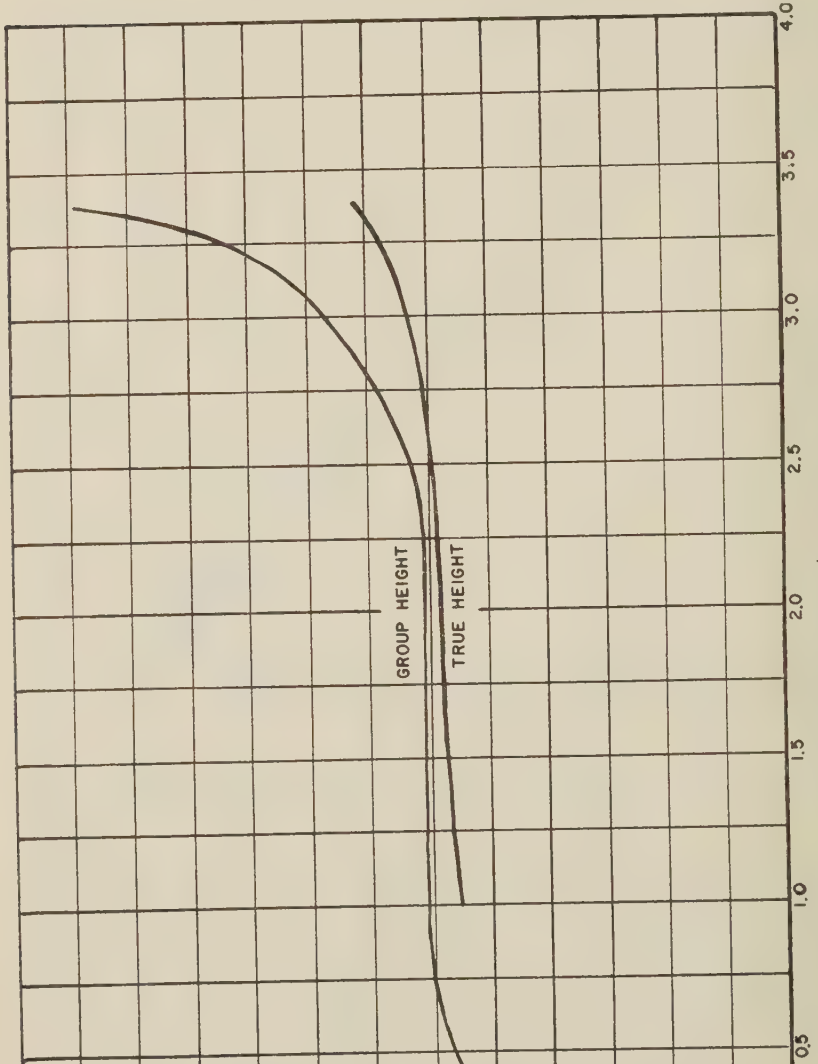

FIG. 2—EXPERIMENTAL GROUP AND COMPUTED TRUE HEIGHTS FOR A "NORMAL E LAYER"—13^h55^m TO 14^h02^m LMST, NOVEMBER 1, 1949

Thus, from equation (9),

$$h_T(f_v) = \frac{1}{n} \sum_{k=1}^{n} h'(f_k) \quad \ldots\ldots\ldots\ldots\ldots\ldots\ldots\ldots\ldots\ldots (26)$$

To determine h_T at some frequency f_v, the following steps are needed: (1) Find the n roots θ_k of the nth polynomial $\cos n\theta$, from the relation $\theta_k = [(2k - 1)/2n]\pi$; (2) compute the values $x_k = \cos \theta_k$; (3) evaluate $f_k = x_k f_v$; (4) from the experimental h'—f curve, read h' corresponding to each value of f_k; and (5) average the values of h' in (4). This give $h_T(f_v)$.

Several steps can be taken in order to reduce the labor involved in the program outlined above. From the symmetry of the problem, it is clear that for each positive value of x_k, there is a corresponding negative value of the same magnitude. Since we have defined $h'(f)$ as an even function, it is readily seen that we have only $n/2$ or $(n + 1)/2$ values of h' to be used in the procedure above, according to whether n is even or odd. Thus, if $n = 20$, we must read $h'(f)$ at 10 values of f; while if $n = 21$, we need 11 values of $h'(f)$.

A second simplification in procedure can be achieved by noting that the values of x_k depend only upon n. Thus, we could choose in advance a set of values of f_v to be used in all the scaling to be done, and then note the values of f_k to be used for each value of f_v listed. This is facilitated by using Figure 1. The range of f_v shown is ample for scaling records for normal E region (the use of the entire procedure for sporadic conditions would be most suspect, in view of the uncertainty as to the nature of sporadic E).

SAMPLE RESULTS

The procedures outlined above have been applied to a number of sets of experimental data. Two rather typical samples are given here. The curves given in Figure 2 are for what is usually called "normal E," while the curves in Figure 3 are for "sporadic" conditions.

The data for both Figures were taken on manual sweep-frequency equipment down to about one megacycle. Then two points were added, the first taken for the appropriate time from 150 kc/sec records of group height as a function of time obtained by our Laboratory and the second taken from the mean value of the 16 kc/sec work reported at Cambridge, England [11]. The difference between the records thus extended, and records extended by extrapolating the data as a constant equal to the value at one megacycle, is found to be small, usually less than one kilometer. The low frequency points were included in the present analysis, since they provided a more severe test of the method.

The curves in Figure 3, from the viewpoint of the application of the present method, are the most interesting. Both the cusp and the gentle rise in the middle of the record are frequently noted under suitable conditions. It will be noted that, for frequencies greater than the cusp frequency, the true heights decrease with frequency. When these true heights are converted to electron densities, the electron densities are then double-valued functions of height—a physically meaningless result. Thus, it is clear that, in some way, the analysis fails when the $h' - f$ record shows a cusp. From planimetric integration, it is found that it is

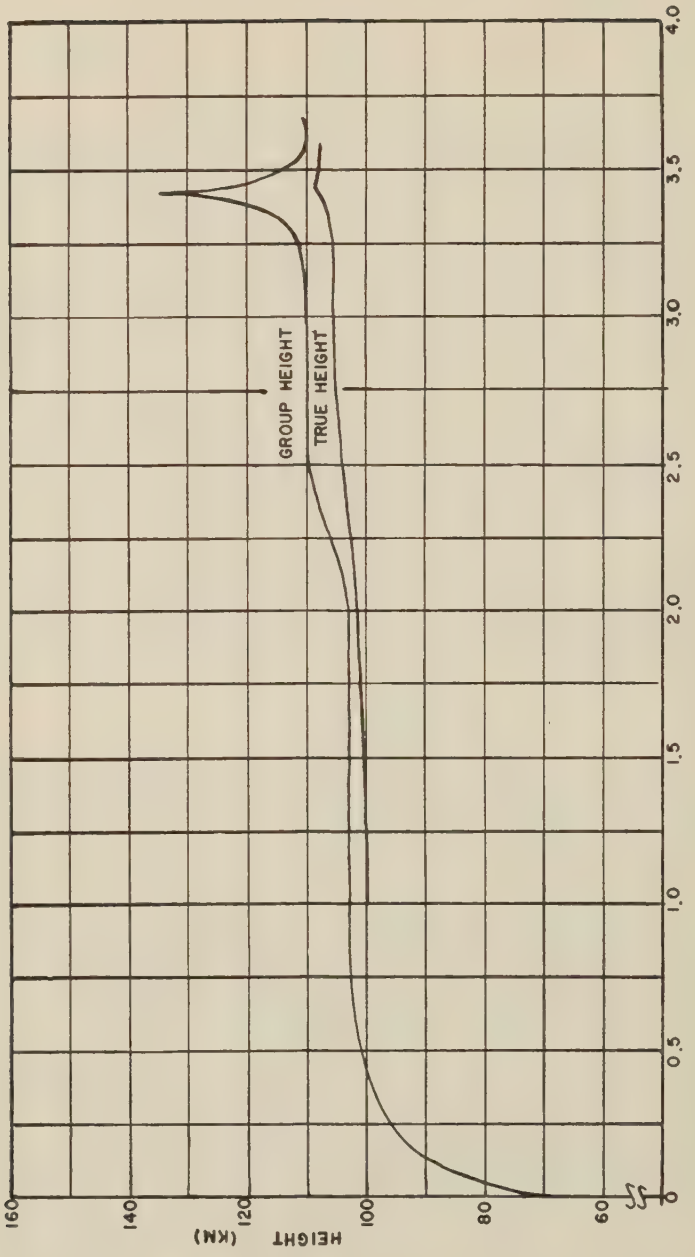

FIG. 3—EXPERIMENTAL GROUP AND COMPUTED TRUE HEIGHTS FOR A "SPORADIC E LAYER"—10^h10^m TO 10^h16^m LMST, APRIL 29, 1949

not the conditions on the quadrature formula used here, so that it must lie in a failure of the expression for true height given in equation (9). This may be due to our neglect of some quantity such as the earth's field, or may be due to the nature

of "sporadic E" itself. From the point of view of the present work, the most interesting observation to be made concerning Figure 3 is that, despite the several types of misbehavior of the $h' - f$ curve, the difference between the true heights obtained in the manner suggested here, and the results from planimetric integration, is of the order of one kilometer for the worst disagreement. All other points were separated by less than one-half of this amount. Since Figure 3 is typical of the most complicated of the records obtained at this Laboratory, it is felt that the ten-point analysis should be adequate for most purposes.

ACKNOWLEDGMENTS

The author would like to thank Prof. L. Kraus, of New York University, who was the first to apply the quadrature formula used here to the present problem, and with whom several interesting and informative discussions were held. A similar debt is acknowledged to Prof. B. Friedman, also of New York University. Finally, the author is greatly indebted to Prof. Norman Davids, of our own Laboratory, for revision of certain portions of the manuscript and for the preparation of Figure 1.

References

[1] C. L. Pekeris, The vertical distribution of ionization in the upper atmosphere, Terr. Mag., **42**, 205–211 (1940).
[2] O. E. H. Rydbeck, On the propagation of radio waves, Trans. Chalmers Univ. Tech., Gothenburg, **34**, (1944).
[3] L. A. Manning, Determination of ionospheric electron distribution, Proc. Inst. Radio Eng., **35**, 1203–1207 (1947).
[4] L. Kraus, New York University, Mathematics Department, Research Group, Progress Report No. 6 (1950).
[5] B. Friedman, Numerical methods for evaluation of the integrals for virtual height, New York University, Mathematics Department, Research Group, Research Report EM-17 (Feb. 1950).
[6] W. E. Milne, Numerical calculus, Princeton, Princeton University Press (1949).
[7] H. Margenau and G. M. Murphy, The mathematics of physics and chemistry, New York, D. Van Nostrand Co., Inc. (1943).
[8] R. Courant and D. Hilbert, Methoden der Mathematischen Physik, Julius Springer, Berlin (1924).
[9] L. A. Manning, Reliability of ionospheric height determinations, Proc. Inst. Radio Eng., **37**, 599–603 (1949).
[10] F. G. Mehler, J. Reine U. Angewandte Math., **63**, 152–158 (1864).
[11] R. N. Bracewell, *et al.*, The ionospheric propagation of low and very-low-frequency radio waves over distances less than 1,000 km, Proc. Inst. Elec. Eng. (London), **98** Pt. 3, 221–236 (1951).

THE SOLAR CONTROL OF THE E AND $F1$ LAYERS AT HIGH LATITUDES

By J. C. W. Scott

Defence Research Telecommunications Establishment (Radio Physics Laboratory), Defence Research Board, Ottawa, Canada

(Received March 31, 1952)

ABSTRACT

The monthly mean critical frequencies of the E and $F1$ layers at high latitudes are shown to vary diurnally with solar angle according to a modified Chapman law. The seasonal, latitude, and solar-cycle dependence of the E-layer sensitivity to solar angle and the sub-solar frequency are measured.

In the auroral zone, the sensitivity of the E layer to solar angle is shown to be very low, but to the north of the zone it is found to have the theoretical Chapman value.

Introduction

Arctic ionospheric records are notable for their complication and variability. In the auroral zone, several types of sporadic ionization have been distinguished in the E layer and in the $F1$ layer, some of which occur in the dark hours. Records taken at an interval of a few seconds show that in both the E layer and the $F1$ layer sporadic ionization may vary with extreme rapidity. Some of this sporadic ionization occurs in clouds which move horizontally with high velocities. Other types are certainly associated with auroral displays. In the auroral zone, and to the north of it, spread echoes are normal in the dark hours; during daylight they frequently complicate the $F1$ layer.

It is therefore of interest to find that in the arctic both the E layer and $F1$ layer on the average vary with solar angle quite regularly, as they do at lower latitudes.

It is found that the sensitivity to solar angle varies seasonally and with the solar cycle. A notable conclusion is that in the auroral zone the sensitivity of the E layer to solar angle is sharply reduced, but that it recovers again to the north of the zone.

The Chapman law

Chapman showed that under simple conditions an ionospheric layer should vary with solar zenith angle according to the law

$$f = f_s \cos^n \chi$$

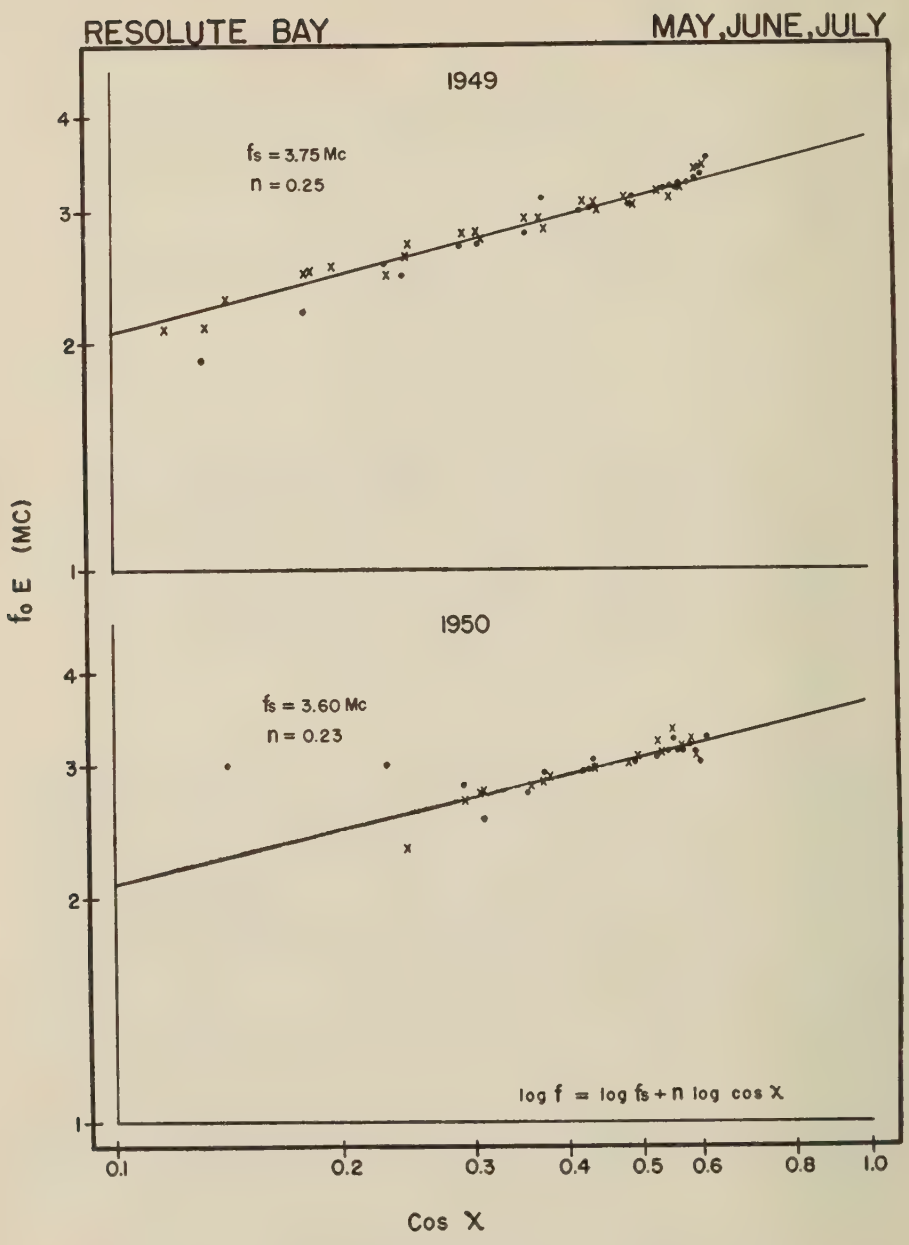

FIG. 1—THE RELATION BETWEEN f_0E AND THE SOLAR ZENITH ANGLE AT RESOLUTE BAY NEAR THE MAGNETIC POLE (LOG f_0E = LOG f_s + n LOG COS X)

where f is the critical frequency, f_s the sub-solar frequency, χ the solar zenith angle, and $n = 0.25$ [see 1 and 2 of "References" at end of paper].

This law is found to hold with fair accuracy at medium latitudes for the E and $F1$ layers, except that n is normally greater than 0.25. When the sun is low on the horizon, other factors must be taken into account, so that the law cannot be expected to hold without modification. In preparing the following plots, care has been taken to discount measurements for zenith angle greater than about 80°.

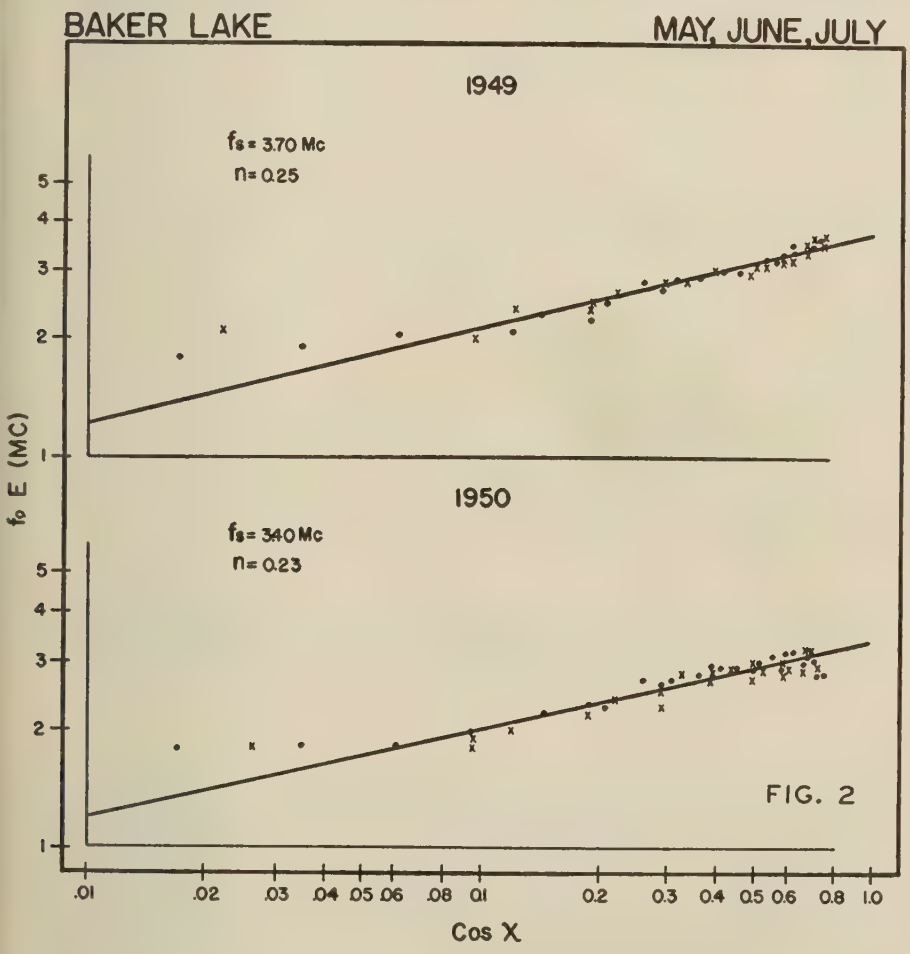

FIGS. 2,3, AND 4 — THE RELATION BETWEEN f_0E AND THE SOLAR ZENITH ANGLE AT THREE STATIONS ON A LINE RUNNING SOUTHWARD FROM RESOLUTE BAY, AND CROSSING THE AURORAL ZONE

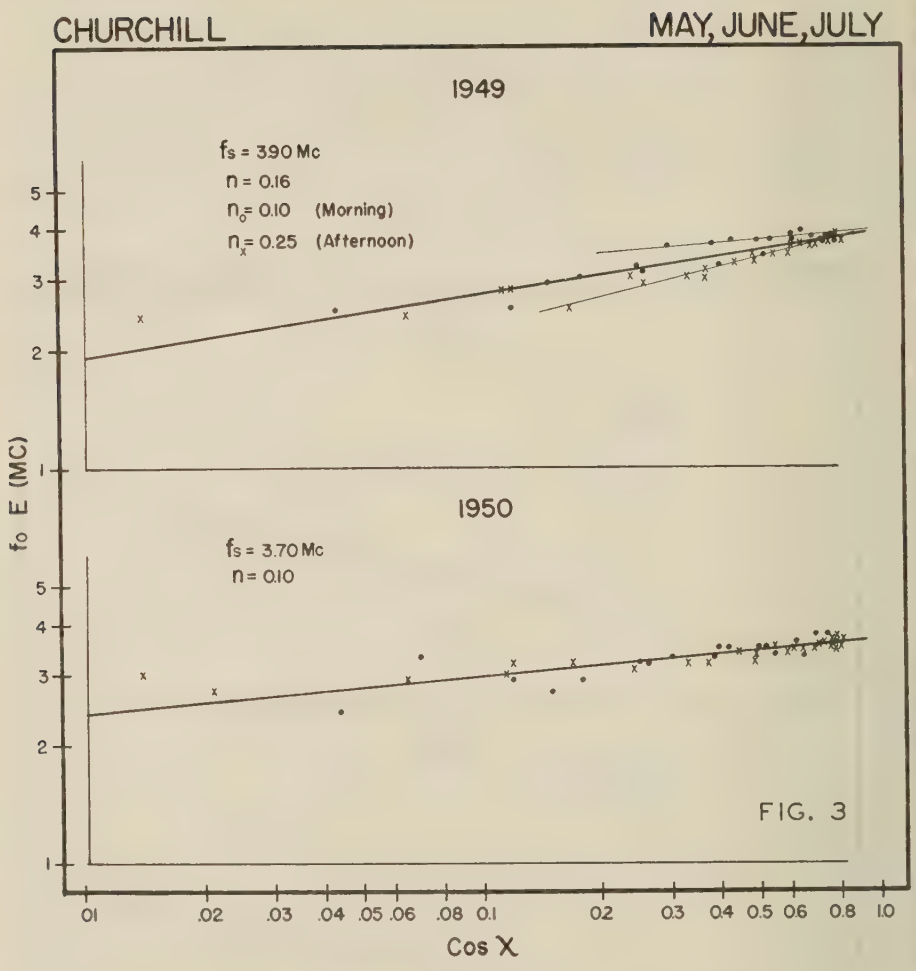

FIG. 3

The first Figure shows a logarithmic plot of f_0E against cos χ for the most northerly Canadian ionospheric station, Resolute Bay, situated near the dip pole at latitude 74.7° north, longitude 94.9° west. The data are for 1949 and 1950, in the arctic summer months of May, June, and July. Hourly median frequencies for each month are plotted against hourly mean zenith angles. It is clear that the Chapman law for a simple region is obeyed with remarkable accuracy.

Figures 2, 3, and 4 show the same data for three stations situated on a line

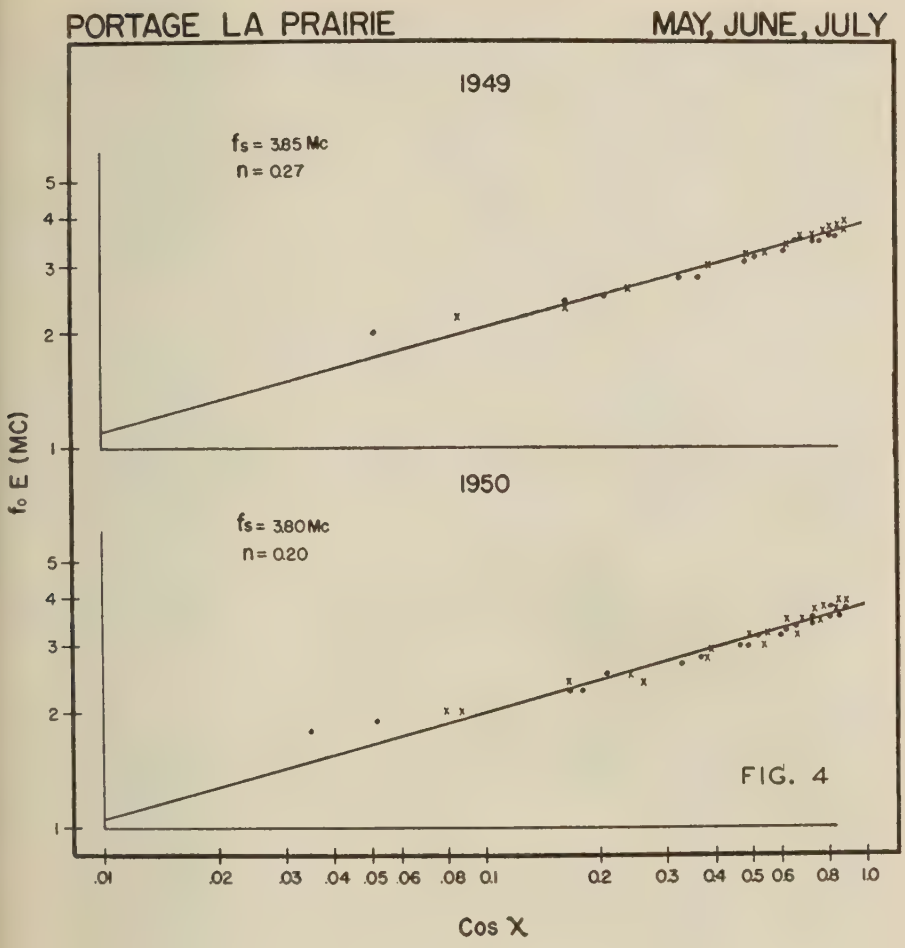

running southward from Resolute Bay. These are Baker Lake at latitude 64.3° north, longitude 96.0° west; Churchill at latitude 58.8° north, longitude 94.2° west; and Portage la Prairie at latitude 49.9° north, longitude 98.3° west. Baker Lake is north of the auroral zone, Churchill at the zone maximum, and Portage la Prairie south of the zone.

It is clear that a linear relationship exists at all these stations, but at Churchill the average value of the cosine power is only 0.16 in 1949 with a value for the morning hours of only 0.10, while in 1950 the average is only 0.10. Fort Chimo is also at the auroral zone maximum at latitude 58.1° north, longitude 68.3° west, and shows similar low values of n. For the same months, these values were 0.17 in 1949 and 0.10 in 1950.

The seasonal variation

The relation $f = f_s \cos^n \chi$ has been plotted for the E layer at Canadian stations since the beginning of operation. From logarithmic plots of the hourly monthly median critical frequency against the hourly monthly mean zenith angle, f_s and n have been derived for each month. Figures 5 and 6 show the monthly variation of the sub-solar frequency and of the power of cos χ, for Prince Rupert at latitude 54.3° north, longitude 130.3° west, and for Ottawa at latitude 45.4° north, longitude 75.7° west. Maximum and minimum curves have been drawn to show the deviation of the data from the mean. The data for Ottawa in 1942, the first year of operation of the first Canadian station, may be of doubtful validity.

The curves have several interesting features. It is evident that f_s and n are not independent, but rise and fall together month by month. Both clearly depend on solar activity, rising and falling with the solar cycle. Also, there is a pronounced seasonal variation, with minima occurring regularly in the winter and maxima either at the equinoxes or in the summer. There is an indication that equinoctial maxima occur together at the two stations and likewise summer maxima. Equinoctial maxima are shown in 1946 and 1947, and summer maxima in 1948, 1949, and 1950.

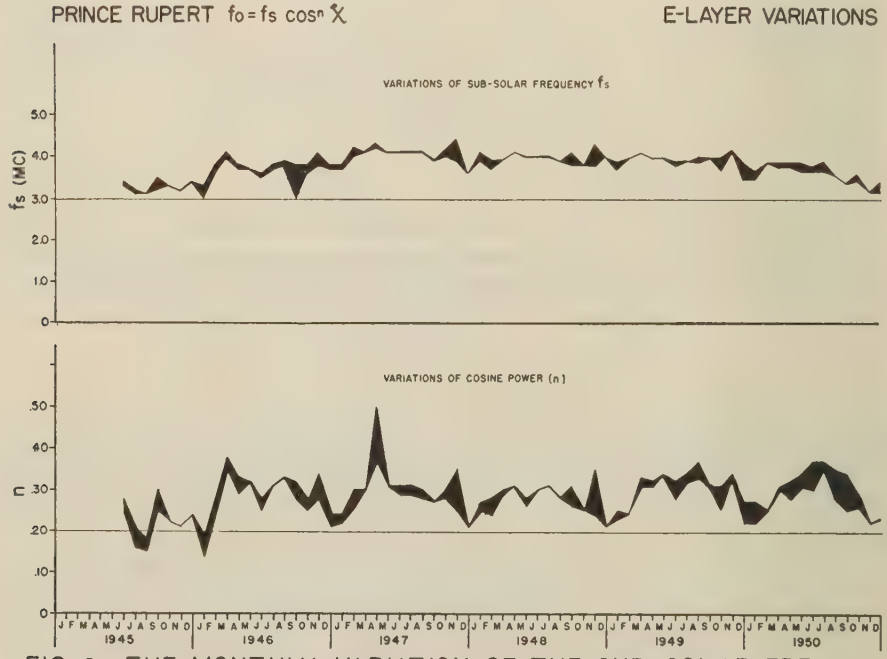

FIG. 5—THE MONTHLY VARIATION OF THE SUB-SOLAR FREQUENCY AND OF THE SENSITIVITY TO SOLAR ANGLE AT PRINCE RUPERT, SHOWING THE SEASONAL AND SOLAR-CYCLE VARIATION

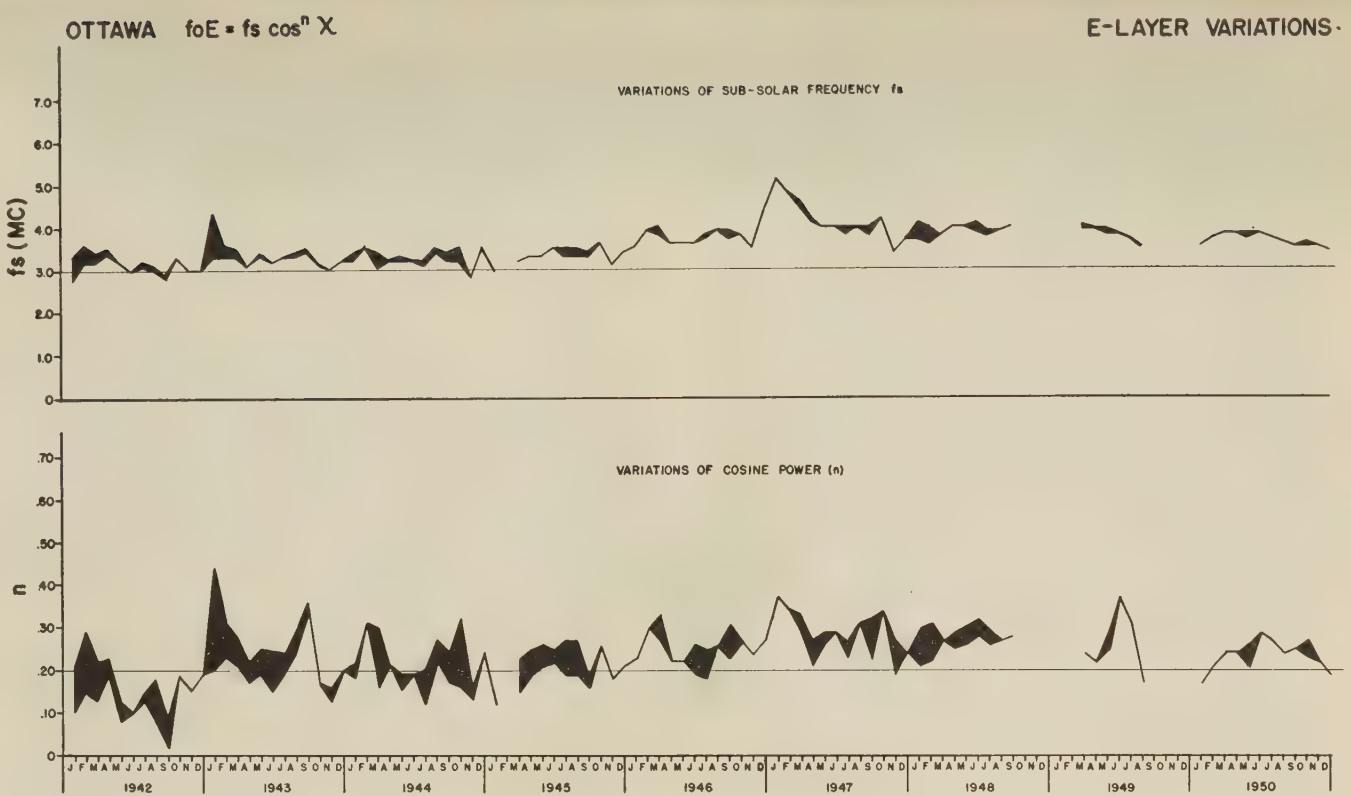

FIG. 6—THE MONTHLY VARIATION OF f_s AND OF n AT OTTAWA; THE VARIATION IS SIMILAR TO THAT AT PRINCE RUPERT

In Figures 7 and 8, the monthly values of f_s and n are superimposed from 1946 to 1950, for the four stations—St. John's, Ottawa, Prince Rupert, and Churchill. The position of St. John's is latitude 47.6° north, longitude 52.7° west.

It is immediately apparent that at Churchill, in the auroral zone, the sensitivity of the normal E layer to changes in the solar zenith angle is consistently lower than at stations outside the zone. The sub-solar frequency, however, is usually not much lower than at the other stations, except in the winter when it drops to an abnormally low value.

We conclude that, in the auroral zone, ionization by solar radiation is modified by other factors. This situation is not surprising, in view of the well-known importance of ionization by charged particles in the auroral zone.

The latitude variation

The evidence, that in the auroral zone the daytime E layer was relatively insensitive to solar angle, prompted us to examine the variation of n and f_s as a function of latitude. The average values of these quantities for May, June, and July were derived for 1949 and 1950, using all stations for which data were available. Figures 9 and 10 show the sensitivity, n, plotted against geographic and geomagnetic latitudes, respectively. Those points marked with a square are of doubtful accuracy.

At moderate latitudes, n is found to be usually about 0.33. The value drops sharply to between 0.10 and 0.20 at the northern auroral zone and to the north of the zone recovers again to about 0.25.

At Calcutta, some 12° north of the magnetic equator, there is apparently another sharp drop. Unfortunately, E-layer data from India were available only from Calcutta. However, Bhar confirms that abnormal E-layer ionization occurs at Calcutta during the summer months [3].

Data from the southern hemisphere have been included for comparison. But it must be remembered that, in the southern hemisphere, May, June, and July are winter months.

The sub-solar critical frequency, f_s , is plotted in the same manner in Figures 11 and 12. It is clearly much more constant from station to station than the sensitivity, and had an average value of about 4.0 Mc in 1949.

While the evidence cannot be considered conclusive, the latitude-variation curves strongly indicate that the sharp drop in sensitivity at Churchill and at Fort Chimo is a geomagnetic rather than a geographic phenomena. Plotted geographically, the points near those of Churchill and Chimo are actually higher than to the north and south. Plotted geomagnetically, however, there is a smooth depression in the curve with the minimum at Fort Churchill (and Fort Chimo).

The low value of sensitivity at Churchill is established by the curves of Figures 7 and 8, which include four years of data. Figure 10 shows other regions of low sensitivity, notably at Calcutta at geomagnetic latitude 12° north and at Falkland at 41° south. The minima at these stations are partially substantiated by adjacent points and by the fact that the latitude-variation curves for 1949 and 1950 are very similar. However, until they are verified by more data, they must be treated with reserve.

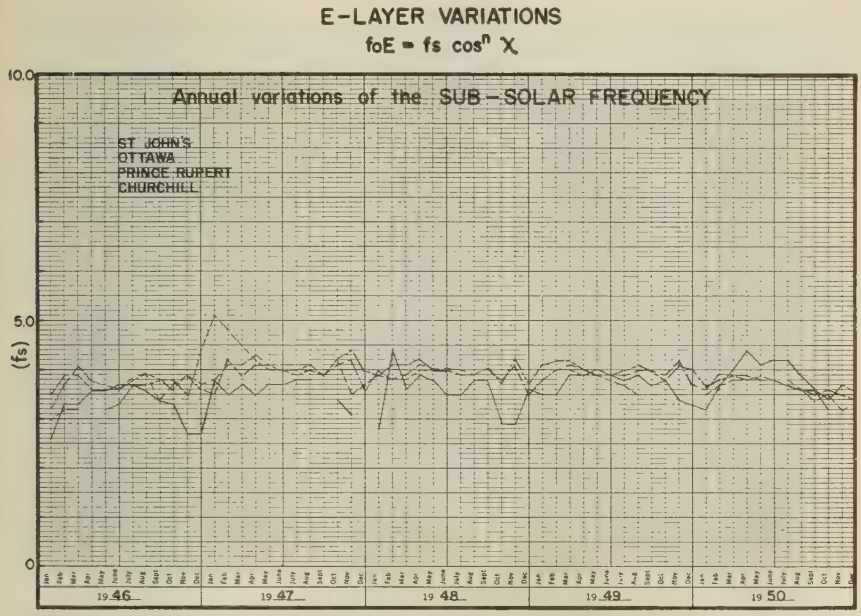

FIG. 7—THE MONTHLY VARIATION OF THE SUB-SOLAR FREQUENCY COMPARED AT FOUR CANADIAN STATIONS

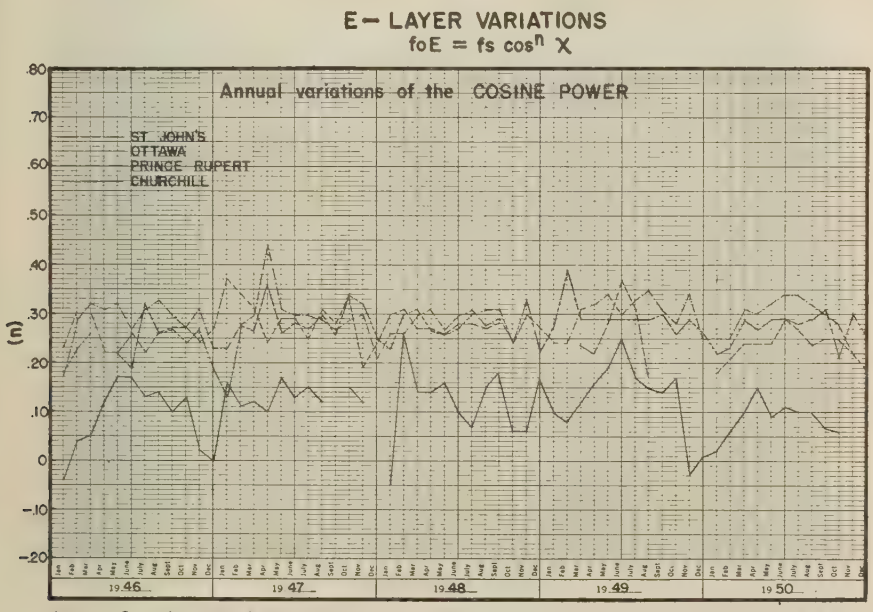

FIG. 8—THE MONTHLY VARIATION OF THE SENSITIVITY TO SOLAR ANGLE AT FOUR CANADIAN STATIONS

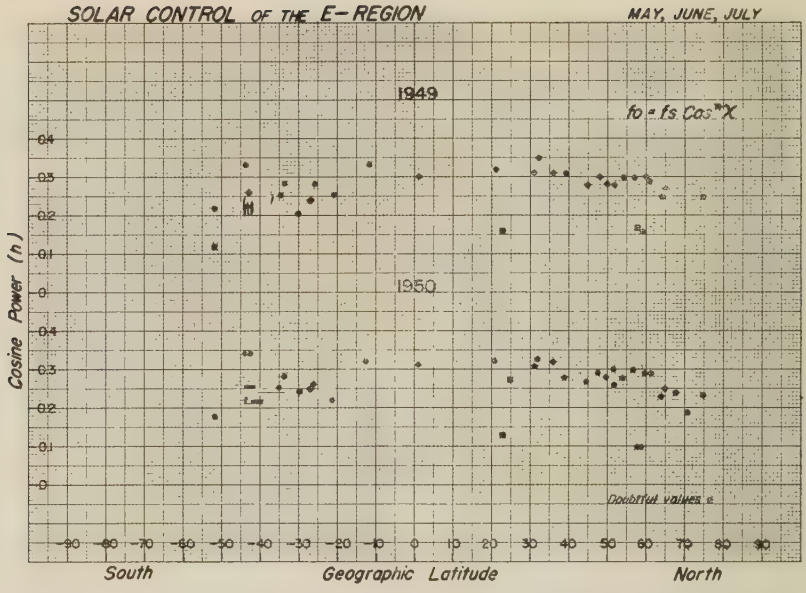

FIG. 9—THE VARIATION OF E-LAYER SENSITIVITY TO SOLAR ANGLE AS A FUNCTION OF GEOGRAPHIC LATITUDE

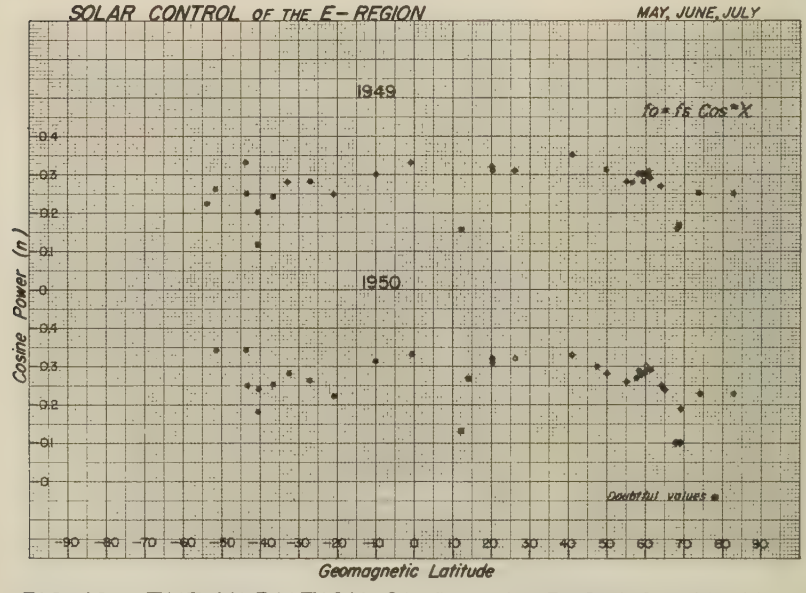

FIG. 10—THE VARIATION OF E-LAYER SENSITIVITY AS A FUNCTION OF GEOMAGNETIC LATITUDE

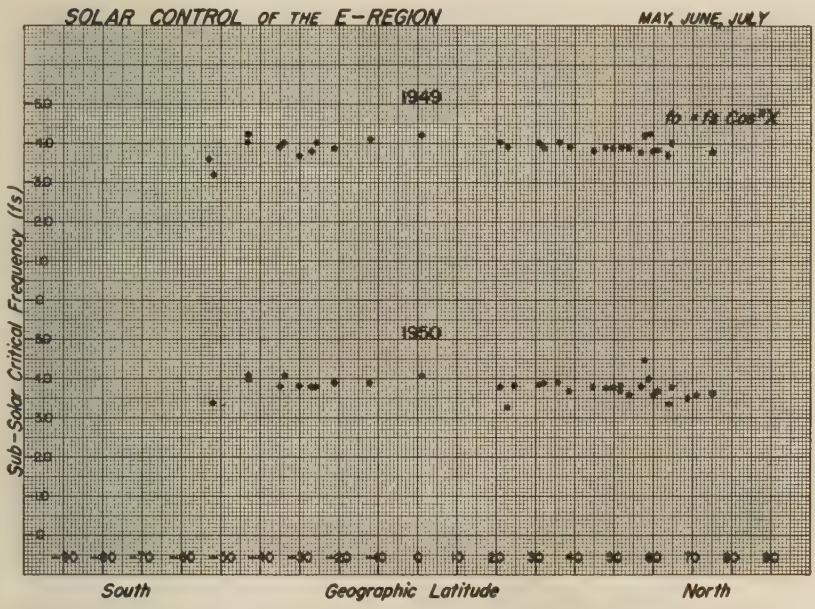

FIG. 11—THE VARIATION OF THE SUB-SOLAR FREQUENCY AS A FUNCTION OF GEOGRAPHIC LATITUDE

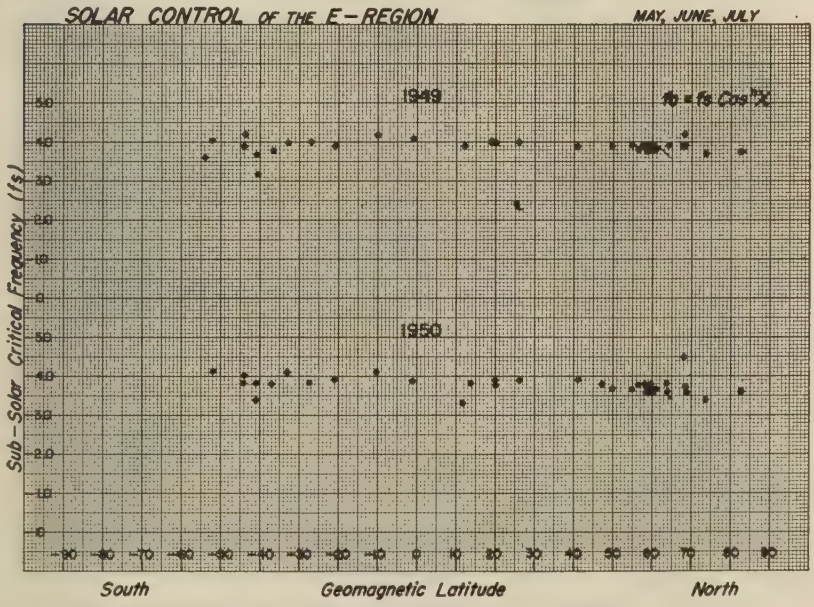

FIG. 12—THE VARIATION OF THE SUB-SOLAR FREQUENCY AS A FUNCTION OF GEOMAGNETIC LATITUDE

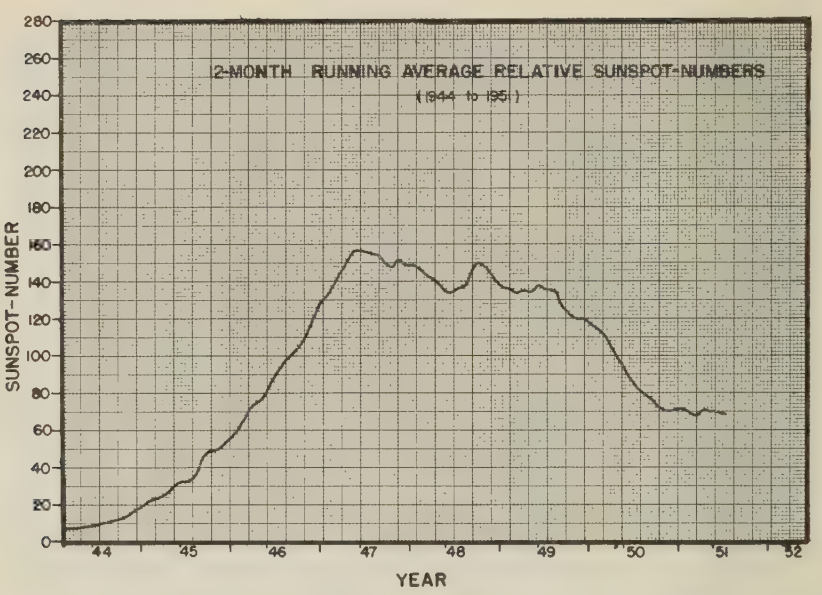

FIG. 13—THE SOLAR CYCLE, 1944-1951

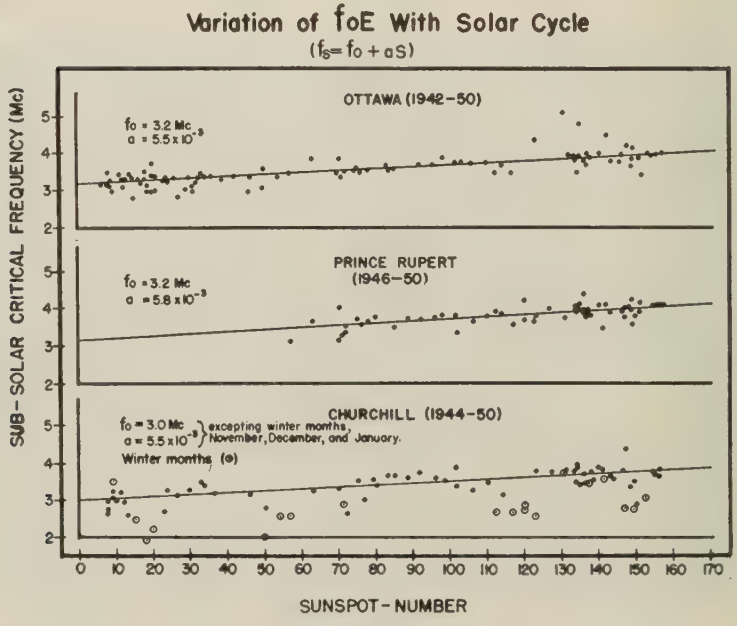

FIG. 14—THE DEPENDENCE OF THE SUB-SOLAR CRITICAL FREQUENCY ON THE 12-MONTH RUNNING AVERAGE SUNSPOT-NUMBER

The solar-cycle variation

For convenience, a plot of the 12-month running average sunspot-number is included in Figure 13. The seasonal-variation curves of f_s and of n clearly show a dependence on the solar cycle. To obtain a quantitive measure of this dependence, the monthly mean values of f_s have been plotted against the 12-month running average sunspot-number. Figure 14 shows such plots for Ottawa, Prince Rupert, and Churchill over the period of operation of these stations.

An approximately linear relationship is apparent, which we write $f_s = f_0 + aS$. The variation of the sub-solar critical frequency with sunspot-number is measured

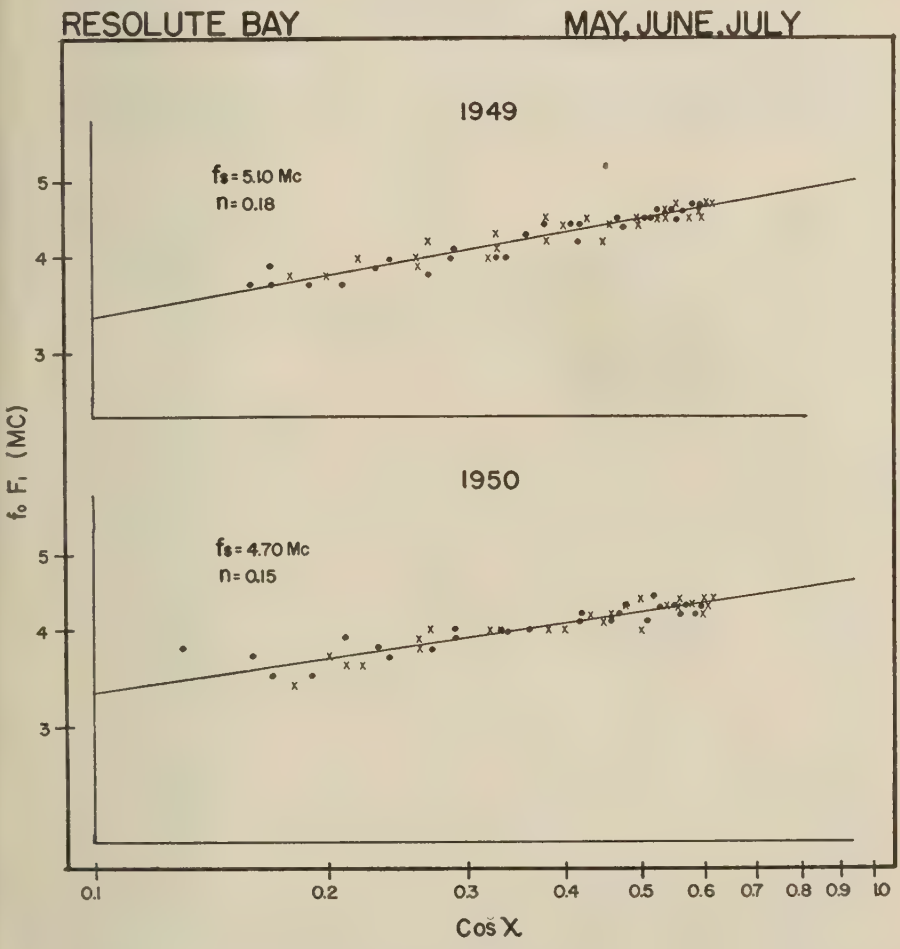

FIG. 15—THE CHAPMAN RELATIONSHIP FOR THE F1 LAYER AT RESOLUTE BAY ($\log f_0 F1 = \log f_s + n \log \cos X$)

by the slope, a, and has a value of about 5.5×10^{-3}. The value of the sub-solar critical frequency extrapolated to zero sunspot-number is f_0 and has a value of 3.2 Mc at Ottawa and Prince Rupert.

At Ottawa and Prince Rupert, the seasonal variations of f_0 and a were not significant. At Churchill, however, f_0 appears to be lower in the winter months. Excepting the months of November, December, and January, the dependence of f_s on sunspot-number is very similar to that at Ottawa and Prince Rupert. The circled points for the winter months show that for this period f_0 is near 2.2 Mc at Churchill.

The F1 layer

A regular $F1$ layer exists only during the summer daylight hours. Consequently, the relationship $f = f_s \cos^n \chi$ has been plotted for the $F1$ layer only for the months

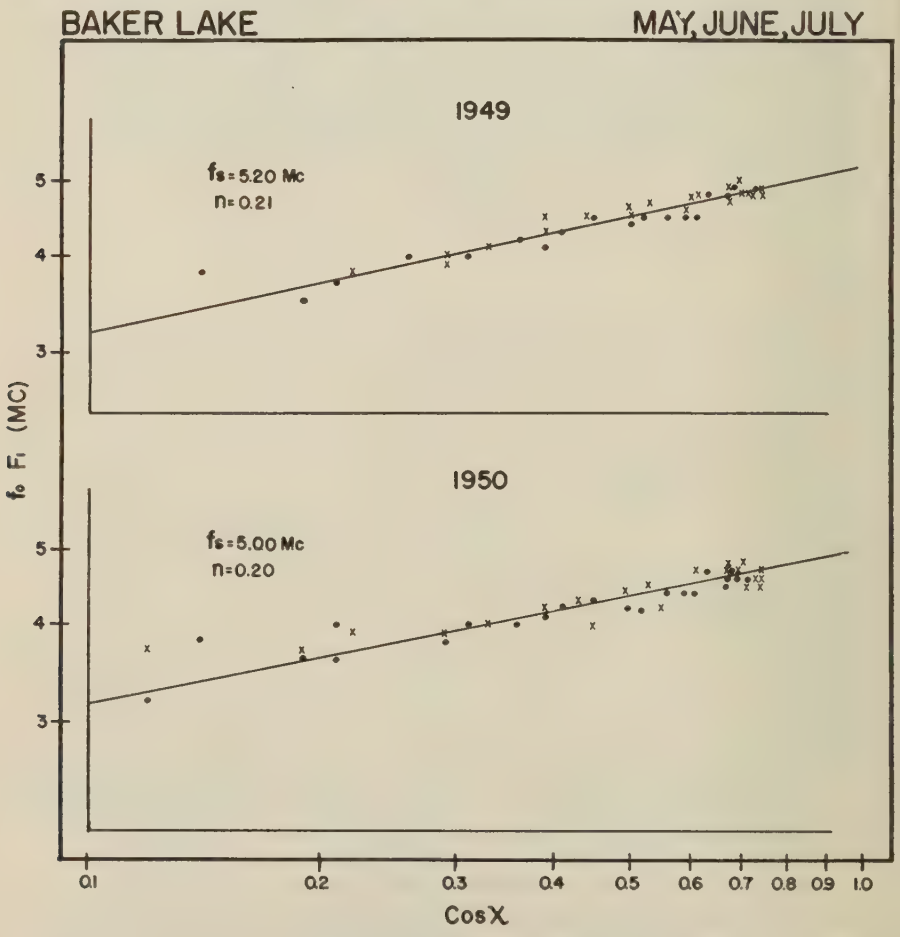

FIG. 16—THE CHAPMAN RELATIONSHIP FOR THE F1 LAYER AT BAKER LAKE

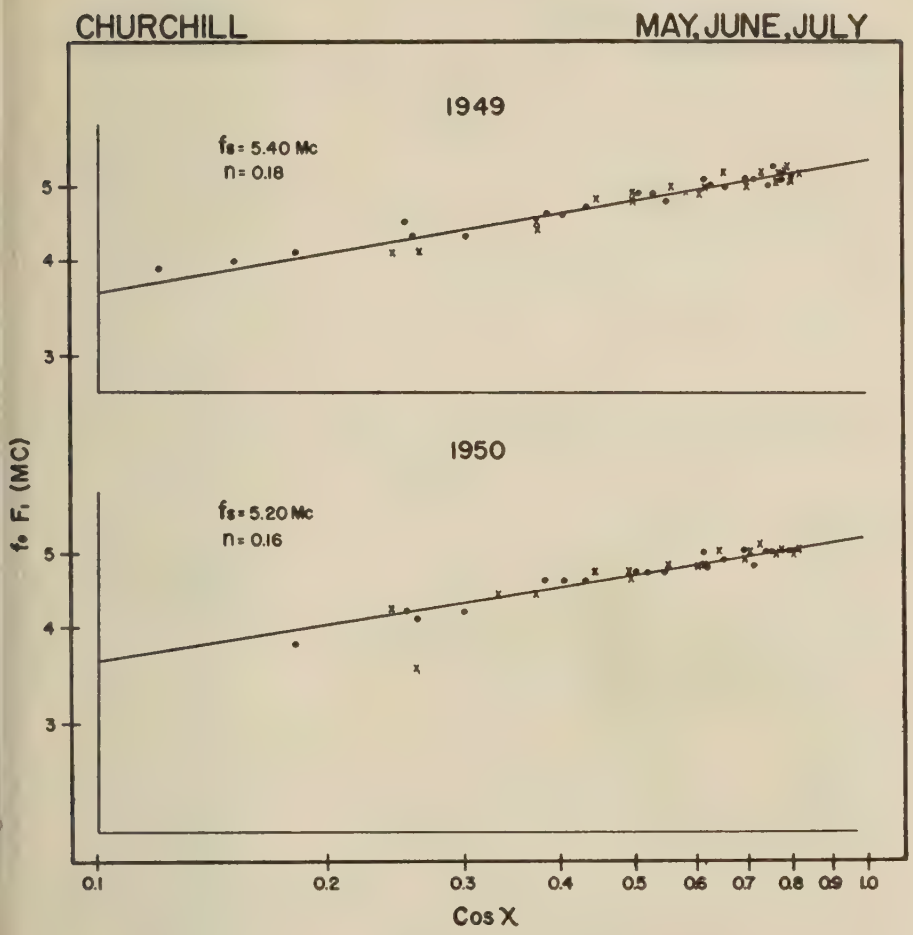

FIG. 17—THE CHAPMAN RELATIONSHIP FOR THE F1 LAYER AT CHURCHILL

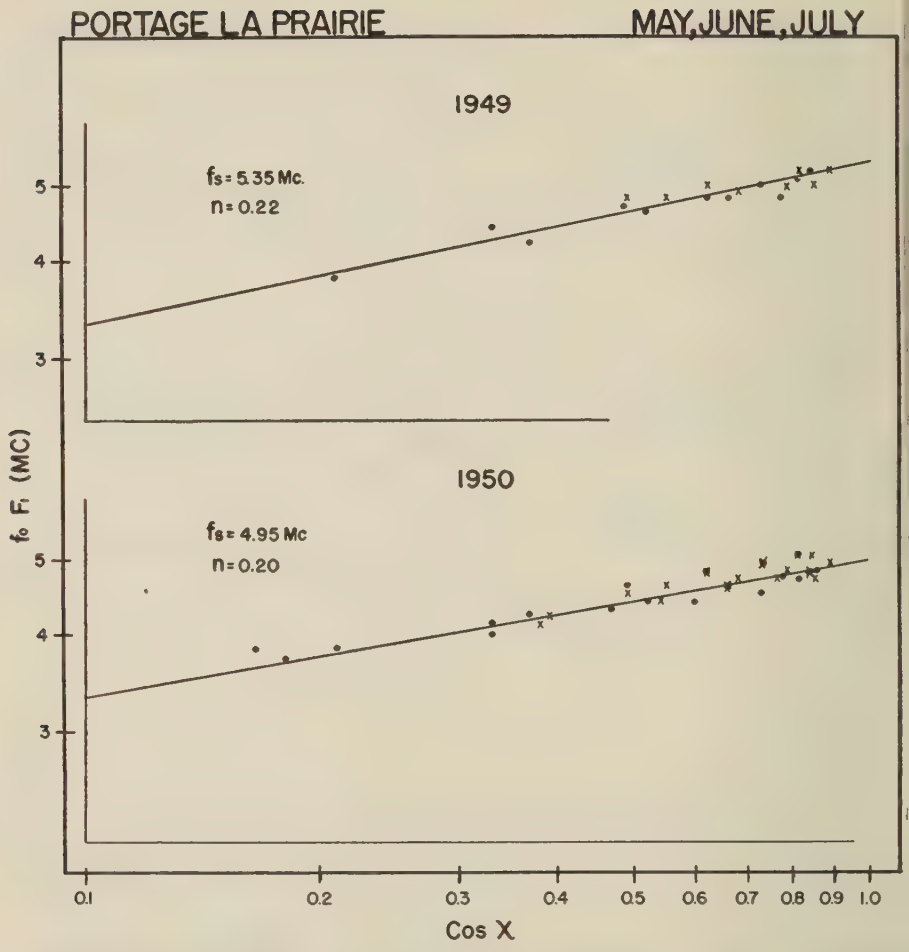

FIG. 18—THE CHAPMAN RELATIONSHIP FOR THE F1 LAYER AT PORTAGE LA PRAIRIE

of May, June, and July. In Figures 15, 16, 17, and 18, logarithmic plots of f_0F1 against cos χ are shown for Resolute Bay, Baker Lake, Churchill, and Portage la Prairie for 1949 and 1950 during this summer period. In Figure 19, similar plots for 1949, 1950, and 1951 are shown for Fort Chimo.

The curves indicate that in the arctic the $F1$ layer also behaves like a simple Chapman region, except that the sensitivity to solar angle is low at all stations from Resolute Bay in the far north down to the latitude of Portage la Prairie. Unlike the E layer, the $F1$ layer does not show a sharp drop in sensitivity at the auroral zone.

The sub-solar frequency f_s probably also depends on solar activity in the $F1$ layer as in the E layer. The average values for the stations measured were 5.27

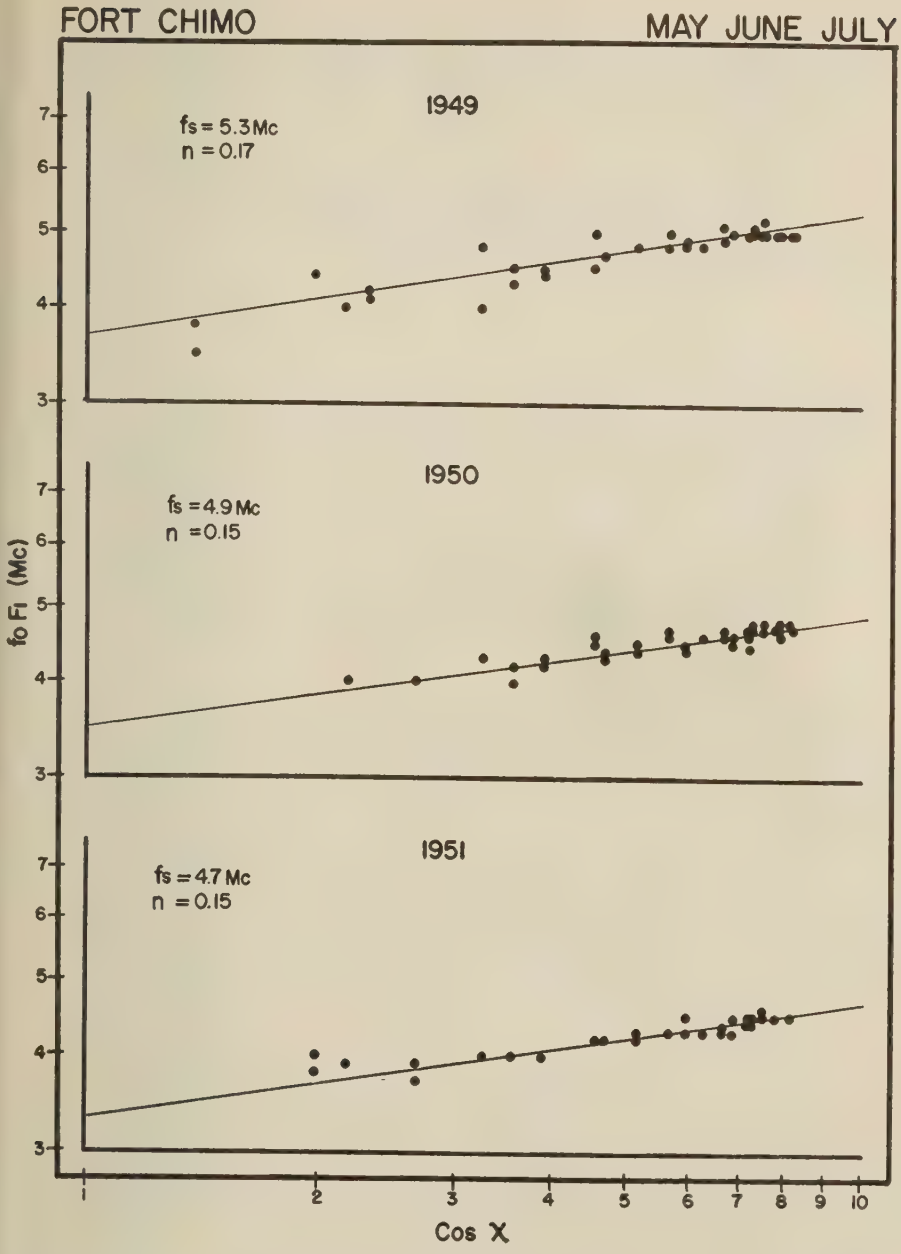

FIG. 19—THE CHAPMAN RELATIONSHIP FOR THE F1 LAYER AT FORT CHIMO

Mc in 1949 and 4.95 Mc in 1950. At Fort Chimo in 1951 the value had fallen to 4.7 Mc. The sensitivity to solar angle also decreases somewhat with solar activity, from an average value of 0.19 in 1949 to 0.17 in 1950. More comprehensive measurements on the $F1$ layer are now being made.

References

[1] S. Chapman, Proc. Phys. Soc. (London), **43**, 26 (1931).
[2] S. Chapman, Proc. Phys. Soc. (London), **43**, 483 (1931).
[3] J. N. Bhar, Indian J. Phys., **13**, 253 (1939).

DOUBLE-DOPPLER STUDY OF METEORIC ECHOES*

By L. A. Manning, O. G. Villard, Jr., and A. M. Peterson

Electronics Research Laboratory of the Department of Electrical Engineering, Stanford University, Stanford, California

(Received April 8, 1952)

ABSTRACT

The study of meteoric echoes is greatly facilitated by the use of a twin-channel Doppler presentation, by means of which both the amplitude and phase of the returned signal may be determined independently. Such a "double-Doppler" system has direct application to the verification of the mechanism of meteor-whistle formation, to the determination of the motion of ionization trails drifting under the influence of upper air winds, and to spectrum analysis of those echoes which exhibit amplitude fading. Examples of the application of the double-Doppler technique to these problems are presented.

I—*Introduction*

When considered from the most general point of view, the echoes returned from meteoric ionization columns require description in terms of both amplitude and phase. The amplitude of the echo is clearly dependent upon the range of the reflecting column, and upon the distribution of electron density throughout the column, including the variations with time related to the formation and decay of the trail. The phase of the reflected signal must be measured in relation to the phase of the transmitted wave. The value of phase is dependent upon the total path length to the receiver from the transmitter, by way of the reflecting column. It is dependent upon motions of the column which may alter the effective length of the wave path, including variations which may result from changes in ionization distribution.

Pulsed transmitters are well adapted to the simple determination of echo amplitude. Continuous-wave systems, on the other hand, enable changes of the the phase of the received signal to be easily detected by comparison with an injected signal of the reference transmitted phase. To be of greatest utility in the study of meteoric reflections, a system is needed which simultaneously gives both the amplitude and phase of the received signal. A method of obtaining this information using a "double-Doppler" technique, applicable either to continuous-wave or pulse-Doppler systems, and a number of the important applications of the technique, will be presented.

*This work was supported jointly by the U. S. Navy Office of Naval Research and by the U. S. Army Signal Corps.

The need for a complex presentation of echo amplitude and phase became evident first in connection with the Doppler frequency recording of "meteor whistles." It was verified by the Stanford group during the Giacobini-Zinner meteor shower of 1946, that the passage of meteors was accompanied by a short-duration echo shifted in frequency by an amount generally falling within the audio spectrum [see 1 of "References" at end of paper]. This shift was believed to be a measure of the velocity of the meteoric particle. A theory was developed relating the rate of change of the Doppler frequency shift to the meteoric velocity [2]. The theory was based upon the concept, described by Skellett [3] and by Pierce [4], that the radius and density of the ionization column were large, with the diameter perhaps as great as one kilometer. Under these assumptions, geometrical optics would be useful in determining the amplitude and phase of the reflected signal, and diffraction effects would not be observed. Early in 1947, a number of plots of meteor-whistle waveforms were made, using whistles recorded by the continuous-wave technique employed during the Giacobini-Zinner shower [1]. The Doppler frequencies reduced from the oscillograms behaved as predicted by the theory, and confirmed our expectation that meteor speeds could be measured by the Doppler method.

Working with the pulse technique, an independent approach to the problem of determining meteoric velocities was described by Ellyett and Davies in a 1948 paper [5]. Their discovery of a diffraction fluctuation in the amplitude of the received echo demonstrated that, at least for many meteors, the trail diameter is no more than a few meters. Ellyett and Davies gave an analysis of the diffraction phenomenon which applies only to the amplitude of the received signal. However, if the received signal be regarded as a complex vector having both amplitude and phase, it is simple to extend their analysis in such a way as to predict the initial Doppler shift giving rise to the "meteor whistle," as well as to predict the subsequent "diffraction fluctuations." When this extension of the diffraction theory was completed, it was found that, to the first approximation, the same relation between Doppler frequency and meteor velocity was obtained as for the geometrical optics solution previously postulated. The one whistle waveform is but the derivative of the other as far as phase is concerned. For this reason, no distinction between the two theories was made in subsequent velocity studies by the Stanford group [6]. From a theoretical point of view, the distinction between the theories, especially in cases where the column radius might be intermediate, seemed of great importance. Instantaneous plotting of the vector amplitude and phase of the received echoes was originally undertaken with this objective in mind.

In the early continuous-wave recordings of Doppler effects, a new phenomenon was uncovered which we have called the "body Doppler." This effect is a small frequency shift in the echo signal which must be produced by velocities of the effective reflection point of the order of 100 meters per second. It has since been attributed to drifts of the ionization trails under the influence of upper atmosphere winds [7]. A complete description of the wind drift requires knowledge of the sense of the motion, whether to or away from the observer. A determination of the complex amplitude and phase of the echo was felt to be the simplest means of measuring this sense. The direction of rotation of the echo vector specifies the direction of motion of the reflector.

A further use of the double-Doppler, vector-echo presentation is based upon its ability to make available for study separately the components producing fading of an enduring meteor echo. It will be shown that it is possible to distinguish fading caused by amplitude variations from fading caused by the beating of separate echo components, and to obtain some knowledge of the frequency spectrum of the beating components.

II—*Vector properties of meteoric echoes*

By the time it has entered the input terminals of a radio receiver, the signal returned from a meteoric ionization column can be described by two quantities, amplitude and relative phase. The standard of comparison for the phase is most conveniently that of a signal of transmitted frequency. In Figure 1, the echo

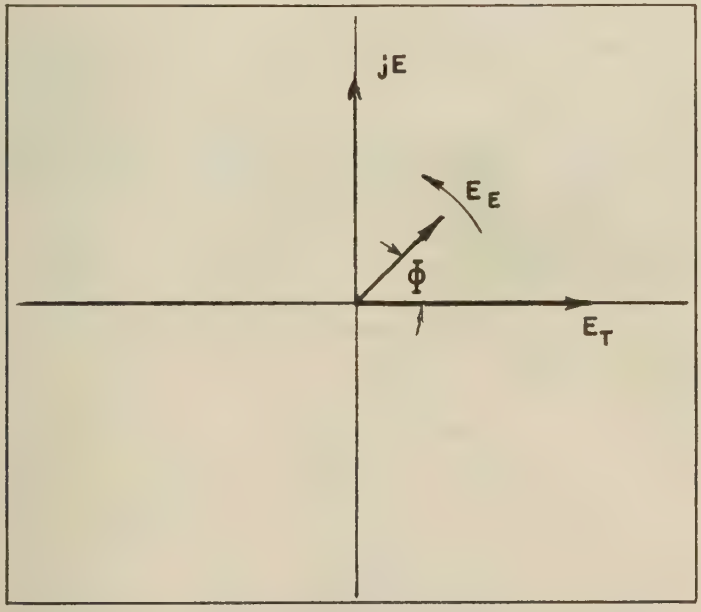

FIG. 1—VECTOR DIAGRAM SHOWING AN ECHO SIGNAL E_E AND THE QUADRATURE REFERENCE SIGNALS E_T AND jE_T

signal E_E is shown plotted as a vector, its phase Φ being relative to a signal E_T of transmitted frequency. If the echo signal has been subjected to a Doppler frequency shift f, the phase will be a function of time, so that $(d\phi/dt) = 2\pi f$. Using the elementary single-channel Doppler technique, the signals E_E and E_T are combined, and the amplitude of the difference signal $E_E - E_T$ is recorded. If the beating signal E_T is made much greater than E_E, notice that the alternating component of $E_E - E_T$ is equal to the projection of E_E along the X axis.

The rectangular component of the vector E_E in the E_T direction is obtained

by beating E_E with E_T . It is evident that by beating E_E with another signal, jE_T , the other rectangular component of E_E can be obtained. If the received signal E_E is combined separately with both E_T and the signal jE_T , a "double-Doppler" receiving system is created. This system has two output channels which represent two quadrature rectangular components of the received vector E_E .

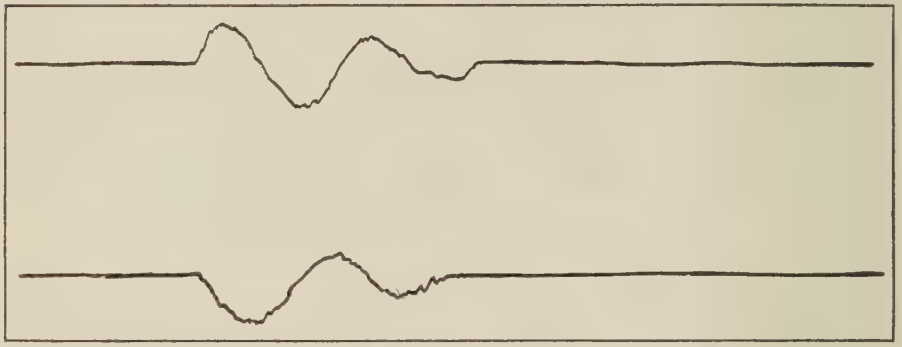

FIG. 2—A SIMPLE METEOR ECHO RECORDED ON THE DOUBLE-DOPPLER CHANNELS; THE REGULAR DOPPLER FREQUENCY SHIFT IS CAUSED BY WIND DRIFT OF THE TRAIL

Note the 90° phase shift between the Doppler components in the two channels. The direction of rotation of the echo vector may be inferred by noting which channel (rectangular component) has the leading phase.

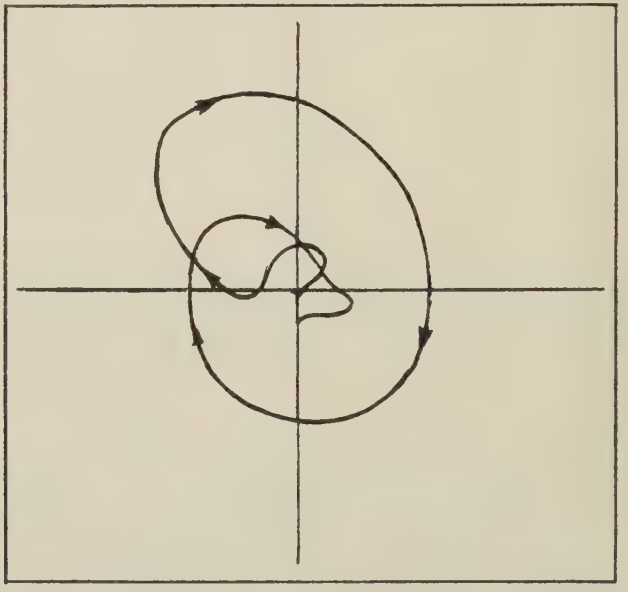

FIG. 3—THE ECHO OF FIGURE 2 RECORDED IN POLAR FORM BY AN OSCILLOSCOPE

Alternatively, the two quadrature receiver channels may be applied to the x and y plates of an oscilloscope, so that the excursions of the tip of the echo vector may be traced out as a polar plot of amplitude and phase. Figure 3 shows an example of the resulting presentation.

III—*Application to meteor whistles*

The theory first used in the analysis of the Doppler effect associated with the formation of a meteoric ionization column was based upon the assumption that the phase of the received echo is dependent only upon the path length to the nearest portion of the ionization column [2]. Physically, such an assumption is justified in two cases: first, if the ionization is confined to the vicinity of a moving point; second, if the trail is of half-infinite length, and is densely ionized throughout such a diameter in wavelengths that a single "reflection point" can be determined by geometrical optics. In contrast, if the trail is assumed weakly ionized, or of small diameter, over a great length, the phase of the received echo is dependent upon integration of elementary signals scattered from the whole of the trail.

Consider first that the ionization column can be correctly represented by a single moving reflection point. If the perpendicular range to the trail is D, and if the meteor is traveling with velocity V, the observed Doppler frequency shift was shown to be [2] $f = -2v^2t/\lambda D$ when $|V| \ll D$. The time t is measured from the moment the meteor arrives at O, and λ is the wavelength in the medium. By inte-

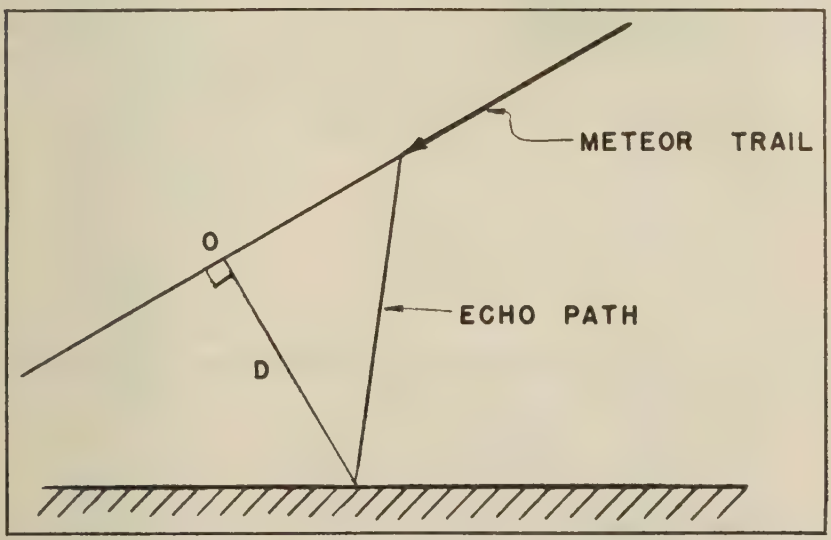

FIG. 4—GEOMETRY OF REFLECTIONS FROM A METEOR TRAIL

grating the expression for Doppler frequency shift with respect to time, the relative phase of the complex vector reflected wave can be obtained. Based upon either the moving ball, or the large-column geometrical optics assumption, then, the

vector received signal will be

$$Eg = A(t) \exp [-i2\pi v^2 t^2/\lambda D] \quad (1)$$

Notice that $A(t)$, the amplitude variation, is not determined. For a moving ball reflector, A will be determined by the variation of ionization production with time. For the large-column geometrical optics reflector, $A(t)$ will depend upon the convexity of the reflection surface at the reflection point. Equation (1) assumes that no component of Doppler shift need be considered to result from trail expansion; differently expressed, (1) assumes no changes in path length result from change in position of the reflection point on the column.

An alternative description of the returned signal may be formulated if different physical assumptions are made with respect to column shape. If the column diameter be assumed small in wavelengths, it must be assumed that each element of path length is effective in returning a signal to the receiver. Taking the signal from the element between vt and $v(t + \mathrm{d}t)$ as

$$E = K \exp [-i(2\pi v^2 t^2)/\lambda D] \, dt \quad (2)$$

the total signal received on diffraction theory will be

$$E_d = K \int_{-\infty}^{t} \exp -i(2\pi v^2 t^2)/\lambda D \, \mathrm{d}t \quad (3)$$

Although the lower limit of integration is infinity, it has been assumed that $|vt| \ll D$, so that the amplitudes of signal returned from each element $v\mathrm{d}t$ are

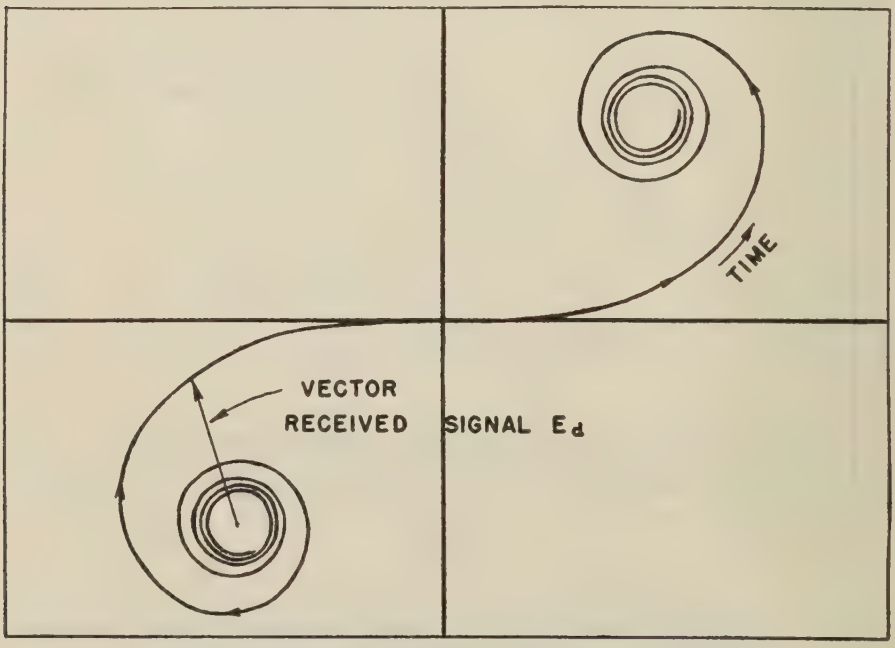

FIG. 5—THEORETICAL CORNU SPIRAL

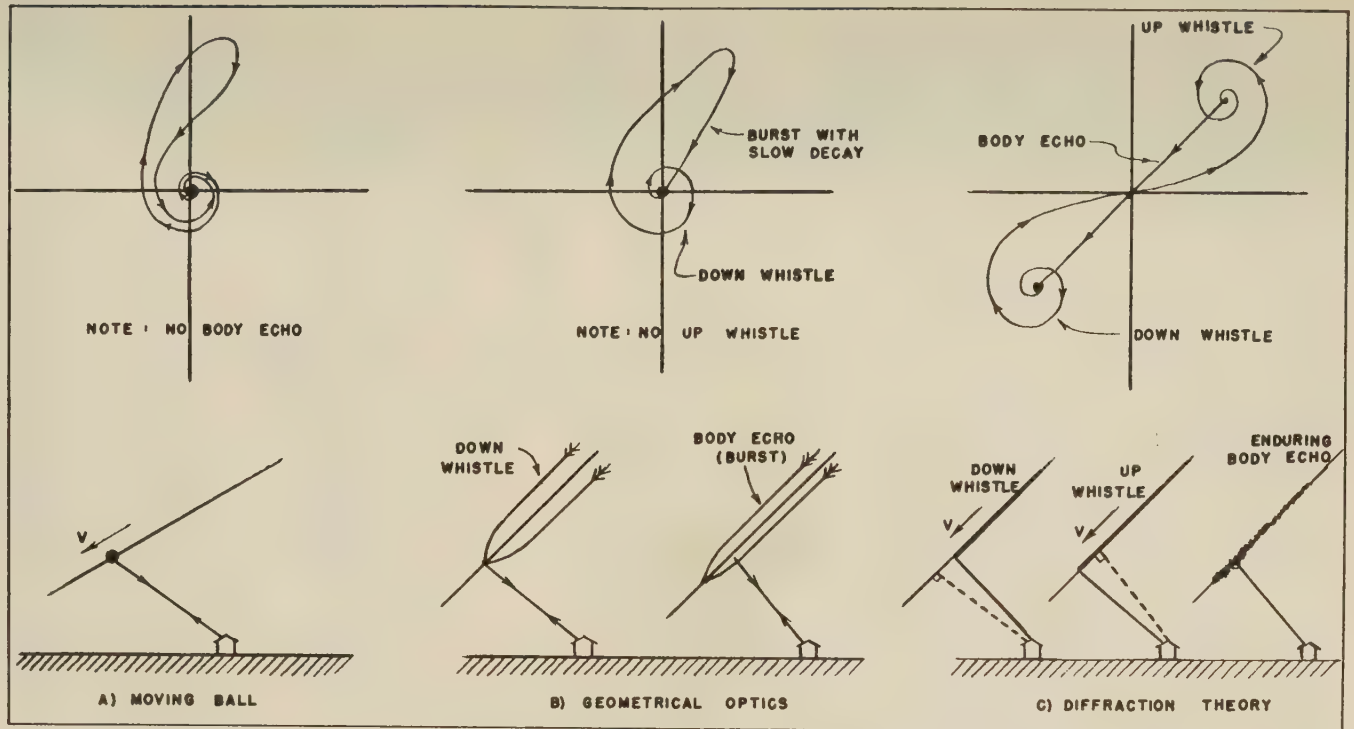

FIG. 6—PREDICTED PLOTS OF VECTOR RECEIVED-SIGNAL STRENGTH FOR THREE IONIZATION DISTRIBUTION MODELS; POSSIBLE TRAIL EXPANSION AND WIND-DRIFT EFFECTS ARE NEGLECTED

equal. The component of the integral resulting from large negative t is negligible. The constant K depends upon range, transmitted power, antenna gains, etc.

It will be seen that, neglecting amplitude variation, the Doppler waveform predicted by the diffraction theory of (3) is just the time integral of the waveform (1) of geometrical optics. Since the frequency of a sine waveform is not changed by integration, to the first approximation it is irrelevant whether formula (1) or (3) is used in velocity analysis.

The real and imaginary parts of (3) would be the cosine and sine Fresnel integrals of the argument $2vt/\sqrt{\lambda D}$, if the lower limits were zero rather than infinity. As a result, the vector E_d describes a cornu spiral as shown in Figure 5, but with E_d measured from the center of the lower spiral instead of from the origin.

The vector received-signal strength predicted by diffraction theory, and plotted in Figure 5, may be compared with predictions based on the moving ball and geometrical optics assumptions of equation (1). In the two latter cases, the exact shapes of the curves will depend on the nature of the amplitude variation. However, a clear distinction between the three cases does exist in terms of the vector diagram. As shown in Figure 6, the vector representing the moving bal lease does not sustain its amplitude after the vaporization of the meteoric particle. There is no body to the echo, and the up whistle appears as a "rewrapping" of the spiral about the zero amplitude point.

In the large-column geometrical optics case, it is the up whistle which is not

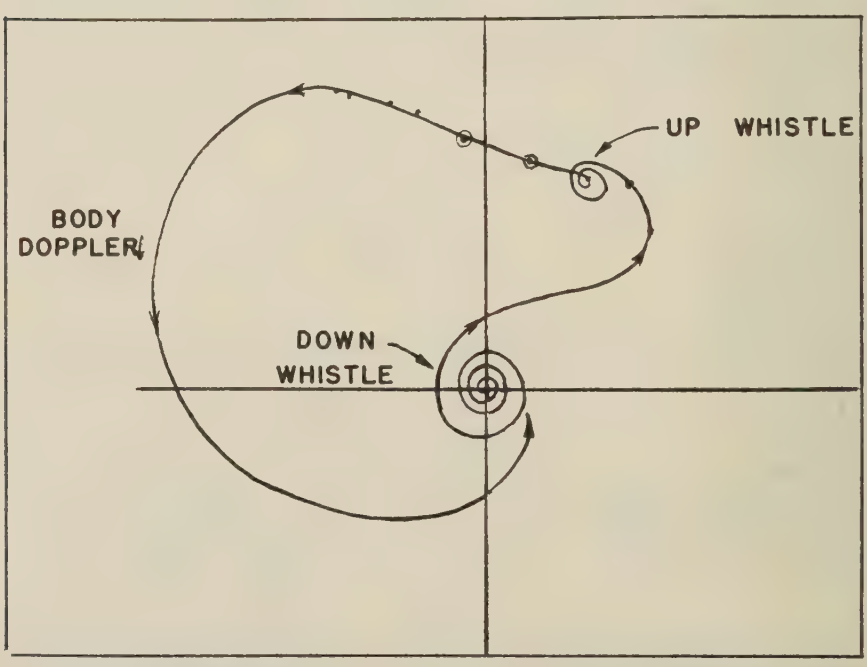

FIG. 7—VECTOR PRESENTATION OF AN ECHO SHOWING BOTH WHISTLE AND BODY-DOPPLER EFFECTS

observed. After the nose of the column passes the perpendicular point, the geometrical reflection point is fixed, except for possible shifts caused by trail expansion or wind drift. A long-duration "burst" or "body echo" is received as the trail gradually decays.

In the diffraction case, a down whistle, up whistle, and body echo will be expected. The distinguishing feature is the isolated coil of the spiral representing the up whistle [8].

Experimental plots of vector echo strength generally most nearly resemble the predictions based upon diffraction theory. Figure 7 shows an example of a meteor reflection observed on a frequency of 23.1 Mc, which exhibits a very common behavior. It will be noted that the initial down-whistle is followed by an up whistle much as predicted by diffraction theory. Following the whistle, a further brief increase in amplitude occurs, presumably as a result of trail expansion. During the decay period, a Doppler shift, the "body Doppler," is caused by wind drift of the trail. When the amplitude and body-Doppler effects are removed, as in

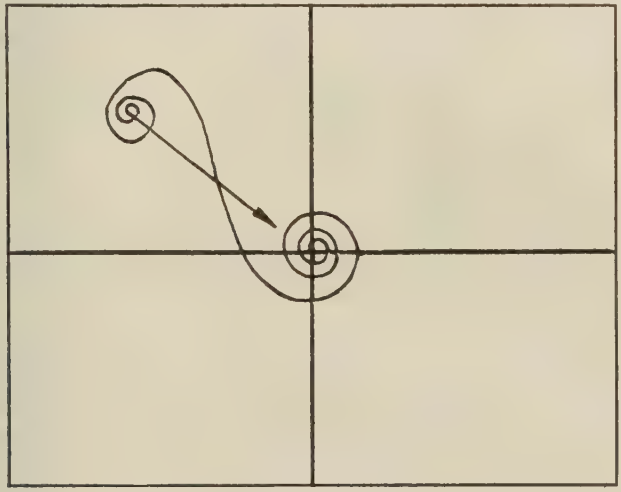

FIG. 8—THE ECHO OF FIGURE 6 WITH THE BODY-DOPPLER FREQUENCY SHIFT SUBTRACTED OUT; COMPARE THIS RECORD WITH THE THEORETICAL CORNU SPIRAL OF FIGURE 5

Figure 8, a good resemblance to the cornu spiral of Figure 5 is seen. Recorded whistles frequently exhibit inferior amplitude in the up-whistle portion of the spiral in comparison with that of the down whistle. It is partly because of this effect that velocity study using the continuous-wave Doppler technique, which reveals the down whistle, is superior to pulse amplitude techniques which depend entirely upon the up-whistle "diffraction fluctuations." Continuous-wave records have been obtained in which as many as 250 oscillations of the down whistle can be discerned.

IV—*Application to wind drift*

When the first Doppler recordings of meteor echoes were made using recorders with good low-frequency response, a constant-frequency Doppler shift was discovered following the meteor whistle, and persisting for the duration of the echo. This low-frequency shift was named the "body Doppler." It has since been shown that the body Doppler is a measure of the drift of the fully-formed ionization trail which results from the action of ionospheric winds [7].

In order to fully utilize the body-Doppler effect, it is necessary to be able to distinguish between a positive frequency shift corresponding to motion towards the observer, and a negative shift corresponding to motion away from the observer. The actual magnitude of the shift is usually between ± 15 cycles per second on a 23-Mc carrier. Vector presentation of the received echo has been found a most convenient way to observe the direction of the shift. Since a positive frequency shift corresponds to a positive rate of change of phase, and negative shift

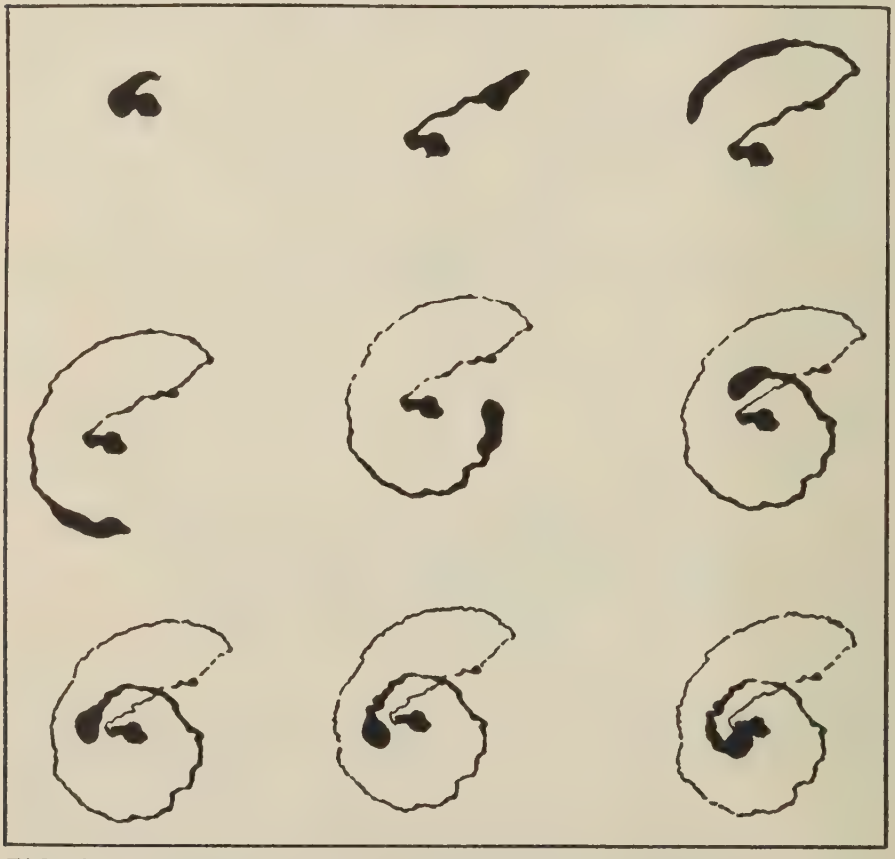

FIG. 9—MOTION-PICTURE SEQUENCE SHOWING VECTOR DISPLAY OF A SIMPLE ECHO

similarly to a negative rate of change of phase, the direction of revolution of the spot representing the tip of the reflected-wave vector is a most simple index of sense of motion.

In Figure 9 is a sequence of motion-picture frames showing the formation of a meteor echo as observed on the vector oscilloscope display. The camera was operated at 16 frames per second, and a long persistence screen was used. It will be noticed that the direction of revolution of the spot is easily determined. The pulse repetition frequency of the pulse-Doppler system used in obtaining the record was not high enough to reveal the cornu spiral, although good definition is obtained in the wind shift and decay portion of the echo.

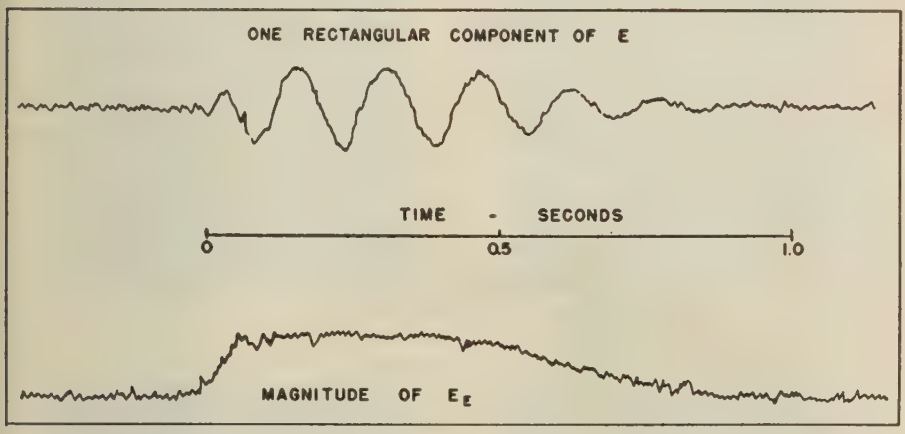

FIG. 10—A METEOR ECHO HAVING NO AMPLITUDE FADING

Another presentation of the behavior of the echo vector during a body Doppler which illustrates the effects involved in a simple wind record is shown in Figure 10. In this Figure, the body-Doppler beat corresponding to the wind motion is clearly evident in the rectangular component of the echo vector, shown in the upper trace. The lower curve is a representation of the magnitude of the reflection

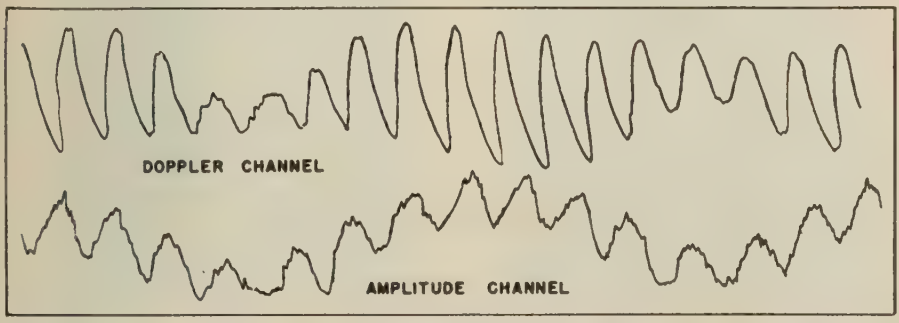

FIG. 11—A PORTION OF A LONG-DURATION METEOR ECHO EXHIBITING AMPLITUDE FADING; NOTE INDEPENDENCE OF DOPPLER AND FADING FREQUENCIES

vector. The fact that the body-Doppler effect as observed in a single channel is in no way the result of amplitude fading is clearly seen. Records of the simple type shown in Figure 10 are used in the wind studies.

V—*Analysis of echo fading*

Vigorous fading of meteor echoes has been apparent in the earliest observations of nearly all investigators. Not all echoes fade, and the fraction which does fade varies markedly from night to night. In general, the longer-duration echoes do exhibit fading. In Figure 11 is shown a record similar to that of Figure 10, but for a fading echo. Again, it is clear that a body-Doppler frequency exists independently of either of the two fading rates.

In seeking an explanation of the cause of the fading effect, one is led first to distinguish between an amplitude modulation of the echo intensity, and an amplitude fluctuation resulting from the beating of two or more separate echo components. The polar plot of the echo vector makes it possible to resolve this question. Figure 12 shows portions of such plots for four fading meteors. It will be noted that the amplitude changes are intimately associated with a reversal of the instantaneous Doppler frequency in the loops. This type of pattern is easily explained as the resultant of two vectors of unequal amplitude and rotational speed, but is inconsistent with an amplitude modulation. The explanation of fading, therefore, must be sought in some mechanism which will return two or more echoes, each with its own independent Doppler frequency shift.

Some information on the spectrum of energy returned in a complex fading echo can be obtained by inspection of the vector waveforms. Consider Figure 12. The waveforms may be interpreted as consisting of two components. The stronger component, say F_1 , determines the average rate of rotation. From the shape of the loops, which point out in these examples, it is seen that the weaker beating component, F_2 , must have a negative frequency shift with respect to the stronger component. The beat frequency $\Delta F = F_2 - F_1$ is the frequency of fading, so that in these rather simple cases the echo spectrum may be easily reconstructed. It will be recognized that the spectrum is not exactly defined, and that the components decay with time. In more complex cases, where more than two components may exist, the analysis is overly complex.

More generally, the spectrum of echo signals may be determined by Fourier analysis of the echo vector. A definite limitation is placed upon the precision of the results by the finite duration of the echo, and by variations in component amplitude with time. The durations of meteor echoes are usually barely adequate to provide resolution between spectral components separated by the lower fading frequencies.

It will be assumed that the echo signal E is expressed in terms of its complex amplitude and phase, in the form

$$E = A(t)e^{j\phi(t)} = A(t)\cos\phi + jA(t)\sin\phi \quad \ldots\ldots(4)$$

Call the two rectangular components of (4) E_c and E_s , so that

$$E = E_c + jE_s \quad \ldots\ldots(5)$$

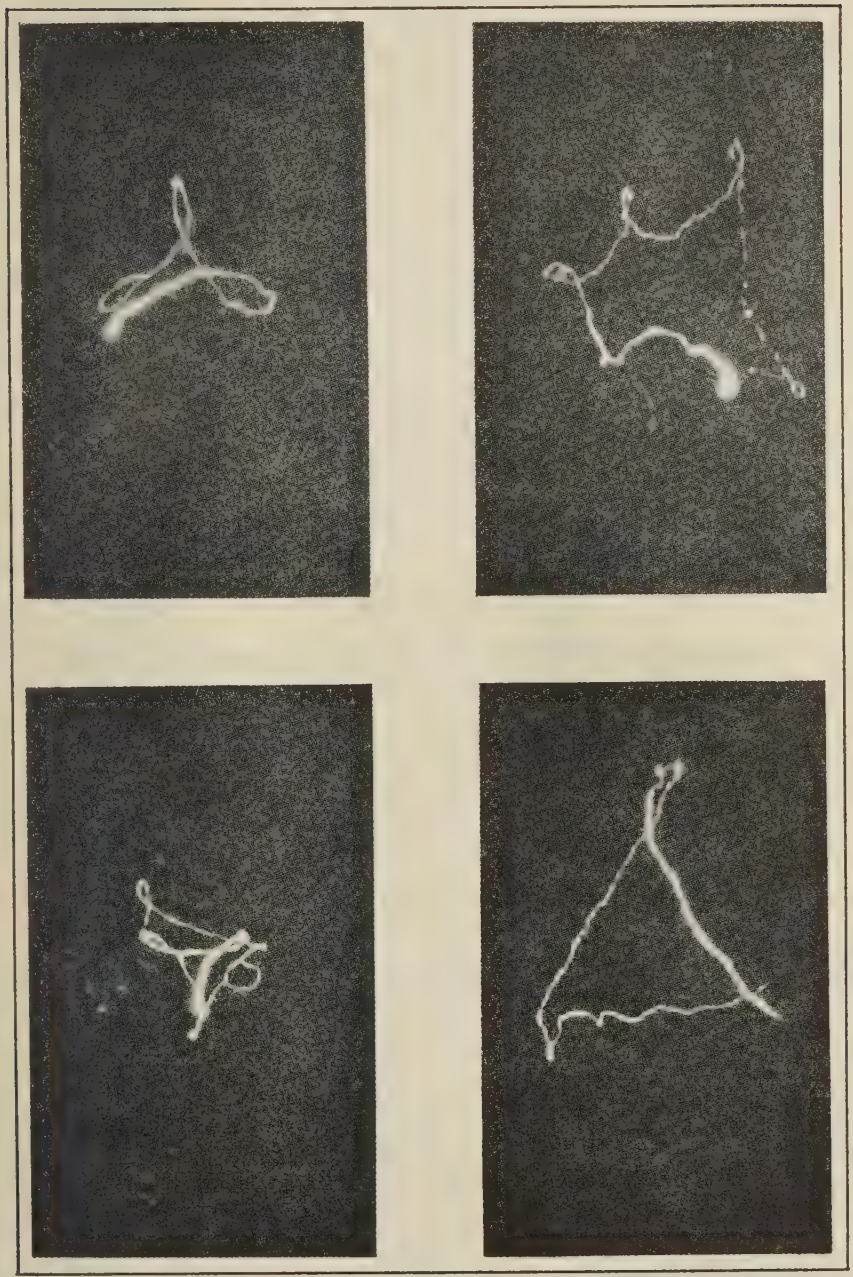

FIG. 12—EXAMPLES OF FADING ECHOES SHOWN BY THE VECTOR DISPLAY

In terms of calibration procedure, E_c is the receiver channel in which a signal with a single sinusoidal component will lead in phase, when the echo frequency is greater than the carrier frequency. In order to define in some way the spectrum we are trying to determine, it will be necessary to make an assumption which will be, in practice, the weakest link in the procedure. Assume that during the duration of the echo,

$$E = \sum_i A_i e^{j\omega_i t} \quad \ldots\ldots\ldots\ldots\ldots\ldots\ldots\ldots\ldots\ldots (6)$$

In other words, the received signal is made up of a number of constant amplitude side-frequency components. The assumption is not quite as bad as it sounds, since fading echoes tend to be of relative fixed peak amplitude during much of their duration, but in many cases, where the fading components are of different duration, this type of spectrum analysis necessarily becomes crude. Another factor affecting the method is the modulation of the spectrum by the echo amplitude, even when considered constant for the duration T. The initial rise and fall of amplitude broadens the component frequency spectra to such an extent that the resolution in terms of Doppler frequency is of the order $1/T$. With the limitations in mind, the analysis proceeds as follows: From (6),

$$(E_c + jE_s)e^{-j\omega t} = \sum_i A_i e^{j(\omega_i - \omega)t}$$

and if we integrate over the duration of the meteor, orthogonality will take effect, whenever $\omega = 2\pi n/T$, where T is the echo duration.

$$\left.\begin{aligned} A_i = \frac{1}{T}\Bigg(\int_0^T E_c \cos\omega_i t\, dt \pm \int_0^T E_s \sin\omega_i t\, dt \\ + j\int_0^T E_s \cos\omega_i t\, dt \mp j\int_0^T E_c \sin\omega_i t\, dt\Bigg) \end{aligned}\right\} \quad \ldots\ldots\ldots (7)$$

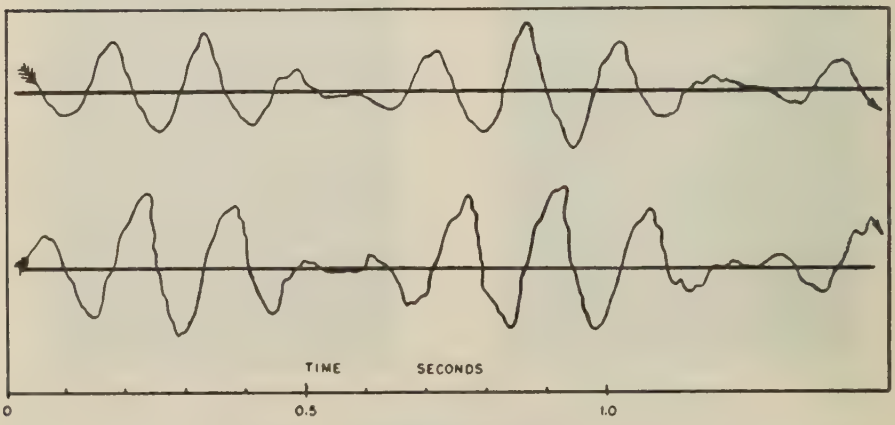

FIG. 13—PORTION OF A DOUBLE-DOPPLER RECORDING OF A FADING ECHO

where the upper sign gives the amplitude of the positive Doppler frequency component, and the lower sign the amplitude of the negative Doppler frequency component; by definition, E_c and E_s are two rectangular components of E, such that a positively revolving vector produces a waveform in E_c leading that in E_s. The magnitude of A_1 gives the magnitude of the side frequency ω_1, while its phase is that of the side frequency at time $t = 0$, relative to that of the E_c channel.

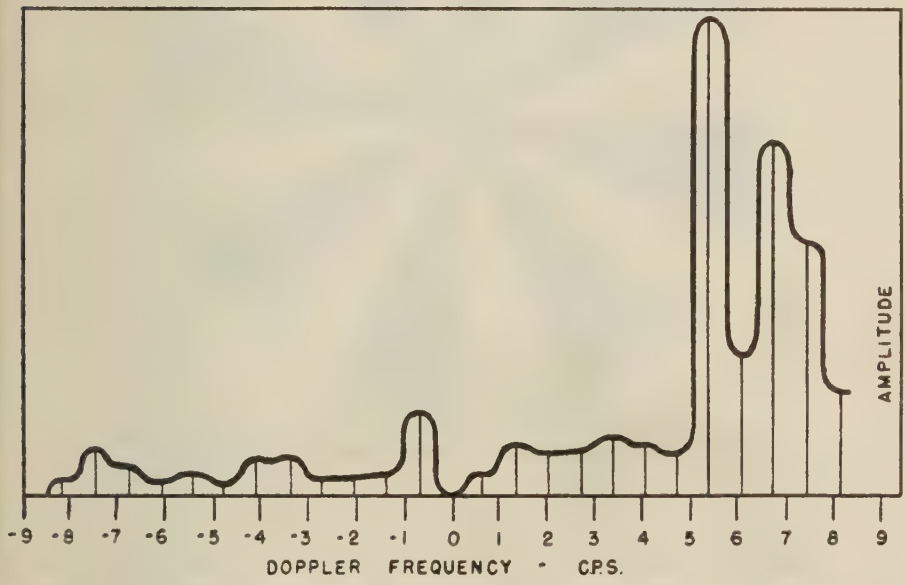

FIG. 14—DOPPLER FREQUENCY SPECTRUM OF THE ECHO IN FIGURE 13

In Figure 13 is shown an example of a complex fading echo; in Figure 14 is the frequency spectrum deduced using equation (7).

VI—*Automatic Doppler frequency recording*

One of the attractive features of the vector presentation of echo waveforms is that a much quicker determination of Doppler frequency can be made. Frequency shift is determined by the angular velocity of the spot on the cathode-ray tube screen, and it is not necessary to await a complete cycle of the body Doppler in order to obtain a measure of trail drift. With the aid of photoelectric monitoring of the screen, it is relatively simple to obtain automatic multiplication and recording of the Doppler shift. Suppose the mask shown in Figure 15 is placed in front of the oscilloscope screen, and the light from the revolving spot picked up by a photocell. A square wave output will be obtained of fundamental frequency six times the Doppler frequency shift. By applying such an output to a frequency meter, it has been possible to automatically record body-Doppler frequencies without the necessity of utilizing a time as great as the body-Doppler period.

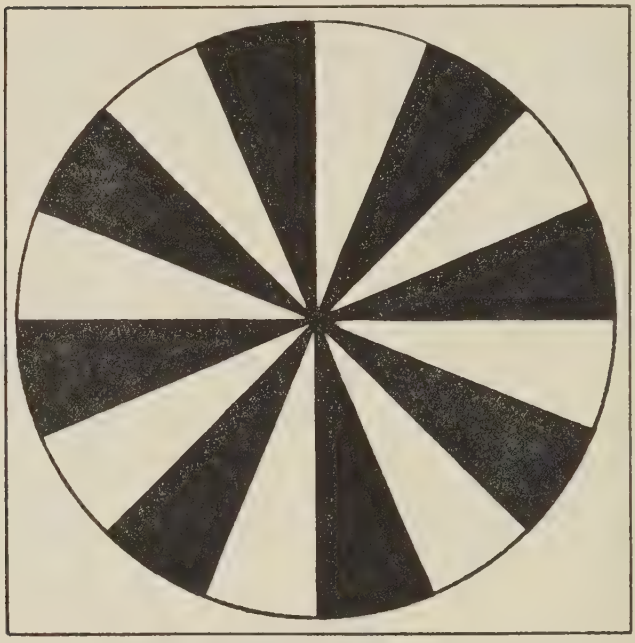

FIG. 15—FREQUENCY MULTIPLYING MASK

Recording of this nature is a considerable help in reducing the large masses of data which accumulate in wind studies.

It is interesting to note the extremely fine resolution which the Doppler technique affords with respect to motions of the column. Using the vector presentation, phase changes of 5° can be measured conservatively. At a wavelength of 13 meters, such an observed change in phase corresponds to a motion of the reflector of only 9 cm. A change in the range of a 120-km meteor of only 0.0001 per cent is thus detectable. The advantage with respect to pure pulse techniques is obvious.

VII—*Conclusions*

The signal returned from a meteoric ionization column is characterized by both amplitude and phase. Neither pulse techniques nor simple single-channel Doppler methods of investigation provide a recording of both of these quantities simultaneously. By using a double-Doppler receiving technique, the true vector nature of the received echo is revealed.

As applied to the determination of meteoric velocities, the double-Doppler technique enables plots of the Cornu spirals predicted by diffraction theory to be obtained experimentally. Confirmation is thus obtained of the assumption of that theory, that each element of the trail adds to the signal.

Application of the double-Doppler technique to study of the frequency shift during the body of the echo, which results from wind drift of the trail, removes the ambiguity in the sense of the drift. The technique serves also to facilitate automatic recording of the shifts.

In the case of those complex echoes with amplitude fluctuations, analysis of the double-Doppler records demonstrates the fading to result from the beating of two or more components of reflected signal. Spectrum analyses of the frequency components producing a complex record can be carried out using these data.

The use of double-Doppler reception enables a more complete picture of the received signal to be obtained, a picture which is essential for many of the analyses and applications of meteoric phenomena.

References

[1] L. A. Manning, R. A. Helliwell, O. G. Villard, Jr., and W. E. Evans, Jr., On the detection of meteors by radio, Phys. Rev., **70**, 767–768 (1946).

[2] L. A. Manning, The theory of the radio detection of meteors, J. App. Physics, **19**, 689–699 (1948).

[3] A. M. Skellett, The ionizing effect of meteors in relation to radio propagation, Proc. Inst. Radio Eng., **20**, 1933 (1932).

[4] J. A. Pierce, Abnormal ionization in the *E*-region of the ionosphere, Proc. Inst. Radio Eng., **26**, 892–902 (1938).

[5] C. D. Ellyett and J. G. Davies, Velocity of meteors measured by diffraction of radio waves from trails during formation, Nature, **161**, 596–597 (1948).

[6] L. A. Manning, O. G. Villard, Jr., and A. M. Peterson, Radio Doppler investigation of meteoric heights and velocities, J. App. Physics, **20**, 475–479 (1949).

[7] L. A. Manning, O. G. Villard, Jr., and A. M. Peterson, Meteoric echo study of upper atmosphere winds, Proc. Inst. Radio Eng., **38**, 877–883 (1950).

[8] D. W. R. McKinley, Meteor velocities determined by radio observations, Astroph. J., **113**, 225–267 (1951).

THE RELATION BETWEEN ELECTRICAL AND DIFFUSION CURRENTS

By M. H. Johnson*

United States Naval Research Laboratory, Washington 25, D. C.

(Received April 25, 1952)

ABSTRACT

A linear relation between the electrical current through a gaseous conductor in a magnetic field and the diffusion currents of the charge bearing particles is deduced from the kinetic theory of diffusion. For conduction by positive ions and electrons, a magnetic field does not alter the diffusion currents parallel to the electrical current, but does move the ions and electrons together transversely to the electrical current and to the magnetic field. The presence of additional negative ions can enhance transverse electronic diffusion and causes new components of the diffusion currents to appear along the magnetic lines of force. By this linear relation, the vertical lunar displacements of the *E*-layer are derived from the lunar current system in the ionosphere. The derived amplitudes and phases can account for the observed motions on the hypotheses that the main lunar current flows in the lower part of the *E*-layer and that approximately equal numbers of negative ions and electrons are present at the point of observation.

Introduction

Martyn[1] has shown that electric fields generated by horizontal air motions through the earth's magnetic field can cause vertical displacements of ions and electrons in the ionosphere, and has attempted to relate the displacements to air velocities. The global system of electromotive forces, induced by winds, establishes a current density, **j**, and concomitant polarization electric field, **E**, throughout the ionosphere. The calculation of **j**, or **E**, from a given distribution of air velocities, taking into account the anisotropic conduction in the earth's magnetic field, is a fundamental problem of the dynamo theory that has not yet been satisfactorily solved.

Our uncertain knowledge of upper atmosphere winds, as well as the difficulty just mentioned, led us to try to interpret the observed vertical displacements without recourse to the dynamo theory. From the kinetic theory of diffusion, we deduce a linear relation between **j** and the vertical electron diffusion current.

*Now at the Radiation Laboratory, University of California.

[1]D. F. Martyn, Proc. R. Soc., A, **190**, 273 (1947).

The diffusion current governs the vertical displacements of the electron layers, which we find may be downward, even though the diffusion current is upward. With a lunar current system inferred from temporal changes in the earth's magnetic field, we derive the lunar height variations in the E-layer. Both the amplitude and phase are consistent with observations if we assume the main lunar current flows in the lower part of the E-layer with a decreasing current density at higher altitudes and we assume the negative ion to electron ratio is about one at the point of observation.

CONDUCTION BY ELECTRONS AND POSITIVE IONS

According to kinetic theory, hydrodynamic equations govern the diffusion velocities, $\mathbf{v}_i$, of charged particles through a neutral gas.[2] Positive ions, electrons, and negative ions will be indicated by subscripts 1, 2, and 3, respectively. In the present application, the number density of the gas, n, is sufficiently large compared to y_i , the number density of charged particles, that the center of mass is at rest with respect to the gas and that the collisions between charged particles can be neglected.[3] The hydrodynamic equations become

$$e(\mathbf{E} + \mathbf{E}_e)y_1 + ey_1\mathbf{v}_1 \times \mathbf{H} = (kT/D_1)y_1\mathbf{v}_1 \quad \ldots\ldots(1a)$$

$$-e(\mathbf{E} + \mathbf{E}_e)y_2 - ey_2\mathbf{v}_2 \times \mathbf{H} = (kT/D_2)y_2\mathbf{v}_2 \quad \ldots\ldots(1b)$$

where $\mathbf{E}_e$ is the electromotive force generated by winds[4] and $\mathbf{v}_i$ are now relative to the neutral gas. The terms on the right side, in which D_i is the binary diffusion coefficient for the charged particles in the neutral gas, are frictional forces from the collisions of the charged particles with the neutral gas. The electrical current density, $\mathbf{j}$, is expressed in terms of the diffusion currents, $y_i\mathbf{v}_i$, by

$$\mathbf{j} = e(y_1\mathbf{v}_1 - y_2\mathbf{v}_2) \quad \ldots\ldots(2a)$$

and the condition of electrical neutrality requires

$$y_1 = y_2 \quad \ldots\ldots(3a)$$

According to the foregoing equations the electronic diffusion current,, $y_2\mathbf{v}_2$ can be expressed as a linear vector function of $\mathbf{H}$ (or of $\mathbf{n}$, a unit vector along $\mathbf{H}$) and $\mathbf{j}$, that is

$$ey_2\mathbf{v}_2 = K_0\mathbf{j} + K_a\mathbf{n}(\mathbf{n}\cdot\mathbf{j}) + K_t\mathbf{j} \times \mathbf{n} \quad \ldots\ldots(4)$$

The terms in Eq. (4) with the factors K_0 , K_a , and K_t will be called parallel, axial, and transverse diffusion currents, respectively. Putting $\lambda_i = (eHD_i)/(kT)$, the elimination of $\mathbf{E} + \mathbf{E}_e$ and $\mathbf{v}_1$ from the equations of the previous paragraph gives

[2]M. H. Johnson, Phys. Rev., 84, 566 (1951); M. H. Johnson and E. O. Hulburt, Phys. Rev., 79, 802 (1950).

[3]T. G. Cowling, Proc. R. Soc., A, 183, 453 (1945). As the collision cross-section for ions is about 10^5 that for neutral atoms, collisions between ions do not become important until $y_i \cong n\ 10^{-5}$.

[4]The letters e, k, and T have their usual significance of electronic charge, Boltzman's constant, and absolute temperature.

$$K_0 = -\lambda_1(\lambda_1 + \lambda_2)^{-1} \quad (5a)$$

$$K_a = 0 \quad (5b)$$

$$K_t = \lambda_1\lambda_2(\lambda_1 + \lambda_2)^{-1} \quad (5c)$$

It is noteworthy that the magnetic field does not alter the parallel diffusion. The result can be seen directly by adding Eqs. (1*a*) and (1*b*) and applying Eqs. (2) and (3); whence the components of $\mathbf{v}_1$ and $\mathbf{v}_2$ parallel to $\mathbf{j}$ are in the ratio $-(D_1/D_2)$, just as in the absence of the magnetic field. Transverse diffusion stems from the necessity of balancing the ampere force, $\mathbf{j} \times \mathbf{H}$, by a frictional force from the motion of ions and electrons together through the gas. In directions perpendicular to $\mathbf{j}$, the condition of electrical neutrality, Eq. (2), constrains the ions and electrons to move together. Consequently, Eq. (5*c*) remains valid when the friction from collisions between electrons and ions is included in Eq. (1).

Let the colatitude, measured from the north pole, and the longitude of a point on the earth's surface be θ and ϕ, and assume that the overhead currents are horizontal so that $\mathbf{j}$ has only two components, j_θ (positive southward) and j_ϕ (positive eastward). If z is the vertical coordinate, j_θ and j_ϕ are functions of z as well as θ and ϕ. The vertical component of Eq. (4) becomes

$$ey_2v_{2z} = \cos I(K_t \sin D + K_a \sin I \cos D)j_\theta + \cos I(K_t \cos D - K_a \sin I \sin D)j_\phi \quad (6)$$

where D and I are the declination (positive eastward) and inclination (positive downward) at the point θ, ϕ. The vertical electronic diffusion current can be computed by Eq. (6) whenever the diffusion factors K_t and K_a and the current densities are known.

CONDUCTION BY ELECTRONS, POSITIVE IONS, AND NEGATIVE IONS

The hydrodynamic equation for negative ions reads

$$-e(\mathbf{E} + \mathbf{E}_e)y_3 - ey_3\mathbf{v}_3 \times \mathbf{H} = (kT/D_1)y_3\mathbf{v}_3 \quad (1c)$$

The diffusion coefficient for negative ions has been taken equal to that for positive ions.[5] Eqs. (2*a*) and (3*a*) must be replaced by

$$\mathbf{j} = e(y_1\mathbf{v}_1 - y_2\mathbf{v}_2 - y_3\mathbf{v}_3) \quad (2b)$$

$$y_1 = y_2 + y_3 \quad (3b)$$

The elimination of $\mathbf{E} + \mathbf{E}_e$, $\mathbf{v}_1$, and $\mathbf{v}_3$ now gives

$$K_0 = -(\lambda_2/\lambda_1)(1 + \lambda_1^2)A(A^2 + B^2)^{-1} \quad (7a)$$

$$K_a = -(\lambda_2/\lambda_1)(B^2 - \lambda_1^2A^2)A^{-1}(A^2 + B^2)^{-1} \quad (7b)$$

$$K_t = (\lambda_2/\lambda_1)(1 + \lambda_1^2)B(A^2 + B^2)^{-1} \quad (7c)$$

[5]The collision radii of positive ions in N_2, which somewhat exceed usual kinetic theory radii, are probably determined by the electrostatic force between the ionic charge and the N_2 electric quadrupole moment. [Cf. M. H. Johnson, Phys. Rev., **80**, (1950).] On that assumption, all singly charged ions should have the same cross-section for collisions with N_2 and the diffusion coefficient should vary with the molecular weight, m_i, as $[1 + (28/m_i)]^{1/2}$.

where

$$A = 1 + (\lambda_2/\lambda_1) + 2(y_3/y_2)$$

$$B = \lambda_1 + \lambda_2 + 2\lambda_2(y_3/y_2)$$

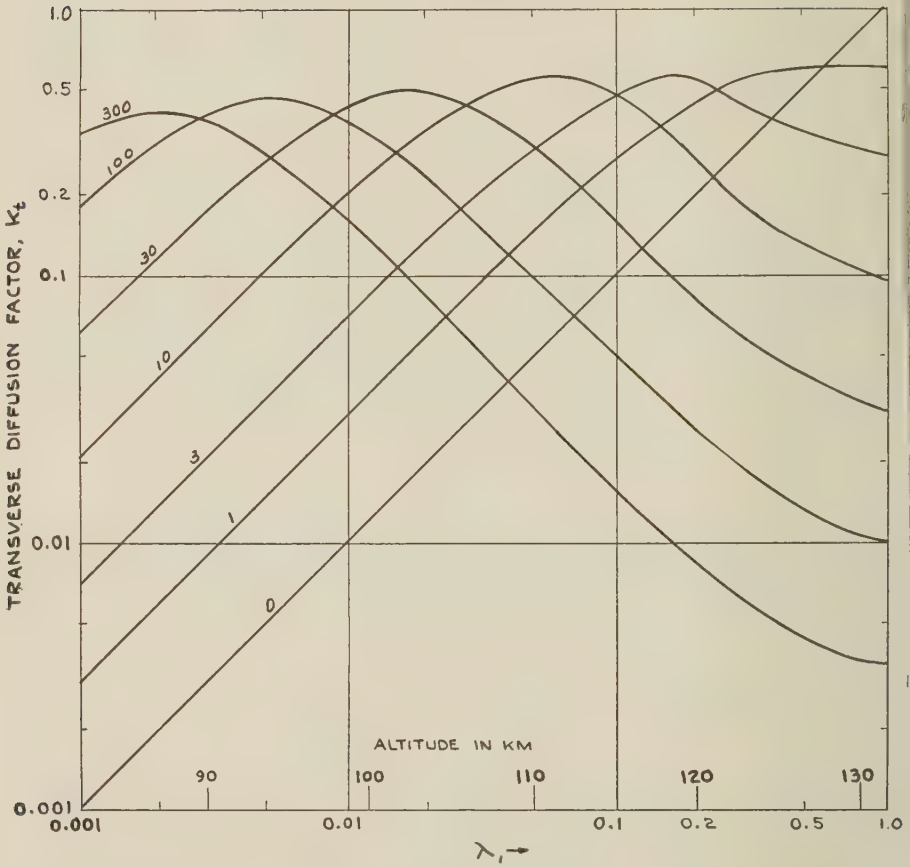

FIG. 1—THE TRANSVERSE DIFFUSION FACTOR, K_t, AS A FUNCTION OF λ_1 AND OF ALTITUDE; THE DIFFERENT CURVES ARE FOR NEGATIVE ION TO ELECTRON RATIOS OF 0, 1, 3, 10, 30, 100, AND 300

The diffusion factors, K_t and K_a, are plotted as functions of λ_1 in Figures 1 and 2 for various values of y_3/y_2, the ratio of negative ions to electrons. The ratio λ_2/λ_1 has been taken as 3500.[6] The second abscissa scale, the altitude in

[6]Two recent and entirely different experiments, L. G. H. Huxley and A. A. Zaazou, Proc. R. Soc., A, **196**, 402 (1949), and Phelps, Fundingsland, and Brown, Phys. Rev., 84, 559 (1951), give a collision probability for thermal electrons in N_2 at 1 mm Hg pressure of about 20 cm^{-1}. Then, at normal pressure and temperature, $D_2 = 250$ cm^2 sec^{-1}. The measured mobility of ions with approximately the molecular weight of N_2 is 2.8 cm^2 sec^{-1} volt $^{-1}$, Mitchell and Ridler, Proc. R. Soc., A, **146**, 911 (1934), and the corresponding value of $D_1 = 0.072$ cm^2 sec^{-1}. Whence $\lambda_2/\lambda_1 = D_2/D_1 = 3500$.

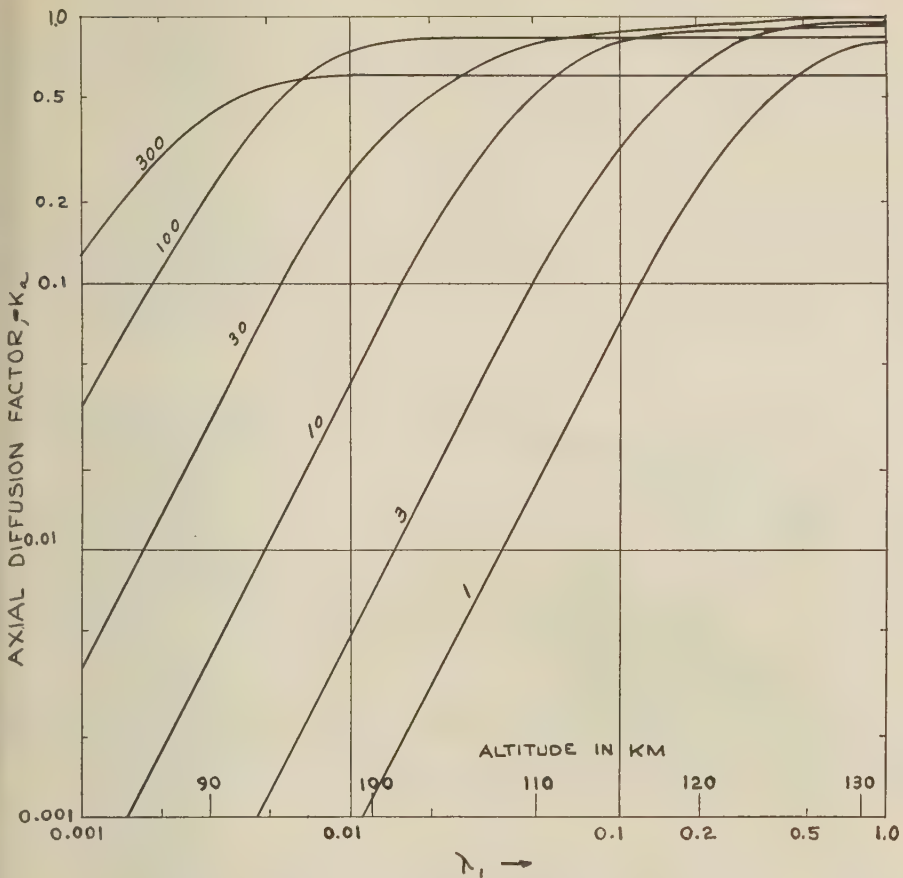

FIG. 2—THE AXIAL DIFFUSION FACTOR, K_a, AS A FUNCTION OF λ_1 AND OF ALTITUDE; THE DIFFERENT CURVES ARE FOR NEGATIVE ION TO ELECTRON RATIOS OF 1, 3, 10, 30, 100, AND 300

kilometers, has been fixed by rocket measurements of density.[7]

Negative ions complicate the diffusion because electrical neutrality no longer constrains the ions and electrons to move together for directions perpendicular to **j**. They make possible axial diffusion in which the electronic diffusion current is deflected from the direction of $-\mathbf{j}$ toward the magnetic lines of force. They can considerably enhance transverse electronic diffusion in the *E*-region.

[7]Havens, Koll, and LaGow, J. Geophys. Res., 57, 59 (1952), find a density of 8×10^{-10} gm cm^{-3} and a scale height of 7.2 km at an altitude of 100 km. The number density, for an average molecular weight of 25, is 2×10^{13} cm^{-3} compared to 2.7×10^{19} cm^{-3} at sea-level. Whence, at 100 km, $D_1 = 9.6 \times 10^4$ cm^2 sec^{-1} and, for $H = 0.3$ oersted, $\lambda_1 = 0.012$.

HEIGHT CHANGES IN THE *E*-LAYER

In the *E*-region, the rapid recombination insures that, at each instant, equilibrium holds between the electron production rate, q, and the rate of electron loss by recombination and diffusion. Then

$$q = r(y_2) + \mathrm{d}(y_2 v_{2z})/\mathrm{d}z \quad \ldots\ldots(8)$$

where $r(y_2)$ is the electron recombination rate and horizontal diffusion currents have been omitted. Let z' be the altitude at which y_2 , determined by Eq. (8), has a particular value and let z'' be the altitude for which y_2 , determined from the equation $q = r(y_2)$, has this same value. Then, if $z' - z''$ is not too large,

$$\delta h = z' - z'' = \mathrm{d}(y_2 v_{2z})/\mathrm{d}z \div \mathrm{d}q/\mathrm{d}z \quad \ldots\ldots(9)$$

The quantity δh may be called the change in height produced by diffusion. It is positive when diffusion moves the point for the electron density under consideration to a greater height.

An important conclusion follows from Eq. (9): an upward diffusion current need not move the layer to a greater height. If v_{2z} is positive (upward), $y_2 v_{2z}$ may be a decreasing function of z, in which case $\mathrm{d}(y_2 v_{2z})/\mathrm{d}z$ is negative. As $\mathrm{d}q/\mathrm{d}z$ is always positive on the lower side of the layer, δh is then negative and diffusion moves the layer downward. Consequently, for a periodic diffusion current which decreases with altitude, the height variations appear exactly out of phase with the diffusion current.

An approximate value may be assigned to $\mathrm{d}q/\mathrm{d}z$. If the ionizing solar radiation be monochromatic, q has the form $n \exp(-n/n_0)$, where n_0 is the number density at which the radiation produces the maximum number of electrons. Then, in a homogeneous atmosphere of scale height H_0 ,

$$\mathrm{d}q/\mathrm{d}z = (1 - n/n_0)q(\mathrm{d}1 - n/\mathrm{d}z) = -(1 - n/n_0)(q/H_0) \quad \ldots\ldots(10a)$$

If the electron density at which the height is judged lies between 0.96 and 0.3 times the maximum density, q lies between 0.93 and 0.09 its maximum. In the corresponding range of n/n_0 , 1.4 to 5, the factor $-(1 - n/n_0)q$ has a maximum at $n/n_0 = 2.6$ and lies between $0.85q_0$ and $0.36q_0$. As the maximum production rate, q_0 , is about 200 $\mathrm{cm}^{-3}\ \mathrm{sec}^{-1}$, a reasonable value to take for the derivative is

$$\mathrm{d}q/\mathrm{d}z = 100/H_0 \qquad \mathrm{cm}^{-4}\ \mathrm{sec}^{-1} \quad \ldots\ldots(10b)$$

LUNAR CHANGES IN THE *E*-LAYER

The only known mechanism for lunar changes in the earth's magnetic field is the tide that the gravitational field of the moon raises in the ionosphere. Consequently, Eq. (1) may be confidently applied to lunar variations even though electromotive forces of other than electromagnetic origin, which might play a part in solar variations, have been omitted. Moreover, it is likely that the only source of lunar height changes is the diffusion described by Eq. (6). In contrast, solar height variations must certainly reflect the diurnal changes in the atmospheric depth to which the ionizing radiation penetrates.

The following equations represent a current sheet[8] inferred from the lunar variations in H:

$$\bar{j}_\theta = -8.1 \times 10^{-7}(\sin 2\theta/\sin\theta)\cos 2(\phi + \omega t) \quad \text{abamp cm}^{-1} \ldots (11a)$$

$$\bar{j}_\phi = 8.1 \times 10^{-7}\cos 2\theta \sin 2(\phi + \omega t) \quad \text{abamp cm}^{-1} \ldots (11b)$$

where ω is the circular frequency of the moon's passage and the time t is reckoned from the lunar transit over the 180th meridian. As the magnetic field at the earth's surface indicates nothing about the vertical distribution of current density, j_θ and j_ϕ will be written

$$j_\theta = -5.6 \times 10^{-13}\beta(\sin 2\theta/\sin\theta)\cos 2(\phi + \omega t) \quad \text{abamp cm}^{-2} \ldots (12a)$$

$$j_\phi = 5.6 \times 10^{-13}\beta \cos 2\theta \sin 2(\phi + \omega t) \quad \text{abamp cm}^{-2} \ldots (12b)$$

where β is a function of z. The numerical factor in Eq. (12) has been so chosen that β is unity within the sheet if the current is uniformly distributed through a thickness of 15 km. If the main lunar current is localized in the E-region, β should be of the order unity through most of the current layer. If the main current flows elsewhere, β should be much less than one.

As a consequence of the way $\mathbf{j}$ depends on t, δh, Eq. (9), has the form

$$\delta h = Z \cos 2[\phi + \omega(t - t_0)] \ldots (13)$$

The height variation contains only the second harmonic of the lunar period. With $Z > 0$ ($Z < 0$), the maximum upward (downward) displacement occurs at a time t_0 after the transit.

In case the E-region contains no negative ions, $K_a = 0$ and Eqs. (6), (9), and (12) yield

$$Z = (3.5\beta K_i)H_0(-\mathrm{d}ln\beta K_i/\mathrm{d}z) \cdot [4\sin^2 D\cos^2\theta + \cos^2 D\cos^2 2\theta]^{1/2}\cos I \quad km \ldots (14a)$$

$$\tan 2\omega t_0 = -\cot D\cos 2\theta(2\cos\theta)^{-1} \ldots (14b)$$

From Figure 1, $K_i = 0.05$ at an altitude of 110 km and, for $\beta = 1$, the first factor in Eq. (14a) is 0.2 km. If β decreases rapidly enough with altitude, the logarithmic derivative is negative and may be about $-H_0^{-1}$. Then, with D constant, Z has a maximum value 0.2 cos $I(1 + 3\sin^2 D)^{1/2}$ at the poles, a minimum value 0.2 cos I | sin D | at cos $2\theta = -\tan D$, and a value 0.2 cos D cos I at the equator. The observed amplitudes[9] are about four times larger than the amplitudes derived above. It may be noted that the maximum value K_i can have for any negative ion concentration is 0.5, for which the first factor in Eq. (14a) is 2 km. Therefore, the derived amplitudes are compatible with observation only if $\beta \sim 1$.

[8]S. Chapman and J. Bartels, Geomagnetism, Oxford, Clarendon Press (1940), Vol. 1, p. 262, Figure 4. Eq. (11) approximates this Figure, except that Eq. (11) places the current foci at 45° instead of 35° latitude.

[9]E. V. Appleton and K. Weekes, Proc. R. Soc., A, **171**, 171 (1939); D. F. Martyn, Proc. R. Soc., A **194**, 429 (1947).

Again assuming a negative logarithmic derivative, Eq. (14*b*) places t_0 , the time of maximum upward displacement, at 9 lunar hours after transit in high latitudes and at 3 lunar hours after transit in equatorial latitudes. The transition takes place in a belt of latitudes $\sim \pm D$ about the current focii. In the southern hemisphere, as one moves from equatorial to high latitudes, t_0 goes from 3 hours to 9 hours (-3 hours), if $D > 0$ ($D < 0$). Canberra, Australia, lies close enough to the current focus, on the equatorial side, to be in the transition belt. Observations give t_0 as 4.2, 5.3, and 6.3 hours for the southern solstice, equinox, and northern solstice, respectively. The sequence of seasons entails a displacement of the current focus from its highest to its lowest latitude. Since $D > 0$ at Canberra, the approach of the current focus at the northern solstice ought to increase t_0 in just the way that has been observed.

Suppose now that the negative ion to electron ratio is unity [10] at 110 km. From Figure 1, $K_t = 0.15$ and Z is larger by a factor of 3; the amplitude of the height variations agrees better with observation. Moreover, y_3/y_2 may well decrease with altitude in such a way that K_t does not depend on altitude. Then any decrease of β with z, which the decrease in y_3/y_2 could bring about, is enough to insure that the diffusion current decreases with z. The presence of negative ions, therefore, makes a negative logarithmic derivative in Eq. (14) much more plausible.

With $y_3/y_2 = 1$ and $\lambda_1 = 0.05$, axial diffusion is relatively small for, from Figure 2, $K_a = -0.018$ compared to $K_t = 0.15$. It first influences the coefficient of j_θ in Eq. (6) where it becomes important for small declinations. At Canberra, the axial part of the coefficient of j_θ is about one-half the transverse part and should not alter the qualitative description of the seasonal phase changes.

A different value of λ_1 (or of y_3/y_2) can make the axial term dominant. For example, the greater height of the E-layer and the larger magnetic field in England suggest $\lambda_1 = 0.25$ at the height of observation so that, with $y_3/y_2 = 1$, $K_t = 0.5$ and $K_a = -0.35$. The axial part of the j_θ coefficient is now three times the transverse part and is nearly as large as the coefficient of j_ϕ . Therein lies a possible explanation of the phase, $t_0 = 11.2$ hours observed in England. In the absence of axial diffusion, the westward declination in England, according to Eq. (14*b*), makes t_0 less than 9 hours, its value for $D = 0$. Suppose that the more rapid increase of $-K_a$ with altitude has the consequence that $d(-\beta K_a)/dz$ is positive although $d(\beta K_t)/dz$ is negative. Then the maximum upward displacement from the term in j_θ alone would occur at $t_0 = 12$ hours. The combination with the term in j_ϕ for which the maximum upward displacement occurs at 9 hours would now result in an intermediate value of t_0 in agreement with observation. Whenever axial diffusion plays a part, the phase of lunar displacements depends upon altitude and negative ion concentration, because K_t and K_a vary with these quantities in entirely different ways.

[10] A negative ion to electron ratio of one at 110 km exceeds the most favorable theoretical estimate by a factor of five. Cf. D. R. Bates and H. W. S. Massey, J. Atmos. Terr. Phys., 2, 1 (1951).

GEOMAGNETIC AND SOLAR DATA

FINAL RELATIVE SUNSPOT-NUMBERS FOR 1951

Table 1 contains the final sunspot-numbers for 1951 for the whole disk of the sun, based on observations made at the Zurich Observatory, supplemented by series furnished by other cooperating observatories. Table 2 gives the number of

TABLE 1—*Final relative sunspot-numbers for the whole disk of the sun for 1951*

Day	Jan.	Feb.	Mar.	Apr.	May	June	July	Aug.	Sep.	Oct.	Nov.	Dec.
1	32	97	74	41	62	38	17	64	46	41	45	32
2	22	84	62	27	56	38	16	71	47	44	57	24
3	32	62	50	24	78	37	36	55	48	43	46	20
4	42	53	45	20	51	26	50	57	55	38	53	22
5	42	60	38	40	46	65	32	73	64	31	61	20
6	64	46	50	61	20	103	56	74	84	19	56	34
7	71	43	55	69	26	115	69	83	77	16	62	41
8	75	53	54	78	17	130	86	102	91	25	43	54
9	60	60	33	75	32	138	105	121	108	54	61	42
10	57	70	26	74	84	137	109	132	118	71	62	22
11	54	74	40	84	102	133	112	121	129	81	76	22
12	46	69	61	88	125	147	96	112	123	95	65	28
13	17	63	43	78	155	159	95	82	114	72	41	31
14	26	67	36	103	170	163	92	66	110	52	40	26
15	15	63	26	118	184	158	90	62	100	63	40	40
16	16	54	31	126	212	147	40	58	89	67	50	49
17	30	50	26	130	220	152	45	54	93	56	46	59
18	35	38	35	148	229	157	48	49	98	58	44	63
19	45	36	38	150	204	146	40	66	89	81	42	62
20	40	41	49	132	180	138	33	67	91	78	43	68
21	50	44	59	149	180	134	26	54	104	43	45	76
22	51	51	60	144	154	123	28	62	109	32	52	102
23	63	55	83	140	140	93	70	38	104	21	54	106
24	77	61	110	119	117	63	78	42	80	14	54	66
25	90	67	108	115	114	60	61	24	76	22	54	52
26	105	72	97	103	93	63	52	8	70	41	60	29
27	115	80	84	110	87	48	60	6	63	55	75	27
28	130	65	74	96	81	45	79	8	58	71	59	41
29	120		70	81	51	43	61	24	23	73	55	43
30	125		65	65	48	18	66	15	31	72	31	50
31	111		52		46		58	40		70		68
Mean	59.9	59.9	55.9	92.9	108.5	100.6	61.5	61.0	83.1	51.6	52.4	45.8

Table 2—*Daily numbers of the sunspot-groups for 1951*

Day	Jan.	Feb.	Mar.	Apr.	May	June	July	Aug.	Sep.	Oct.	Nov.	Dec.
1	4	7	5	4	6	4	2	6	5	3	5	4
2	2	6	6	3	5	4	2	8	4	3	5	3
3	2	5	5	3	6	4	5	6	4	3	5	3
4	4	5	4	2	5	3	6	5	4	3	6	3
5	3	4	4	5	4	7	3	7	4	3	5	3
6	2	4	6	6	1	7	6	7	7	2	5	4
7	3	6	5	6	3	5	8	6	6	2	6	5
8	5	7	5	6	2	7	8	6	9	3	3	6
9	5	6	3	6	4	6	9	6	9	5	5	4
10	6	7	3	6	4	7	9	5	10	7	4	3
11	6	7	3	6	7	5	8	7	12	8	7	2
12	6	6	5	9	8	7	7	9	12	8	5	3
13	2	7	3	5	8	10	7	6	10	6	5	4
14	3	7	3	6	7	8	7	5	9	5	4	3
15	2	7	3	6	11	9	7	6	8	6	4	5
16	1	6	3	5	11	8	6	6	7	5	6	4
17	2	5	3	4	11	7	4	4	7	5	6	4
18	2	4	4	5	12	8	5	3	7	4	5	4
19	3	5	3	5	12	6	4	6	6	6	5	3
20	3	4	5	6	11	6	4	5	5	7	5	4
21	4	3	7	9	11	6	3	4	7	6	4	5
22	5	3	6	7	9	6	3	5	8	4	6	5
23	6	3	6	8	8	6	7	4	9	3	6	5
24	6	2	7	7	7	5	7	5	6	2	6	3
25	4	2	8	7	8	6	6	3	6	3	7	4
26	5	4	8	7	7	7	4	1	7	5	7	3
27	6	5	8	6	7	6	5	1	6	6	6	2
28	5	4	7	6	7	6	7	1	6	7	5	2
29	6		7	6	5	5	8	3	2	6	5	4
30	7		7	5	5	2	8	2	3	5	3	3
31	7		5		4		7	5		5		4
Mean	4.1	5.0	5.1	5.7	7.0	6.1	5.9	4.9	6.8	4.7	5.2	3.7

spot-groups on each day for the year 1951. The yearly mean of the group-numbers is 5.4, against 6.9 in 1950. The yearly mean of the relative numbers is 69.4, against 83.9 in 1950. Figure 1 gives a graphical representation of the daily relative sunspot-numbers for 1951, the times being plotted as abscissas and the relative numbers as ordinates. The limits of successive solar rotations are indicated by vertical arrows in the upper edge of the diagram. The general decline of solar activity has been

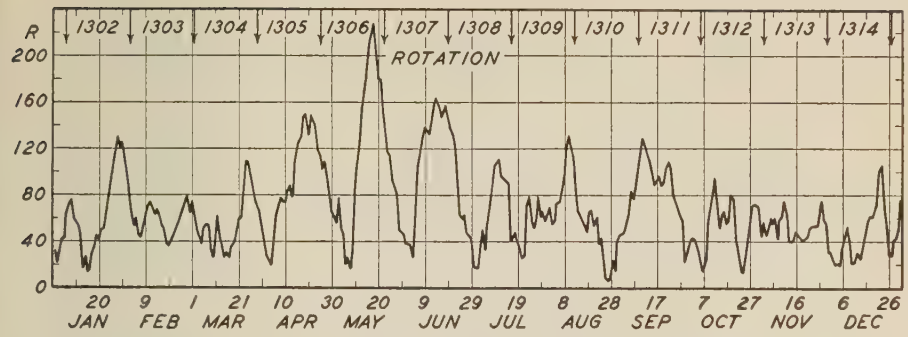

FIG. 1—DAILY RELATIVE SUNSPOT-NUMBERS FOR 1951

rather slow compared with the preceding year and was interrupted by the large increase from April to June produced by a huge spot-group. No spotless days occurred in 1951.

M. Waldmeier

Swiss Federal Observatory
Zurich, Switzerland, May 16, 1952

INTERNATIONAL DATA ON MAGNETIC DISTURBANCES, FIRST QUARTER, 1952

Preliminary Report on Sudden Commencements

S.c.'s given by five or more stations are in italics. Times given are mean values, with special weight on data from quick-run records.

Sudden commencements followed by a magnetic storm or a period of storminess (s.s.c.)

1952 January 03d 18h 04m: Te Ka.—03d 20h 20: So.—04d 21h 09: Te Ka Hr.—09d 20h 26: Am.—16d 09h 58: Eb.—24d 19h 08: So.—27d 09h 29: Wn Ni Ci El.—*29d 15h 30*: fourteen.—30d 11h 55: Ci Eb Va Hr.

1952 February 01d 01h 55m: Tl.—01d 08h 09: So.—01d 10h 12: Ci Ka.—*05d 23h 35*: eight.—06d 08h 20: Es Ci.—06d 09h 41: Le.—06d 17h 22: So.—06d 23h 35: Hu.—16d 13h 06: Ci.—19d 17h 35: So.—*23d 21h 26*: thirty—24d 00h 05: So.—28d 15h 00: SF.

1952 March *03d 07h 31m*: eighteen.—19d 12h 25: Es.—21d 04h 18: Ci.—23d 23h 33: Wi Ci Tn.—24d 14h 00: Es Wn Wi Fu.—27d 20h 00: So.—30d 19h 39: Do.—31d 16h 13.5: Tr.

Sudden commencements of polar or pulsational disturbances (p.s.c.)

1952 January 08d 16h 41m: Es CF.—09d 19h 10: Es Tl.—10d 23h 31: Wn CF.—13d 22h 34: Tl SF Hr.—21d 19h 50: So CF.—27d 12h 00: So Ka.—*28d 21h 32*: six.—29d 18h 10: Es Wi CF Fu.—*30d 18h 41*: five.—*30d 21h 35*: six.—30d 22h 15: Wn Fu Tl.

1952 February 06d 21h 44m: Tr CF Ci Hr.—10d 22h 12: Ci Tl.—11d 18h 55: Tr Wi Tn.—13d 20h 36: Tr Wn.—14d 17h 44: Wn Hr.—14d 23h 44: Le Tl.—15d 22h 13: CF Fu.—15d 22h 56: CF Fu.—15d 23h 40: CF Ci SF.—16d 20h 30: Tr Ni CF Ci.—18d 00h 00: CF Eb.—19d 00h 15: Tl SF.—19d 02h 28: Ci SF.—*19d 20h 34*: eight.—19d 23h 28: Wn Ci.—22d 19h 46: Wn CF Tl.—24d 00h 13: Ci Hr.—*24d 18h 34*: six.—25d 12h 54: Wi Ka To.—*26d 01h 02*: eight.—*27d 19h 46*: five.—*27d 20h 43*: six.—28d 18h 39: Es Ci Tl.

1952 March 03d 12h 58m: Ci Am.—03d 22h 40: Tn Ci.—*04d 19h 30*: nine.—05d 19h 09: Tr Hr.—06d 21h 15: Fu Tl.—07d 09h 24: Es Ci Am.—07d 16h 57: CF Ci.—07d 22h 27: Wn Fu Ci Hr.—08d 16h 13: Fu Ci.—08d 18h 22: Fu Ci Tl.—08d 23h 56: Ci SF.—10d 16h 42: Do CF Eb Hr.—11d 17h 52: Ci Tn.—*11d 18h 50*: five.—11d 21h 36: So Ci.—*13d 21h 43*: eight.—16d 04h 10: CF Va.—16d 23h 50: CF Ci.—*18d 22h 47*: five.—19d 19h 57: Wn CF Fu.—*21d 00h 31*: five.—*21d 22h 31*: five. 22d 01h 03: Wn Va.—*22d 19h 24*: five.—22d 19h 40: Es Ci.—*22d 23h 51*: seven.—23d 17h 48: Ni Ci Ka Tn.—26d 01h 30: CF Ci.—26d 19h 20: So Fu.—27d 03h 56: CF SJ Va.—27d 04h 12: Ci Va.—27d 21h 07: So Wn Fu.—28d 04h 20: CF Tl Va.—30d 13h 18: To Am.—30d 21h 30: Ci Hr.—31d 00h 36: Ci Hr.—31d 08h 13: Ci Am.—31d 14h 51: Ci Ka.

Geomagnetic planetary three-hour-range indices Kp, preliminary magnetic character-figures, C, and final selected days, January to March, 1952

January 1952									
E	1	2	3	4	5	6	7	8	Sum
1	5o	4 −	4o	4o	3 +	3o	3o	3 −	29 −
2	2 +	3 −	2o	1 +	1 +	2 −	3 −	1 +	15 +
3	2 −	2 +	2 −	1 +	2 +	1o	3 +	3o	17 −
4	4o	2o	2 −	2 +	3o	3 +	3o	5 −	24o
5	4 −	6o	6o	5 −	5o	4 +	3o	4 +	37o
6	5 −	5 −	5 −	4o	3o	4 +	3o	2 +	31 −
7	3o	3o	3 −	3 −	4 +	4 +	3 +	4o	27 +
8	3 +	4o	2 +	3o	3o	3o	2o	1o	22 −
9	0 +	3o	3 +	2 −	2o	3o	4 −	3 −	20 −
10	3o	5 +	5 −	3 +	3 +	5 −	4 −	5 −	33 −
11	4o	4 −	4 −	3o	4o	5 −	4 −	4 −	30 +
12	5 −	5 +	4o	4o	4o	5 −	4 +	5o	36o
13	4o	4 +	4 −	5o	6 −	5 −	5 −	5 +	37 +
14	4 +	5o	5 −	4 +	5 −	5o	5 −	5o	38 −
15	4 −	4 +	4 +	4 −	6o	5o	4o	2 +	33 +
16	3 +	2 +	3 −	3 +	3 −	3o	3o	3o	23 +
17	2o	3 −	2o	2 −	1 −	1 +	2 +	2o	15 −
18	2o	2 −	1 −	1o	1 −	1o	1o	1o	9o
19	1 −	1o	1 −	1o	2o	2 −	2 +	2 −	11o
20	0 +	2 −	1 +	1 +	1 −	1 +	2o	2o	11 −
21	2 +	2 −	2 −	2o	1 +	1 +	1 +	2 −	13 +
22	2o	2 +	2o	2 −	2 −	2o	2 +	3o	17o
23	3o	2o	3 −	3 +	4 +	4 +	4 +	4 −	28 −
24	4 −	2 +	2o	2 −	3o	4 −	3o	3o	22 +
25	3 +	1 +	2 +	3o	3o	3o	3 −	2o	21 −
26	0o	0 +	1 +	3 −	3 −	2o	1o	1 −	11 −
27	1 +	4 −	4o	4 +	6 −	5 +	4 −	4 −	32 −
28	3 +	5o	4 −	4 −	4o	4 −	2o	3o	28 +
29	2o	1o	3 −	4 −	4o	5o	6 +	6 −	30 +
30	4 −	4o	4o	2 +	3o	1o	3 −	2 +	23o
31	1 +	1 +	2 −	1 +	4 −	4 −	2o	3 −	18 −

February 1952									
1	2	3	4	5	6	7	8	Sum
3 +	2o	4 +	6 −	5 −	4o	5o	4 +	33 +
3 +	4 +	3o	2 +	2 +	3o	2o	2o	22 +
2 −	2 +	2 −	2 −	2 −	1 +	2o	1o	13 +
2o	2 −	1o	1 −	2o	1 −	1o	0 +	9 +
0 +	1 +	1 −	1 −	1o	0 +	0 +	1 −	5 +
2o	4 −	4 −	4 +	4 +	6 −	6o	6 +	36o
5 −	4 +	5 +	5 +	4o	4o	4 +	5 −	37 −
5 +	4 +	6o	4o	4 +	5o	5 −	4 +	38o
4o	4 +	3 −	3 +	4 +	5 −	4 +	4o	32 −
3o	3o	3o	4 −	3 −	4 +	5 +	7 −	32 −
6o	5 −	3 +	5 −	3 +	3 +	4 +	5 +	35o
5 +	5o	4 −	4 +	5 −	4 −	4 +	5o	36o
5 −	4 −	3 +	3 +	4 +	5 −	4o	5o	33o
4o	3 −	3 −	3 +	3o	3 +	4 −	3o	26 −
2o	3o	4 −	3 −	1 +	2o	1 −	3 −	18o
4 −	6 −	6 +	6 −	5 +	4o	5o	5o	41 −
5 −	3 −	1 +	3o	3o	2 +	2o	2 −	21 −
4 −	3 −	2o	4 −	3 −	2o	3 +	4o	24o
5o	4 +	5 −	4 −	4o	4 −	5o	5o	35 +
3o	4 −	4 +	3o	2o	2 +	1 +	1 +	21o
2o	2o	1o	0 +	2 +	2 −	2 −	1 +	12 +
1 −	1o	2o	1 +	1 +	1 +	3o	2 −	12 +
2 +	2 −	2o	1o	1 +	1 +	1 +	4 +	15 +
7 −	7o	4 −	6o	6 −	5o	6o	4 +	44 +
5 −	3 −	2o	3 +	5 −	2o	2 +	2 −	23 +
3 +	3 +	4 +	4 +	3 −	4 +	4o	5o	31 +
4 +	6 −	6 +	4o	3 −	4o	4 +	5o	36 +
5 −	5 +	6 −	5o	4o	5 −	4 +	2o	36 −
2o	4 +	4 −	4o	4o	4 −	2o	4 −	27 +

March 1952									
E	1	2	3	4	5	6	7	8	Sum
1	4 −	4 −	3 +	3 +	4 −	3 +	1 +	1 −	23o
2	1o	3 −	1 −	2 −	1 +	1o	1 −	1 −	10 −
3	0 +	1o	2 +	2 −	6 −	5 −	6 +	7 −	29 −
4	6 −	6 +	6o	6 +	5o	5 +	6 −	5 +	46 −
5	6o	7 −	5 +	6 +	6o	6 +	6o	7 +	50o
6	8o	7 +	6 +	5 −	4 +	4o	5o	5 +	45o
7	4 −	5o	3 +	6 +	5 +	6 −	5o	7 −	41o
8	6 −	5o	4 +	5 −	5 −	6 −	6o	5 +	41 +
9	6o	4o	5 −	5o	4 +	5 +	5o	6o	40 +
10	4 +	4 +	5 −	4 −	4 +	6 −	5o	5 +	37 +
11	5 +	4o	4 −	4 −	4o	4 +	5 +	4 −	34o
12	4 +	3 +	3 −	3o	4o	3 +	4o	3o	28 −
13	3 −	2 +	3o	2o	3 +	2o	2 +	3 +	21o
14	2o	2 +	1o	3o	2 +	1 +	1 −	2 +	15o
15	2o	3o	3o	2o	3o	3 −	4o	4 +	24o
16	2o	3 +	4 +	4o	3o	4 −	4 −	4o	28o
17	4 −	5 −	4o	4 −	5 −	4 +	3o	3o	31o
18	2 +	3 +	3 +	3 −	2 +	4 −	1o	2o	21 −
19	2o	1o	2 −	1o	2 −	2 +	3 −	2o	14 +
20	0 +	1 +	2 −	2 +	1 −	0 +	1o	1o	9 −
21	3 −	4 −	5 −	5 −	6 −	5 −	4 −	6 −	35 +
22	5 −	5o	4o	3 +	2 +	3o	4 +	6 −	32 +
23	7o	4 +	5o	4 +	3 +	4o	6 −	4o	38 −
24	5o	6 −	5o	5 +	5o	5o	5 −	4 +	40o
25	2 +	3 +	5 −	4 +	5 −	4 −	4o	3 +	30 +
26	5 −	3o	1 +	2 −	3o	3 −	4o	3 −	23o
27	2o	4o	4 −	3 +	3 +	4 +	3 −	3 −	26o
28	2 −	2o	1o	1 −	1 +	1 −	1 +	1o	10 −
29	1 −	1o	1o	3 −	3 −	1 +	2o	3o	14 +
30	3 +	4 −	2o	2o	4 +	6o	6o	7 −	34o
31	8 −	6o	7 −	5 +	4o	6o	5 +	5o	46o

Preliminary *C*, 1952		
Jan.	Feb.	Mar.
1.0	1.4	0.8
0.2	0.5	0.1
0.6	0.1	1.5
1.0	0.1	1.6
1.3	0.0	1.7
1.2	1.6	1.6
1.0	1.3	1.5
0.5	1.4	1.5
0.7	1.2	1.5
1.2	1.4	1.4
1.2	1.3	1.2
1.3	1.4	1.0
1.5	1.2	0.7
1.4	0.9	0.2
1.3	0.4	1.0
0.5	1.6	1.0
0.2	0.8	1.1
0.0	0.9	0.6
0.1	1.3	0.4
0.2	0.5	0.0
0.2	0.0	1.3
0.5	0.2	1.2
1.1	0.6	1.5
0.8	1.7	1.4
0.6	1.0	1.0
0.2	1.2	0.8
1.5	1.4	0.9
1.0	1.2	0.1
1.5	1.0	0.4
0.7		1.4
0.8		1.6

Final selected days		
Jan.	Feb.	Mar.
Five quiet		
18	3	2
19	4	14
20	5	19
21	21	20
26	22	28
Five disturbed		
5	6	4
13	8	5
14	16	6
27	24	7
29	27	31
Ten quiet		
2	2	1
3	3	2
8	4	13
17	5	14
18	15	18
19	17	19
20	20	20
21	21	26
22	22	28
26	23	29

Sudden impulses found in the magnetograms (s.i.)

1952 January 01d 17h 13m: So.—02d 22h 46: Tr So.—03d 19h 37: Es Hr.—04d 22h 20: Ci.—06d 16h 09: So Do Ka.—09d 04h 00: Te.—09d 08h 30: Ka.—11d 12h 45: Va Hr.—11d 13h 09: Ka.—12d 17h 09: Es.—13d 10h 30: Ni Ci.—13d 17h 46: Ci.—14d 17h 59: Es.—15d 13h 11: Va Hr.—16d 06h 11: Le Es.—23d 00h 19: Hr.—24d 00h 49: Ci.—27d 19h 21: Es.

1952 February 01d 20h 08m: Ka.—11d 18h 46: Le Wn Fu.—12d 13h 03: Ka.—16d 13h 22: Ci Ka.—17d 10h 33: Es.—23d 23h 53: Fu.—24d 15h 38: Es.—25d 02h 28: Ci.—26d 06h 06: Ka.—26d 16h 56: So Es Wn Fu.

1952 March 01d 14h 10m: Ci Ka.—01d 18h 34: So.—03d 17h 20: Ci Ka.—03d 20h 20: Wn Hr.—04d 02h 20: Ci.—04d 04h 20: Ci Hr.—06d 14h 10: Ci.—07d 14h 12: Ci Te.—11d 17h 37: Fu.—11d 23h 33: SF.—15d 20h 14: Wn Fu.—17d 08h 09: Es Tl.—17d 18h 43: Ka.—19d 14h 35: Va.—20d 05h 55: Hr.— 21d 04h 30: Va.—21d 14h 12: Ci Ka Tn Hr.—23d 23h 42: Ci Tn.—24d 00h 00: Te.—24d 01h 58: Te.—24d 04h 54: Tl SF.—25d 06h 45: Es Wi.—28d 12h 17: Hr.—28d 21h 30: Tr.

Preliminary Report on Solar-flare Effects

Effects confirmed by ionospheric or solar observations are in italics.

1952 January 03d 18h 04m: Hu (s.c. after Te Ka Wi).—03d 19h 36-21h 00: Tu (s.i. after Es Wi Hr).—*09d 10h 42–11h 15*: CF(?) Hr.—15d 13h 07: Eb (s.i. after Va Hr).—15d 14h 15-15h 04: Te.—*24d 00h 36-01h 00*: Ka.—26d 14h 24-18h 00: Tu.—27d 09h 32: Eb (s.c. after Wi Ni Ci El).—31d 21h 18-22h 10: Tu.

1952 February 03d 13h 54m-14h 00m: Ch.—03d 16h 38-57: Ch Tu.—08d 10h 27–36: Es.—11d 23h 24-24h 21: Te.—13d 15h 02-10: CF(?).—15d 06h 03-24: Ap.—16d 16h 51-58: SJ.—17d 16h 45-17h 10: SJ Tu Hu Ap.

1952 March 27d 13h 18m: Tu Hu Va.—29d 15h 00: Tu.

Ionospheric or solar disturbances without clear geomagnetic effect

None.

Minor disturbances reported by one station only are listed in the De Bilt quarterly circular, but omitted here.

Committee on Characterization of Magnetic Disturbances

J. Bartels, *Chairman*
University
Göttingen, Germany

J. Veldkamp
Kon. Nederlandsch Meteorologisch Instituut
De Bilt, Holland

PROVISIONAL SUNSPOT-NUMBERS FOR APRIL TO JUNE, 1952

(Dependent on observations at Zurich Observatory and its stations at Locarno and Arosa)

Day	April	May	June
1	28	30	12
2	16	15	19
3	21	8	14
4	26	19	7
5	37	30	7
6	33	34	6
7	37	30	26
8	40	27	21
9	32	23	8
10	30	0	17
11	46	7	10
12	28	6	18
13	22	8	20
14	19	15	22
15	7	14	46
16	8	8	36
17	7	10	45
18	17	18	45
19	33	22	55
20	53	36	50
21	62	26	50
22	50	25	55
23	38	32	70
24	26	31	58
25	15	17	56
26	26	10	56
27	16	43	52
28	17	57	66
29	32	49	63
30	42	36	76
31		23	
Means	28.8	22.9	36.2
No. days	30	31	30

Mean for quarter: 29.2 (91 days)

M. Waldmeier

Swiss Federal Observatory
Zurich, Switzerland

CHELTENHAM THREE-HOUR-RANGE INDICES *K* FOR APRIL TO JUNE, 1952

[K9 = 500γ; scale-values of variometers in γ/mm: $D = 5.4$; $H = 2.5$; $Z = 4.0$]

Gr. day	April 1952		May 1952		June 1952	
	Values *K*	Sum	Values *K*	Sum	Values *K*	Sum
1	4544 4343	31	5645 4355	37	2423 2222	19
2	6456 3456	39	6443 4345	33	3321 1232	17
3	6665 3455	40	5443 3346	32	3311 1223	16
4	6454 3456	37	5543 3444	32	3212 0122	13
5	5465 4445	37	5344 3334	29	2331 1222	16
6	6455 3336	35	3443 2334	26	3331 0112	14
7	5454 3344	32	4455 5455	37	2122 1122	13
8	4543 3344	30	5433 3332	26	3344 3455	31
9	5333 2343	26	1210 0012	7	3543 5435	32
10	7543 2233	29	2211 2111	11	4332 3334	25
11	4233 2132	20	0122 4333	18	4352 2343	26
12	4232 0132	17	4332 2123	20	3232 2223	19
13	4522 2132	21	2213 4243	21	0131 1233	14
14	1123 2323	17	4431 1122	18	2344 3355	29
15	4333 4223	24	2111 1212	11	3444 3333	27
16	3452 3233	25	2211 1212	12	3553 3332	27
17	4433 1212	20	1221 1224	15	3443 2322	23
18	0122 3234	17	5355 4443	33	4412 2234	22
19	5322 3344	26	4546 3333	31	2112 2222	14
20	2422 1123	17	4444 3333	28	2211 1223	14
21	2454 8765	41	3334 3322	23	2101 1222	11
22	5654 2234	31	1321 0112	11	1232 4444	24
23	4543 2233	26	1122 2323	16	5544 4344	33
24	2212 2433	19	3333 2334	24	5644 3444	34
25	1113 1223	14	4443 2322	24	2232 2245	22
26	2112 1233	15	1135 3456	28	4333 3332	24
27	2211 1213	13	7543 3445	35	3442 2333	24
28	5534 3333	29	5234 4545	32	2112 3222	15
29	5653 4556	39	4543 3434	30	2232 1245	21
30	6554 3446	37	4533 2233	25	5776 3233	36
31			4542 2234	26		

Ralph R. Bodle
Observer-in-Charge
Cheltenham Magnetic Observatory
Cheltenham, Maryland, U.S.A.

PRINCIPAL MAGNETIC STORMS

(Advance knowledge of the character of the records at some observatories as regards disturbances)

Observatory (Observer-in-Charge)	Greenwich date	Storm-time		Sudden commencement				C-figure, degree of activity[4]	Maximal activity on K-scale 0 to 9			Ranges		
		GMT of begin.	GMT of ending[1]	Type[2]	Amplitudes[3]				Gr. day	Gr. 3-hr. period	K-index	D	H	
					D	H	Z							
(1)	(2)	(3)	(4)	(5)	(6)	(7)	(8)	(9)	(10)	(11)	(12)	(13)	(14)	(
	1952	*h m*	*d h*		′	γ	γ					′	γ	
College (M. L. Cleven)	Mar. 30	13 20	10 15	.....	....	....	....	ms	30	6	7	350	1800	14
									31	3,4				
									1	6				
									2	4				
									3	3,4,6				
									7	4				
	Apr. 21	05 00	22 12	.....	....	....	....	ms	22	4	7	250	1660	13
	Apr. 28	02 00	5 13	.....	....	....	....	ms	29	6	7	340	1950	10
									30	3				
									2	6				
	May 7	03 00	8 17	.....	....	....	....	s	7	6	8	520	1990	16
	May 26	08 00	31 10	.....	....	....	....	ms	26	5	6	180	1300	9
									27	1,4				
									28	4,5,6				
									29	3,4				
									30	3				
	June 22	07 00	24 17	.....	....	....	....	ms	24	5,6	6	220	1390	9
	June 29	19 30	30 20	.....	....	....	....	ms	30	2	7	410	1040	15
Sitka (T. L. Skillman)	Apr. 21	11 50	22 12	.....	....	....	....	s	21	5	9	227	2021	9
	Apr. 28	03 30	6 12	.....	....	....	.....	.....	28	3	.....	143	1387	7
								s	29	4	8			
	May 7	04 00	8 13	.....	....	....	....	s	7	3,4	9	166	1376	7
	May 17	23 58	20 18	s.c.	−2	+28	+3	s	18	4	8	82	778	6
	May 26	08 35	31 10	.....	....	....	....	ms	27	1	7	110	1047	5
	June 22	07 00	24 18	.....	....	....	....	ms	23	4,5	6	56	617	5
									24	5,6	6			
	June 29	19 30	30 14	.....	....	....	....	s	30	3	9	240	2146	8
Witteveen (D. van Sabben)	Jan. 4	21 10	7 23	.....	....	....	....	ms	4	8	6	30	185	
	Jan. 9	18 00	16 03	.....	....	....	....	ms	10	6	6	35	200	
									11	6	6			
									12	6,7	6			
	Jan. 27	04 00	28 24	.....	....	....	....	ms	27	6	6	28	160	1
	Jan. 29	12 00	30 06	.....	....	....	....	ms	29	7,8	7			
	Feb. 1	07 00	1 22	.....	....	....	....	ms	1	7	6	33	165	
	Feb. 6	05 00	13 24	.....	....	....	....	ms	6	6,7,8	6	52	230	1
									9	7	6			
									10	7,8	6			
									11	1,8	6			
									12	7	6			
									13	8	6			
	Feb. 15	22 00	17 03	.....	....	....	....	ms	16	5,7,8	6	40	180	
	Feb. 19	00 16	19 24	.....	....	....	....	ms	19	7,8	6	28	170	5
	Feb. 23	21 26	25 03	s.c.*	−2	+48	−4	ms	24	2,7	7	55	245	1
	Feb. 26	01 00	28 20	.....	....	....	....	ms	27	8	6	28	185	
									28	7	6			
	Mar. 3	12 00	12 24	.....	....	....	....	ms	5	6,8	7	55	360	2
									6	1,2	7			
									7	8	7			
									8	7	7			
	Mar. 21	03 00	26 03	.....	....	....	....	ms	21	8	6	52	260	1
									23	1,7	6			
	Mar. 30	10 00												
	(Storm of Mar. 30 still in progress at end of month)													

[1]Approximate time of ending of storm construed as the time of cessation of reasonably marked disturbance movements in th traces; more specifically, when the *K*-index measure diminished to 2 or less for a reasonable period.

[2]s.c. = sudden commencement; s.c.* = small initial impulse followed by main impulse (the amplitude in this case is that of th *main impulse only*, neglecting the initial brief pulse); . . . = gradual commencement.

[3]Signs of amplitudes of *D* and *Z* taken algebraically; *D* reckoned positive if towards the east and *Z* reckoned pos tive if ve tically downwards.

[4]Storm described by three degrees of activity: *m* for moderate (when *K*-index as great as 5); *ms* for moderately severe (whe *K* = 6 or 7); *s* for severe (when *K* = 8 or 9).

PRINCIPAL MAGNETIC STORMS—Continued

bservatory (Observer-n-Charge)	Green-wich date	Storm-time GMT of begin.	Storm-time GMT of ending[1]	Sudden commencement Type[2]	Sudden commencement Amplitudes[3] D	H	Z	C-figure, degree of activity[4]	Maximal activity on K-scale 0 to 9 Gr. day	Gr. 3-hr. period	K-index	Ranges D	H	Z
(1)	(2)	(3)	(4)	(5)	(6)	(7)	(8)	(9)	(10)	(11)	(12)	(13)	(14)	(15)
	1952	*h m*	*d h*		′	γ	γ					′	γ	γ
eltenham	Mar. 30	02 ..	10 09	.....	.....	.....	.....	ms	31	1	7	38	153	120
R. Bodle)	Apr. 21	11 51	23 08	s.c.	1	10	4	s	21	5,6	8	32	354	181
	Apr. 28	01 ..	8 04	.....	.....	.....	.....	ms	30	1	6	33	94	86
	May 18	00 ..	21 22	.....	.....	.....	.....	ms	19	4	6	24	58	33
	May 26	08 ..	1 00	.....	.....	.....	.....	ms	27	1	7	50	162	160
	June 8	02 33	11 23	s.c.	3	13	4	m	8	7,8	5	7	86	29
	June 14	04 ..	17 11	.....	.....	.....	.....	m	14	8	5	8	94	16
	June 23	02 ..	25 00	.....	.....	.....	.....	ms	24	1,2	6	23	101	33
	June 29	19 ..	30 12	.....	.....	.....	.....	ms	30	2,3	7	68	339	480
n Juan	Apr. 21	11 49	22 11	s.c.	+1	+8	−2	ms	21	5,6,7,8	6	16	194	74
G. Ledig)	June 29	19 32	30 11	s.c.	0	+17	−3	m	30	2,3	5	7	125	18
nolulu	Jan. 4	18 00	6 12	.....	.....	.....	.....	m	5	2	5	7	129	45
F. White)	Feb. 5	23 35	8 18	.....	.....	.....	.....	m	6	2	5	6	122	40
	Feb. 15	22 00	17 04	.....	.....	.....	.....	ms	16	4	6	5	155	38
	Feb. 23	21 26	25 02	s.c.	0	28	14	ms	24	1	7	6	224	52
	Feb. 26	21 00	28 19	.....	.....	.....	.....	m	27	2,3	5	6	115	33
	Mar. 3	07 30	11 15	.....	.....	.....	.....	ms	3	8	6	10	215	49
									6	1	6			
	Mar. 21	03 00	25 15	.....	.....	.....	.....	ms	21	3	6	7	141	45
	Mar. 30	13 00	8 12	.....	.....	.....	.....	ms	31	1,3	6	10	166	57
	Apr. 21	11 50	22 13	s.c.	0	22	10	ms	21	5	6	15	144	55
	Apr. 26	21 00	6 13	.....	.....	.....	.....	m	28	2	5	8	143	56
	May 26	8 00	31 10	.....	.....	.....	.....	ms	27	1	6	11	196	36
	June 29	19 33	30 11	s.c.	1	18	12	ms	30	2	7	12	254	76
stituto	Mar. 30	03 50	6 02	.....	.....	.....	.....	m	31	1,2,5.8	5	8	295	48
Geofisíco de	Apr. 21	11 50	22 07	s.s.c.	+1	+41	+3	s	21	5,6	9	14	672	54
Huancayo	Apr. 27	22 12	5 02	s.s.c.	0	+12	+2	ms	29	6	6	6	302	45
. A. Giesecke)	May 17	18 00	19 06	.....	.....	.....	.....	ms	18	6	6	7	214	24
	May 26	08 52	31 07	.....	.....	.....	.....	m	26	6,8	5	9	381	46
	June 8	06 22	10 06	.....	.....	.....	.....	m	9	6	5	4	188	28
	June 14	04 17	15 05	.....	.....	.....	.....	m	14	6	5	3	157	43
	June 22	07 05	24 17	.....	.....	.....	.....	m	22	5,6,7	5	6	210	31
	June 29	19 32	30 12	s.s.c.	0	+46	+4	m	30	2,3	5	8	268	35
	1951													
izabethville	Oct. 28	11 54	29 06	s.c.	+3	+63	+8	ms	28	6,7	...	9	511	62
. Alexandre)	Dec. 27	21 36	28 24	s.c.	+1	+50	+4	m	28	5,6	...	5	282	12
	1952													
	Jan. 27	09 27	27 24	s.c.	+2	−50	−3	m	27	5,6	...	9	171	31
	Jan. 29	15 29	30 03	s.c.	....	+17	+1	m	29	6,7	...	6	120	12
	Mar. 3	07 28	6 06	s.c.	−1	+19	....	m	5	6,7	...	11	218	40
	Mar. 30	13 50	31 24	.....	.....	.....	.....	m	30	6,7	...	9	143	23
	(N.B. Il n'y a pas eu d'enrégistrement les: 22 et 23 février 20 mars. Le 6 février fut très agite)													
pia	Jan. 4	19 48	5 16	.....	.....	.....	.....	m	5	2	5	7	145	38
. C.	Jan. 9	20 21	15 21	s.c.	0	+4	0	m	15	6	5	7	86	39
Stanbury)	Jan. 27	04 20	28 18	.....	.....	.....	.....	m	27	5	5	6	85	20
	Jan. 29	15 29	29 23	s.c.	0	+15	−3	m	29	7	5	6	68	20
	Feb. 1	08 06	2 00	.....	.....	.....	.....	m	1	4,7	5	5	64	17
	Feb. 5	23 32	15 01	s.c.	0	+6	0	m	7	4	5	8	122	42
	Feb. 16	00 47	17 04	.....	.....	.....	.....	ms	16	4	6	10	151	28
	Feb. 23	21 26	25 01	s.c.	0	+25	−8	ms	24	1	6	6	240	40
	Feb. 26	20 24	28 18	.....	.....	.....	.....	(m)	..	....	(5)	8	94	20
	(*Note:* Gauss House was under repair during storm of Feb. 26)													
	Mar. 3	07 31	12 16	s.c.	0	+8	−3	ms	3	8	6	6	159	33
	Mar. 21	01 33	26 05	.....	.....	.....	.....	ms	21	3	6	5	169	35
	Mar. 30	13 18	.. ..	.....	.....	.....	.....	m	31	1,3,4	5	5	137	31
	(*Note:* Storm of Mar. 30 still in progress; see following page)													

PRINCIPAL MAGNETIC STORMS—Continued

Observatory (Observer-in-Charge)	Greenwich date	Storm-time GMT of begin.	Storm-time GMT of ending[1]	Sudden commencement Type[2]	Amplitudes[3] D	H	Z	C-figure, degree of activity[4]	Maximal activity on K-scale 0 to 9 Gr. day	Gr. 3-hr. period	K-index	Ranges D	H	
(1)	(2)	(3)	(4)	(5)	(6)	(7)	(8)	(9)	(10)	(11)	(12)	(13)	(14)	(1
	1952	*h m*	*d h*		′	γ	γ					′	γ	
Apia— *continued* (A. C. Stanbury)	Mar. 30	13 18	10 04	.....	.....	.....	.....	m	2	1,4	5	3	115	
									3	3	5			
									4	3	5			
									5	2	5			
									6	1,2,4,8	5			
	Apr. 21	11 50	23 12	s.c.	0	+16	−6	ms	21	5	6	6	137	
	Apr. 27	19 39	8 21	.....	.....	.....	.....	m	28	2	5	7	284	
									29	7,8	5			
									30	1,3	5			
									1	3	5			
									2	2	5			
									3	7,8	5			
									4	1	5			
									5	1	5			
									7	2,4,5,7,8	5			
									8	1,2	5			
	May 17	21 30	20 06	.....	.....	.....	.....	m	19	2	5	5	112	
	May 26	08 29	31 10	.....	.....	.....	.....	ms	26	8	6	5	192	
									27	1.2	6			
	June 7	23 03	12 23	.....	.....	.....	.....	m	8	3,4	5	4	88	
	June 22	07 06	26 23	.....	.....	.....	.....	m	24	1,2	5	6	107	
	June 29	19 29	30 17	s.c.	0	+14	−5	ms	30	2	7	6	278	
Hermanus (A. M. van Wijk)	Mar. 30	12 ..	10 14	.....	.....	.....	.....	ms	30	8	6	25	143	1
									31	1	6			
									2	7	6			
									4	7	6			
	Apr. 18	11 ..	20 00	.....	.....	.....	.....	m	18	7,8	5	13	84	
									19	5,8	5			
	Apr. 21	11 50	23 12	s.c.	+1	+5	+5	ms	21	5	7	30	209	1
	Apr. 27	22 *ca.*	8 22	.....	.....	.....	.....	ms	29	6,8	6	28	171	1
									3	8	6			
									5	1	6			
									7	8	6			
	May 17	22 *ca.*	19 21	.....	.....	.....	.....	m	18	3,6	5	16	85	
									19	2,4	5			
		(*Note:* Strong impulse at 23h 56m, May 17 (*H*, −26γ)												
	May 26	07 ..	31 07	.....	.....	.....	.....	ms	26	8	6	36	113	1
									27	1	6			
	June 8	02 ..	12 03	.....	.....	.....	.....	m	9	5	5	11	79	
	June 14	03 *ca.*	16 18	.....	.....	.....	.....	m	14	5,6,8	5	20	64	
	June 22	07 *ca.*	25 00	.....	.....	.....	.....	m	22	6,8	5	19	103	
									23	3	5			
									24	1,2	5			
	June 25	10 49	26 18	s.c.	−1	+2	+2	m	26	1	5	11	58	
	June 29	19 33	30 15	s.c.	0	+11	+10	ms	30	2,3	6	38	161	1
Amberley (H. F. Baird)	Mar. 30	13 18	10 14	.....	.....	.....	.....	ms	31	3	7	42	231	
	Apr. 14	23 49	17 12	s.c.	+1	+8	−5	m	15	5	5	15	101	
	Apr. 21	11 51	22 12	s.c.	+1	+31	−4	ms	21	5	6	23	175	1
	Apr. 27	22 18	9 00	.....	.....	.....	.....	ms	29	3,6	6	33	187	1
									7	4	6			
	May 17	23 59	19 19	s.c.*	−2	−41	+7	m	18	4	5	24	152	
	May 26	08 37	31 14	.....	.....	.....	.....	m	26	4,8	5	29	248	
	June 8	02 30	11 16	.....	.....	.....	.....	m	8	4	5	12	93	
	June 14	02 02	18 05	.....	.....	.....	.....	m	14	5	5	18	95	
	June 22	07 37	28 04	s.c.*	−1	−15	+3	m	23	3	5	17	145	
									24	1,2	5			
	June 29	19 31	30 17	.....	.....	.....	.....	s	29	8	4	40	250	1
									30	3	7			

LETTERS TO EDITOR

NOTE ON GIBBONS-NERTNEY PAPER, "A METHOD FOR OBTAINING THE WAVE SOLUTIONS OF IONOSPHERICALLY REFLECTED LONG WAVES, INCLUDING ALL VARIABLES AND THEIR HEIGHT VARIATION"

Equation (2) in the above paper, which appeared in the September 1951 issue of this JOURNAL (**56**, No. 3, pp. 355-371), is the W.K.B. solution to the wave equation and, consequently, neglects all internal reflections taking place due to gradual changes in the physical properties of the medium. Equation (23) clearly demonstrates this fact. It appears that the objective is to determine a way in which the physical properties of the medium can be modified so that the W.K.B. solution becomes the exact solution to the wave equation, that is, $p(x)$ such that

$$\frac{3}{4}\left(\frac{p'}{p}\right)^2 - \frac{p''}{2p} = 0$$

Schelkunoff[1] has considered this case in detail and shown that, in spite of the fact that the resulting solution appears to yield two independently progressive waves, reflection is total.

J. B. SMYTH

UNITED STATES NAVY ELECTRONICS LABORATORY,
San Diego 52, California, March 14, 1952
(Received March 24, 1952)

REPLY TO PRECEDING NOTE OF J. B. SMYTH

We wish to thank Dr. J. B. Smyth for indicating some points apparently requiring clarification in our paper "A method for obtaining the wave solutions of ionospherically reflected long waves, including all variables and their height variation," which appeared in this JOURNAL, Volume 56, pp. 355–371, September, 1951.

We believe that the situation is best illustrated by an example. We shall consider the case of a real index of refraction $K_0\epsilon$ for simplicity. The problem is shown in Figure 1. In this case, we have a dielectric "well" with its minimum at the origin. We shall consider a wave of $\lambda = 2$ km entering this region from the left. Any solution of the equation

$$K_0^2\epsilon^2 = p^2 - \frac{3}{4}\left(\frac{p'}{p}\right)^2 + \frac{1}{2}\frac{p''}{p}$$

may be used, but for convenience we shall select the one which *starts off* as a W.K.B., that is, $p \to K_0\epsilon$, $p' \to 0$ as $x \to \infty$. We shall then obtain the p solution

[1] S. A. Schelkunoff, Communications on Pure and Applied Mathematics, **4**, 117–218 (June 1951).

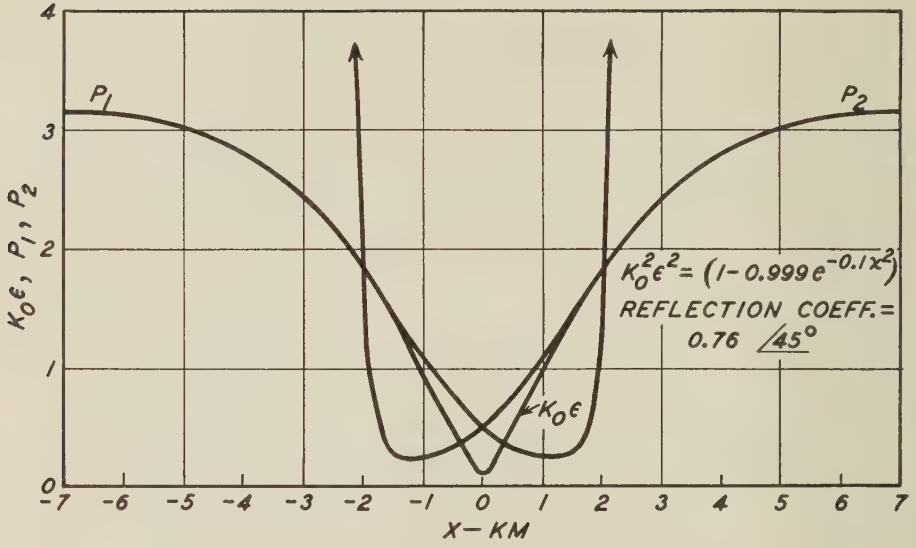

FIG. 1 — A SIMPLE EXAMPLE OF THE USE OF "p" FUNCTIONS

numerically. This solution is indicated in the Figure as p_1 and defines a pair of wave solutions

$$\pi_{1,2} = \frac{1}{\sqrt{p_1}} e^{\pm j \int p_1 dx}$$

We find that a few kilometers to the right of the minimum of the index of refraction, p_1 becomes rather difficult to calculate numerically and we shall drop this solution for the moment. Next, we will consider the p solution which starts as a W.K.B. solution for large *positive* values of x. This solution will be the mirror image of p_1 about $x = 0$ and is indicated as p_2 . Our entire p function will then consist of p_1 in the negative half plane and p_2 in the positive, with a region where the two solutions overlap.

We may now examine these p solutions. We see that in the negative half plane p_1 represents a pair of W.K.B. solutions ($p = K_0\epsilon$) in the region for $x < -1.5$ km, and only in this region. In the region $x > -1.5$ km, the terms in p_1' and p_1'' have become important. This is indicated by the fact that $p \neq K_0\epsilon$ and, in fact, if one took $p = K_0\epsilon$, we would have solutions to quite another differential equation.

Let us now consider the meaning of our solutions. These "p solutions" will not, in general, represent progressive waves. They represent two linearly independent solutions to the wave equation, and we may only determine the reflection coefficient of the "well" by emerging again into a homogeneous medium.

In order to determine the reflection coefficient, we must work a boundary value problem across the plane at $x = 0$, if we are to maintain continuity on the wave

functions and their derivatives. This is true because of the discontinuity in the derivative of the p function as we transfer from p_1 to p_2 .

The points which we wish to stress are as follows: (1) The p solution may reduce to the W.K.B. solution $p = K_0\epsilon$ only in a region where the W.K.B. solution is valid and even this is not necessary. It is possible even in the homogeneous medium to obtain a pair of p solutions which contain mixtures of "right-going" and "left-going" waves in a standing wave pattern. (2) The contribution of

$$\left[\frac{3}{4}\left(\frac{p'}{p}\right)^2 - \frac{p''}{2p}\right]$$

is not, in general, negligible and, in fact, it is the effect of these derivative terms which indicates the location of a reflection region in the example. We see, in this case, that the p_1 , p_2 solutions may be reduced W.K.B. or "very nearly reflectionless" solutions in the region $|x| > 1.5$ km, and it is therefore the region -1.5 km $< x < +1.5$ km which is principally responsible for the reflection of the wave. (3) Although equation (23) has the appearance of the reflection coefficient of a W.K.B. region backed by a metallic reflector, this is not true, since the p function is not equal to $K_0\epsilon$ in the reflection region and, in fact, the terms in p' and p'' are very important in this region.

We hope that this argument will help to clarify the points which Dr. Smyth brings up in his note.

R. J. Nertney

Ionosphere Research Laboratory,
The Pennsylvania State College,
State College, Pennsylvania, March 31, 1952
(Received April 2, 1952)

CONCLUDING COMMENTS REGARDING THE GIBBONS-NERTNEY PAPER

I would like to reemphasize the fact that the "p solutions" in the paper by Gibbons and Nertney are W.K.B. approximate solutions to the wave equation. When $p(x) = K_0\epsilon(x)$, the authors state that their "p solutions" are W.K.B. solutions representing waves in a medium whose physical properties are given by $K_0\epsilon(x)$. Obviously then, when $p(x) = p(x)$, the solutions are nothing more than W.K.B. solutions representing waves in a medium whose physical properties are given by $p(x)$.

Professor Nertney's note gives an excellent example for discussion. In this example, the dielectric constant and its derivative are continuous functions. Using W.K.B. solutions, yields zero reflection from this dielectric "well." Professor Nertney replaces this problem by another distribution with a discontinuity in the derivative at $x = 0$. However, it is *not* the region -1.5 km $< x < 1.5$ km which is principally responsible for the reflection computed for the above example. The discontinuity in p' at $x = 0$ is entirely responsible for the reflection coefficient obtained. The magnitude of the reflection coefficient obtained by the W.K.B. method depends singly upon the magnitude of the discontinuity in p' at $x = 0$. If, in the limit, I remove the discontinuity in p' at $x = 0$, I have not changed the

physical problem; however, the properties of the W.K.B. solution would state that the physical situation has been modified drastically.

It should be observed that the authors have used a solution which is a very poor approximation to the given problem as an approximate solution to another problem. It is certainly not to be expected that the results obtained in this manner will have any connection with the original problem.

J. B. Smyth

United States Navy Electronics Laboratory,
San Diego 52, California, April 29, 1952
(Received May 1, 1952)

SOME COMMENTS ON L. ELTERMAN'S "THE MEASUREMENT OF STRATOSPHERIC DENSITY DISTRIBUTION WITH THE SEARCHLIGHT TECHNIQUE"

I have read with much interest Mr. L. Elterman's article[1] "The measurement of stratospheric density distribution with the searchlight technique," and feel that both Mr. Elterman and the Geophysics Research Division of the Air Force Cambridge Research Center are to be commended for their efforts in trying to perfect a device that will be of considerable value in upper atmospheric exploration.

Despite the apparently close fit (on a semi-log graph) of the observed densities with the Rand curve, however, I find that the observed densities yield impossible pressures and temperatures aloft in two of the cases I have analyzed, as indicated in Table 1. These values were determined by using the trapezoidal rule to integrate the hydrostatic equation above 14.6 km, at which level Mr. Elterman gives radiosonde data to which his measurements were matched. The pressure values for the August sounding were deliberately underestimated by using arithmetic mean densities (the density-height curve is monotonically decreasing and concave upward) and the values 980 dynes cm^{-2} and 28.90 gm $mole^{-1}$ for the acceleration of gravity and the molecular weight of air, respectively; and those for the November sounding deliberately overestimated by using logarithmic mean densities and the values 960 dynes cm^{-2} and 28.60 gm $mole^{-1}$. Actually, a numerical determination of pressure from the Rand densities for the corresponding levels by the use of the trapezoidal rule and a first-difference Newton-Bessel correction[2] at the lower boundary yields pressure values less than one-fourth of a millibar different from the Rand tabulated pressures,[3] but Mr. Elterman's density values were too erratic from level to level to permit evaluation of the Newton-Bessel correction. The temperatures were calculated from the pressure and density values by means of the equation of state, and are given merely to illustrate how erroneous the pressure values are. Temperature values calculated from the slope of the logarithmic density curve will, of course, not appear so fantastic at the higher elevations, but will, in general, be more in error at the lower levels.

[1]J. Geophys. Res., **56**, 509 (1951).

[2]H. and B. S. Jeffreys, Mathematical physics, London, Cambridge University Press (1946).

[3]G. Grimminger, Analysis of temperature, pressure and density of the atmosphere extending to extreme altitudes, Rand Corporation, R-105 (Nov. 1948).

TABLE 1—*Pressure and temperature values calculated from Elterman's densities*

Height	8/19—8/20/50		11/15—11/16/50	
	Pressure	Temperature	Pressure	Temperature
km	*mb*	°*K*	*mb*	°*K*
15.9	112	203	103	202
17.4	87	191	80	216
18.8	68	183	65	235
20.5	50	182	51	246
22.3	35	161	40	263
24.4	23	150	31	293
27.4	11	114	23	420
29.7	5	78	19	550
31.9	1	22	17	680
34.1	−2	<0	15	930
37.9	−5		14	1,300
41.5	−6		13	1,800
45.9	−7		12	2,700
51.0	−8		11	4,000
56.0	−9		11	6,500
58.6	−9		11	10,000
61.8			10	16,000

It should also be pointed out that Mr. Elterman's value of 7.29×10^{15} for the reciprocal of the Boltzmann constant appears to be too high, in view of the values 7.245×10^{15} and 7.244×10^{15} given by DuMond and Birge, respectively.[4]

In view of the above remarks, it seems to me that Mr. Elterman is unjustified in drawing any conclusions from his measurements as to the seasonal variation of density in the region above 20 km.

LEWIS D. KAPLAN

UNITED STATES WEATHER BUREAU,
Washington, D.C., April 17, 1952
(Received April 18, 1952)

A REPLY TO LEWIS D. KAPLAN'S COMMENTS ON DENSITY MEASUREMENTS WITH THE SEARCHLIGHT TECHNIQUE

The criticism by Lewis D. Kaplan of the method for deriving stratosphere densities with the searchlight technique was received with much interest, although the validity of his analysis is considered questionable. The use of the trapezoidal rule in conjunction with the hydrostatic equation for deriving pressures from densities is indeed dangerous, as is any analytical method which attempts to derive information by successive integration from basic values. Unless these basic values

[4] J. W. M. DuMond and E. R. Cohen, Rev. Mod. Phys., **20**, 82 (1948); and R. T. Birge, Rev. Mod. Phys., **13**, 233 (1941).

are characterized by extreme accuracy, the derived results can readily fall in the realm of fantasy such as the negative pressures and impossible temperatures produced by Kaplan.

The searchlight scattering work is essentially a field technique which cannot possibly contain the refinements of a laboratory experiment. Even if the scattering measurements were conducted with negligible error, the evaluation of the constant for deriving the densities makes use of radiosonde data at 14.6 km and at that altitude the error in pressure is, conservatively, 3 per cent. Thus, the constant and all values of derived densities will be either lifted or reduced by 3 per cent, depending on whether the error is negative or positive. This does not appear serious, but follow-

Calculation of pressure and temperature from Rand densities increased by 3 per cent

h	N	N_e	$\bar{N}_e$	g	dh	dP	P	T
13.176	4.995×10^{18}							
			3.999×10^{18}		3.048	57.1		
16.764	3.109	3.202×10^{18}		976.15			92.1	210
			2.527		3.048	36.1		
19.812	1.937	1.995		975.24			56.0	205
			1.577		3.048	22.5		
22.860	1.210	1.246		974.29			33.5	196
			9.855×10^{17}		3.048	14.0		
25.908	7.568×10^{17}	7.795×10^{17}		973.35			19.5	182
			6.171		3.048	8.78		
28.956	4.743	4.885		972.43			10.7	160
			3.871		3.044	5.49		
32.000	2.979	3.068		971.50			5.21	124
			2.333		3.052	3.44		
35.052	1.722	1.774		970.57			1.77	72.7
			1.384		3.048	1.96		
38.100	1.049	1.080		969.66			−0.19	<0

h = Altitude (km)
N = Number density—Rand (cm^{-3})
N_e = Number density—Rand—plus 3 per cent (cm^{-3})
$\bar{N}_e$ = Logarithmic mean of N_e (cm^{-3})
g = Apparent gravity (cm/sec^2)
dh = Layer thickness (km)
dP = Calculated pressure differential (mb)
P = Calculated pressure (mb)
T = Calculated temperature (°K)
* = Unchanged number density used (4.995×10^{18} cm^{-3})

$$dP = \bar{N}_e m g \, dh$$

$$T = \frac{P}{\bar{N}_e k}$$

m = mean molecular mass (4.8×10^{-23} gm)
k = Boltzmann constant (1.372×10^{-16} erg/degree)

ing through on Kaplan's analysis and applying this error, even to such ideal values as the Rand distributions, the results as shown by the submitted Table are little less than tragic. Obviously, a 3 per cent deviation can arise from many sources other than the radiosonde, and the existence of reasonable error, even though it occurs at low altitudes only, will result in nonsense when the measurements are integrated for pressures to higher altitudes. Under such circumstances, the application of the equation of state for deriving temperatures is equally useless.

The use of 7.29×10^{15} rather than 7.245×10^{15} as the reciprocal of the Boltzmann constant is based on the choice of Mitra's value for the constant in his text book (1.372×10^{16} erg/degree). In any case, use of the lower value would result in a 0.6 per cent difference in density values which is not considered significant.

A brief comment is in order concerning the objectives in submitting the paper to the Journal of Geophysical Research. Primarily, it was meant to describe a technique which permitted the first successful attempt to measure light scattering from a beam to an altitude of 68 km. The agreement between the obtained densities and those of a model atmosphere is a very interesting development and rightfully deserves the emphasis given. This was the thinking which motivated the writing of the paper, and it was not expected that these preliminary results would be subjected to detailed quantitative analysis. The writer was fully aware when analyzing the data that the derived density distributions are of an exploratory nature.

It is recognized that there is much to be done in perfecting this technique. There are such aspects as refinement of calculations pertaining to the selected scattering region of the beam, more accurate use of noise levels, and improvement of light source, method of modulation, and detection instrumentation. These problems are now under study at the writer's laboratory—Geophysics Research Division of the Air Force Cambridge Research Center—and it is expected that these studies will contribute materially to the knowledge of the upper atmosphere through the medium of the searchlight technique.

L. Elterman

Geophysics Research Division,
Air Force Cambridge Research Center,
Cambridge 39, Mass., June 19, 1952
(Received July 10, 1952)

NOTE ON THE SIGNIFICANCE OF INVERSE MAGNETIZATIONS OF ROCKS

For many decades there has existed a fascinating dilemma among students of the earth's magnetic field and students of rock magnetism. Intuitively, and often as a matter of well-founded faith, one regards the earth's magnetic field as an inherent property of such grandeur that reversals of its sense are difficult to grant, and yet there are so many examples of rocks having a magnetic polarity so close to the opposite of the present field that one's faith in this constancy may become shaken (see, for example, Hospers[1]). It thus remains important to understand fully the mechanism by which these "inverse" rocks become magnetized.

As early as 1853, it was recognized[2] that when a molten lava cools through its Curie point it acquires a direction and sense of magnetization that reflects accurately the impressed magnetic field. The experiment has been repeated several times on many different samples and with the same result. Recently, however, Nagata[3] has shown that magnetic material separated from a particular Japanese extrusive rock

[1] J. Hospers, Nature, **168,** 1111–1112 (1951).
[2] M. Melloni, Paris, C.-R. Acad. sci., **37,** 229, 966 (1853).
[3] T. Nagata, Nature, **169,** 704–705 (1952).

acquires the opposite polarity when a magnetic field is applied while it cools through certain temperature intervals. Balsley, Buddington and Fahey[4] report that the material separated magnetically from rocks having reversed polarity is frequently characterized by a high TiO_2 content in the analyses. It is interesting to note that Nagata's material is of this type, having 7.4 per cent TiO_2 .

Néel[5] has worked out in some detail various theoretical mechanisms by which the polarity of a rock during cooling may become the opposite of the impressed magnetic field. In these, it is required that there be two magnetic phases that interact on one another, whether it be on the scale of adjacent lattice planes, or on the scale of minutely intermingled different crystalline species. His treatment is thus reminiscent of the ingenious explanation given by Smith, Dee, and Mayneord[6] for the curious self-reversal behavior of a particular two-phase iron-carbon alloy. In some Silurian sediments of the Appalachian mountains, stable inverse polarizations are to be found.[7] Magnetization experiments, the details of which will be published later, show for these inverse rocks an anomalous behavior that is not characteristic of a single-phase system.

Based on the foregoing, it is interesting to consider the possibility that inverse polarizations might be used, in some cases at least, to prove the constancy of the earth's magnetic field. Let us assume that in order for an igneous rock to acquire an inverse polarization, the following conditions must be met: (1) The normal earth's field is present; (2) the composition of the melt is favorable so that on cooling the ferromagnetic ingredients can break down by exsolution, and not merely on the scale of lattice dimensions, into two (or more?) magnetically interacting phases; (3) the rate of cooling is slow enough to allow the exsolution to take place.

Granted these three conditions, then one can predict that in the case of deep-seated material making a shallow intrusive or extrusive where the rates of cooling and exsolving are not everywhere uniform, there should be found cases of normal polarizations on the chilled margins or in small offshoots of the main body, whereas the larger interior portions would show an inverse polarity. On the basis of this hypothesis, one can suggest that magnetic surveys would locate only the larger portions of shallow intrusives or flows of material capable of acquiring an inverse polarization. For example, the dike system described by Bruckshaw and Robertson[8] may perhaps be somewhat more continuous than is shown by their magnetic observations. Deep-seated intrusives would not be expected to show this effect on the margins.

Likewise, it can be predicted that the interesting self-reversal property of Nagata's material will be destroyed if the sample is cooled rapidly after it has been heated sufficiently that the exsolved phases recombine. Indeed, partial recombination during his experiments may explain the fact mentioned by Nagata that this material does not follow precisely the addition law of normal thermo-remanent

[4]J. R. Balsley, A. F. Buddington, and J. J. Fahey, Trans. Amer. Geophys. Union, **33**, 320 (1952).

[5]L. Néel, Ann. Géophys., **7**, 90–102 (1951).

[6]S. W. J. Smith, A. A. Dee, and W. V. Mayneord, Proc. Phys. Soc., **37**, 1–14 (1924).

[7]J. W. Graham, J. Geophys. Res., **54**, 131–167 (1949).

[8]J. McG. Bruckshaw and E. I. Robertson, Mon. Not. R. Astr. Soc., Geophys. Sup., **5**, 308–320 (1949).

magnetism first enunciated by Thellier.[9] It can be imagined, too, that in the case of some rocks having a very fine-grained dispersal of the two phases, the recombination rate at the temperatures used in the experiments may be sufficiently high that the curious property of self-reversal is destroyed, and, hence, is never observed. Experiments not depending on heat would then be required to clarify the mechanism of magnetization of these rocks.

These phenomena would not be observed if the two-phase ordering of the ferromagnetic ingredient is an inherent property of the material that takes place on the scale of the lattice dimensions, as exemplified by Néel's type *N* ferrite.[10]

If it should prove correct that some rocks, on cooling under natural conditions, can acquire an inverse magnetization, then, in order to demonstrate the constancy of the earth's field, it will be necessary, by similar field studies, to show that representative rocks having normal polarizations do not possess the self-reversal property, and that therefore their polarizations presumably depict correctly the polarity of the earth's field at the time they cooled.

To summarize, there is reason to doubt that inverse magnetizations of rocks prove a reversal of the earth's magnetic field; indeed, fuller understanding of the mechanism of their magnetization may be crucial in showing the constancy of the earth's field.

John W. Graham

Department of Terrestrial Magnetism,
Carnegie Institution of Washington,
Washington 15, D.C., May 26, 1952
(Received May 26, 1952)

[9]É. Thellier, Ann. Inst. Phys. Globe, **16,** 157–302 (1938).
[10]L. Néel, Ann. Phys., **3,** 137–198 (1948).

NOTES

(14) *Authorization of new geomagnetic station to replace Cheltenham Magnetic Observatory*—The United States Congress has authorized the construction of a geomagnetic station to replace the present Commerce Department observatory at Cheltenham, Maryland, which it is stated is rapidly becoming inadequate for proper standardizing and testing of geomagnetic equipment. The new station will be constructed on the A. P. Hill Military Reservation near Fredericksburg, Virginia, and will be operated by the United States Coast and Geodetic Survey.

(15) *New material for permanent magnets*—A new material which exhibits a coercive force of 3,000 oersteds, the highest recorded coercive force of any known permanent magnetic material, has been developed in the Magnetics Division of the United States Naval Ordnance Laboratory. It has been named "BISMANOL" from its composition of bismuth and manganese and NOL where it was prepared. Because of its high coercive force, BISMANOL exceeds any other permanent magnet, except the platinum-cobalt alloy, in available flux density in short magnets where length to diameter ratio is one or less. BISMANOL magnets are made by the powder metallurgy technique, and complicated shapes can be processed to close tolerances without requiring machining.

(16) *Proposed radio telescope at Jodrell Bank, Manchester, England*—A giant radio telescope, with a paraboloid aerial of 250 feet in diameter and a height of 185 feet to the top of the horizontal axis, is to be built in Britain to map unexplored regions of the universe. It is expected to greatly further the work in radio astronomy. There are regions of considerable astronomical interest which cannot be seen by means of conventional telescopes but which may be observed with the help of radio waves. The work is an outgrowth of the discovery in 1931 by the U.S. scientist Jansky that stars emit radio waves that can be received on earth. It is expected that construction of the radio telescope will be completed in less than four years.

(17) *Venezuelan Geophysical Society formed*—The Society of Exploration Geophysicists, Tulsa, Oklahoma, has announced that forty-three exploration geophysicists met in Caracas, Venezuela, on May 26, 1952, to form the "Sociedad Venezolana Geofisica." The group unanimously agreed to form the society along the same lines and for the same purpose as the Society of Exploration Geophysicists. Regular meetings will be held for the discussion of current exploration problems encountered in Venezuela, and consideration will be given to affiliation at a later date as a local section of the S.E.G.

(18) *Mapping of potential iron-ore area in southwestern Oklahoma*—The possibility of iron-ore production from the titaniferous magnetite deposits of the Raggedy Mountains, northwest of Lawton, Oklahoma, has prompted the release by the United States Geologic Survey of a preliminary aeromagnetic map of the region, covering 120 square miles. By correlating the aeromagnetic and geologic data, it is possible to select favorable areas for drilling to determine amount of overburden and quantity and quality of any ore that may be located.

(19) *Colloquia at the University of Alaska*—The Geophysical Institute, Univer-

sity of Alaska, is holding regular colloquia twice monthly. Members of the staff and visiting scientists will participate in discussions of the aurora, the ionosphere, and back-scatter. A series of lectures by Prof. Sydney Chapman, of Oxford University, dealing with theories of magnetic storms and the aurorae, were scheduled for September 10 to October 3, 1952, while on September 17 Dr. L. A. Manning, of Stanford University, spoke on the determination of winds in the upper atmosphere.

(20) *Establishment of an earthquake seismograph station at Rice Institute, Houston, Texas*—Donation of $25,000 by four geophysical exploration companies toward establishment of an earthquake seismograph station at the Rice Institute, Houston, Texas, was announced recently by the Society of Exploration Geophysicists. The gift was made by General Geophysical Company, Independent Exploration Company, Robert H. Ray Company, and Seismic Explorations, Inc., all of Houston. These consulting geophysical companies, although engaged primarily in the application of seismology to the search for oil, have shown vital interest in the basic earth sciences and feel that the establishment of such a station at Rice will be of great value in fundamental research and will contribute to the solution of geophysical problems. The money will be used to provide the equipment for a seismological station for the continuous recording of the movement of the earth and earthquakes anywhere in the world. The Rice Institute will become a part of the great scientific network which serves to gather information for peoples all over the world on the incidence, direction, and violence of earth tremors and quakes. It is believed that work can be started in setting up the station at the same time as the establishment of the geological courses at the Institute.

(21) *Conference on radio meteorology to be held at the University of Texas in November 1953*—The University of Texas will be host to a four-day conference on radio meteorology scheduled for the second week in November 1953. The meeting will be jointly sponsored by the American Meteorological Society, the Radar Weather Conference, the Institute of Radio Engineers through its Professional Group on Antennas and Propagation, National Commission II on Tropospheric Radio Propagation of the International Radio Scientific Union, and the Joint Commission on Radio Meteorology. The sessions will deal with such topics as tropospheric radio wave propagation mechanisms, radar storm detection and rainfall determination, cloud physics, turbulence, spherics, refractive index climatology and forecasting, and atmospheric reflections.

(22) *Geomagnetic activities of the United States Coast and Geodetic Survey*—Mr. John B. Townshend completed a magnetic field trip in the southern and midwestern United States. Lieut. Renaldo Salgueiro, of Bolivia, accompanied Mr. Townshend.

Mr. Leonard R. Southwick and Mr. Richard G. Green are engaged in magnetic field trips in the western and southeastern United States, respectively.

Dr. Clemente Garavito of Colombia, Major Kasim Yasar of Turkey, and Lieut. Renaldo Salgueiro of Bolivia have been guests of the United States Coast and Geodetic Survey, studying the methods and instruments used in the magnetic work of the Bureau.

Airborne surveys were continued on a limited program.

The following reports were published: Magnetic hourly values for San Juan,

P.R., and Honolulu, T. H., for 1948, and for Cheltenham, Maryland, for 1949; reproductions of San Juan magnetograms for the first half of 1949, and of San Juan and Honolulu magnetograms for the second half of 1949.

(23) *Corrigenda*—In the article by W. Snyder and R. A. Helliwell in this Journal, volume 57, No. 1 (March, 1952, issue) about midway of page 74, the definition of x as used in equation (1) should read $x = Ne^2mK_o\omega^2$ instead of $x = N_e^2mK_o\omega^2$; and on page 78, line 23, following the words "major axis" should be inserted "of the electric vector ellipse." The first-mentioned error was kindly drawn to the authors' attention by Dr. James C. W. Scott, of the Defence Research Board, Ottawa, Canada.

(24) *Personalia*—Dr. *Allen V. Astin* has been named Director of the National Bureau of Standards, Washington, D.C. He has been acting chief of the Bureau since October 1951. Dr. Astin joined the Bureau of Standards in 1932. During World War II he took a leading part in the development of the proximity fuse. After the war, he became assistant director and in 1947 chief of the Bureau's ordnance department. In 1950 he was appointed associate director of the Bureau.

Dr. *Edward V. Appleton*, for his research on the ionosphere, was elected an honorary member of the Institution of Electrical Engineers (London).

Dr. *B. W. Currie*, professor of physics at the University of Saskatchewan, Canada, has been appointed head of the Department of Physics, University of Saskatchewan.

LIST OF RECENT PUBLICATIONS

By W. E. Scott

Department of Terrestrial Magnetism,
Carnegie Institution of Washington,
Washington 15, D. C.

(Received June 23, 1952)

A—*Terrestrial Magnetism*

Akimoto, S. Magnetic susceptibility of ferromagnetic minerals contained in igneous rocks. Kyoto, J. Geomag. Geoelectr., **3**, No. 3-4, 47-58 (1951).

Argentina, Republica. Carta isogona de la Republic Argentina (confeccionada para la epoca 1950.0). Servicio Meteorológico Nacional, Ministerio de Asuntos Tecnicos, Ser. A, Sec. 2*a*, No. 8, 13 + carta isogona (1950). 24 cm.

Argentina, Republica. Datos climatologicos y geomagneticos, Islas Orcadas del Sur (Isla Laurie), periodo 1903-1950. Servicio Meteorológico Nacional, Ministerio de Asuntos Tecnicos, Ser. B, Sec. 1*a*, pt. 1*a*, No. 11, 97 pp. (1951). 36 cm.

Bartels, J., and J. Veldkamp. International data on magnetic disturbances, fourth quarter, 1951. J. Geophys. Res., **57**, No. 2, 305-309 (1952).

Bernard, P. Interprétation de la variation undécennale de la composante horizontale du champ magnétique terrestre. Paris, C.-R. Acad. sci., **234**, No. 8, 866-868 (1952).

Birebent, R. Sur un nouveau dispositif pour la mesure de l'intensité d'un champ magnétique. Paris, C.-R. Acad. sci., **234**, No. 11, 1135-1136 (1952).

Bodle, R. R. Cheltenham three-hour-range indices *K* for January to March, 1952. J. Geophys. Res., **57**, No. 2, 310 (1952).

Cullington, A. L. The magnetic secular variation in New Zealand. N.Z. J. Sci. Tech., B, **33**, No. 5, 355-372 (1952).

Dürschner, H. Enregistrement à distance des variations du champ magnétique terrestre. Ann. Géophys., **7**, No. 4, 199-207 (1951).

Fukushima, N. Development and decay processes of the bay disturbances in geomagnetic field. Kyoto, J. Geomag. Geoelectr., **3**, No. 3-4, 59-76 (1951).

Haalck, H. Zur Frage der Erklärung des erdmagnetischen Kernfeldes und des allgemeinen Magnetismus der Himmelskörper. Beitr. Geophysik, **62**, Heft 1, 1-8 (1952).

Jackson, W. World-wide simultaneous magnetic fluctuations and their relation to sudden commencements. J. Atmos. Terr. Phys., **2**, No. 3, 160-172 (1952).

Lundbak, A. Aeromagnetic survey of vertical intensity over the sound with apparatus of the BMZ type. Tellus, **3**, No. 2, 69-74 (1951).

Macht, H. G. Die Potentialanteile zweiter und höherer Ordnung des Erdmagnetfeldes—I. Beitr. Geophysik, **62**, Heft 2, 127-153 (1952).

Nagata, T. Sudden commencements preceded by the preliminary reverse impulse in a geomagnetic field. Nature, **169**, 446-447 (March 15, 1952).

Nagata, T. Reverse thermo-remanent magnetism. Nature, **169**, 704-705 (April 26, 1952).

Nagata, T., N. Fukushima, and I. Yokoyama. Results of observations of geomagnetic variations at Zenigamezawa, Hokkaido, during the solar eclipse of September 12, 1950. Tokyo University, Geophys. Inst., 7 pp. (1952). 26 cm.

Néel, L. Confirmation experimentale d'un mécanisme d'inversion de l'aimantation thermorémanente. Paris, C.-R. Acad. sci., **234**, No. 20, 1991-1993 (1952).

San Fernando. Anales del Instituto y Observatorio de Marina (publicados de order de la superioridad), Sección 3*a*. Observaciones meteorológicas y magnéticas correspondientes a los años 1949-1950. San Fernando, Imprenta del Observatorio de Marina, iii + 76 (1951). 34 cm.

Sivaramakrishnan, M. V. Geomagnetic field variations at Kodaikanal. Nature, **169**, 409-410 (March 8, 1952).

Stoyko, N. De l'influence de l'irrégularité de la rotation terrestre sur le champ magnétique. Paris, C.-R. Acad. sci., **234**, No. 18, 1798-1800 (1952).

Thellier, É., et O. Thellier. Sur la direction du champ magnétique terrestre, dans la région de Trèves, vers 380 apres J.-C. Paris, C.-R. Acad. sci., **234**, No. 14, 1464-1466 (1952).

Toledo, Observatorio Central Geofísico. Geomagnetismo, año 1947. [Prepared by J. Sancho.] Madrid, Instituto Geográfico y Catastral, 43 pp., 4 pls., 6 graphs (1951). 24 cm.

Tromsö, Auroral Observatory. Results of magnetic observations for the year 1950. Bergen, Pub. Inst. Kosmisk Fysikk, No. 33, 31 pp. (1952). 31 cm.

United States Coast and Geodetic Survey. Magnetic hourly values, Honolulu, T.H., 1948. Washington, D.C., U.S. Coast Geod. Surv., No. HV-Ho48, 46 pp. (1951). 25 cm.

United States Coast and Geodetic Survey. Magnetic hourly values, San Juan, Puerto Rico, 1948. Washington, D.C., U.S. Coast Geod. Surv., No. HV-SJ48, 45 pp. (1951). 25 cm.

United States Coast and Geodetic Survey. Magnetograms, Honolulu, T.H., July-December 1949. Washington, D.C., U.S. Coast Geod. Surv., No. MG-H49.2, 56 pp. (1951). 25 cm.

United States Coast and Geodetic Survey. Magnetograms, San Juan, Puerto Rico, January-June 1949. Washington, D.C., U.S. Coast Geod. Surv., No. MG-J49.1, 53 pp. (1951). 25 cm.

B—*Terrestrial Electricity*

Coroniti, S. C., A. J. Parziale, R. C. Callahan, and R. Patten. Effect of aircraft charge on airborne conductivity measurements. J. Geophys. Res., **57**, No. 2, 197-205 (1952).

Goto, M. A newly designed differential electrometer and its application to the simultaneous measurement of air earth current and potential gradient. Kyoto, J. Geomag. Geoelectr., **3**, No. 1, 22-23 (1951).

Hatakeyama, H., and S. Hudimoto. On the potential gradient and the space charge in the lower stratum of the atmosphere. Geophys. Mag., Tokyo, **23**, No. 1, 15-20 (Dec., 1951). [Prof. S. Fujiwhara's anniversary volume, Pt. 2.]

Holzer, R. E., and D. S. Saxon. Distribution of electrical conduction currents in the vicinity of thunderstorms. J. Geophys. Res., **57**, No. 2, 207-216 (1952).

Kasemir, H. W. Die Feldkomponentenmühle. Tellus, **3**, No. 4, 240-247 (1951).

Norinder, H., and R. Siksna. Height variations in the concentration of ions near the ground during summer nights at Uppsala. Tellus, **3**, No. 4, 234-239 (1951).

Parkinson, W. C. Note on the concentration of condensation nuclei over the western Atlantic. J. Geophys. Res., **57**, No. 2, 314-315 (1952). [Letter to Editor.]

Sheppard, P. A. An experiment in geophysical research. Nature, **169**, 427-428 (March 15, 1952). [Brief résumé on report of the Thunderstorm Project, U.S. Department of Commerce, 1949.]

C—*Cosmic Rays*

Bonnevay, G. Effet de gerbe dans la mesure absolue de l'intensité du rayonnement cosmique. J. Phys. et Le Radium, **13**, No. 2, 68-73 (1952).

Maeda, K., and T. Suda. The annual and diurnal variations of cosmic-ray intensity and the temperature effect. Kyoto, J. Geomag. Geoelectr., **3**, No. 1, 18-21 (1951). [Bihourly data of cosmic-ray intensity at Huancayo and aerological data at San Juan were used.]

Nagashima, K. On the relation between the cosmic ray intensity and the geomagnetic storm. Kyoto, J. Geomag. Geoelectr., **3**, No. 3-4, 100-116 (1951).

Riddiford, L., and S. T. Butler. The origin of cosmic rays in solar or stellar disturbances. Phil. Mag., **43**, No. 339, 447-456 (1952).

D—*Upper Air Research*

Bibl, K. L'ionisation de la couche *E*, sa mesure et sa relation avec les éruptions solaires. Ann. Géophys., **7**, No. 4, 208-214 (1951).

Bowles, K. The fading rate of ionospheric reflections from the aurora borealis at 50 Mc/sec. J. Geophys. Res., **57**, No. 2, 191-196 (1952).

Bullen, J. M. An ionospheric disturbance index. [Based on variations in height and critical

frequency of the *F*2 layers of the ionosphere at Lincoln.] N.Z. J. Sci. Tech., B, **33**, No. 5, 348-354 (1952).

Dieminger, W., und A. E. Hoffmann-Heyden. Reflexionen von Kurzwellen aus Höhen unter 100 km. Naturwiss., **39**, Heft 4, 84-85 (1952).

Gerson, N. C. The terrestrial atmosphere. Sci. Prog., **40**, No. 158, 245-254 (1952).

Greenhow, J. S. Characteristics of radio echoes from meteor trails: III—The behaviour of the electron trails after formation. Proc. Phys. Soc., B, **65**, No. 387, 169-181 (1952).

Heading, J., and R. T. P. Whipple. The oblique reflexion of long wireless waves from the ionosphere at places where the earth's magnetic field is regarded as vertical. Phil. Trans. R. Soc., A, **244**, No. 887, 469-503 (1952).

Johnson, F. S., J. D. Purcell, R. Tousey, and K. Watanabe. Direct measurements of the vertical distribution of atmospheric ozone to 70 kilometers altitude. J. Geophys. Res., **57**, No. 2, 157-176 (1952).

Kelso, J. M., H. J. Nearhoof, R. J. Nertney, and A. H. Waynick. The polarization of vertically incident long radio waves. Ann. Géophys., **7**, No. 4, 215-244 (1951).

Kerr, F. J. On the possibility of obtaining radar echoes from the sun and planets. Proc. Inst. Radio Eng., **40**, No. 6, 660-666 (1952).

Kilpatrick, E. L. Polarization measurements of low frequency echoes. J. Geophys. Res., **57**, No. 2, 221-226 (1952).

Little, A. G., and R. Payne-Scott. The position and movement on the solar disk of sources of radiation at a frequency of 97 Mc/s. I—Equipment, and II—Noise storms. Aust. J. Sci. Res., A, **4**, No. 4, 489-507 and 508-525 (1951).

Lovell, B., and J. A. Clegg. Radio astronomy. London, Chapman and Hall, Ltd., 238 pp. + 120 figs. (1952). 19 cm.

Maeda, K. The effects of atmospheric motion and dynamo current on the electron density of the ionosphere. Kyoto, J. Geomag. Geoelectr., **3**, No. 3-4, 77-89 (1951).

Matsushita, S. Intense *Es* ionization near the magnetic equator. Kyoto, J. Geomag. Geoelectr., **3**, No. 2, 44-46 (1951). [Letter to Editor.]

Meek, J. H. Ionospheric disturbances in Canada. J. Geophys. Res., **57**, No. 2, 177-190 (1952).

Millman, G. H. A note on ionospheric wind measurements at 150 Kc/s. Ann. Géophys., **7**, No. 4, 272-275 (1951).

Nicolet, M. Problèmes de l'émission spectrale du ciel nocturne et des aurores. Inst. R. Mét. Belgique, 18 pp. (1951). 22 cm. [Résumé de l'état de la question.]

Nicolet, M. Les altitudes théoriques des couches d'émission nocturne. Mém., Soc. R. Sci. Liège, **12**, Fasc. 1-2, 71-86 (1952).

Nicolet, M., and R. Pastiels. Atomic and molecular nitrogen in the high atmosphere. Mém., Soc. R. Sci. Liège, **12**, Fasc. 1-2, 147-149 (1952).

Osborne, B. W. Lunar variations in *F*2 region critical frequency at Singapore. Nature, **169**, 661-662 (April 19, 1952).

Piddington, J. H., and H. C. Minnett. Observations of galactic radiation at frequencies of 1210 and 3000 Mc/s. Aust. J. Sci. Res., A, **4**, No. 4, 459-475 (1951).

Ratcliffe, J. A. Radio astronomy. Nature, **169**, 348-350 (March 1, 1952).

Ryle, M. A new radio interferometer and its application to the observation of weak radio stars. Proc. R. Soc., A, **211**, No. 1106, 351-375 (1952).

Sato, T. On the effect of the earth's magnetic field on the virtual height of the ionosphere. Kyoto, J. Geomag. Geoelectr., **3**, No. 3-4, 90-99 (1951).

Schelkunoff, S. A., and H. T. Friis. Antennas, theory and practice. New York, John Wiley and Sons, Inc., xxii + 639 (1952).

Sulzer, P. G., G. F. Montgomery, and I. H. Gerks. An U-H-F moon relay. Proc. Inst. Radio Eng., **40**, No. 3, 361 (1952).

Vasseur, J. P. Diffraction des ondes électromagnétiques par des ouvertures dans des écrans plans conducteurs. Onde Électrique, **32**, No. 298, 3-10, and No. 299, 55-71 (1952).

Watts, J. M. A note on the polarization of low frequency ionosphere echoes. J. Geophys. Res., **57**, No. 2, 287-289 (1952).

Weekes, K., and R. D. Stuart. The ionospheric propagation of radio waves with frequencies near 100 kc/s over short distances. Proc. Inst. Elec. Eng., **99**, Pt. 4, No. 2, 29-37 (1952).

Weekes, K., and R. D. Stuart. The ionospheric propagation of radio waves with frequencies near 100 kc/s over distances up to 1000 km. Proc. Inst. Elec. Eng., **99**, Pt. 4, No. 2, 38-46 (1952).

Wells, H. W. Ionospheric effects of solar eclipse at sunrise, September 1, 1951. J. Geophys. Res., **57**, No. 2, 291-304 (1952).

Yerg, D. G. A tentative evaluation of kinematic viscosity for ionospheric regions. J. Geophys. Res., **57**, No. 2, 217-220 (1952).

E—*Earth's Crust and Interior*

Båth, M. The distribution of microseismic energy with special reference to Scandinavia. Ark. Geofysik, **1**, No. 13, 359-393 (1951).

Båth, M. Earthquake magnitude determination from the vertical component of surface waves. Trans. Amer. Geophys. Union, **33**, No. 1, 81-90 (1952).

Birch, F. Elasticity and constitution of the Earth's interior. J. Geophys. Res., **57**, No. 2, 227-286 (1952).

Burling, R. L. Determination of geologic time. Nucleonics, **10**, No. 5, 30-35 (1952).

Cooper, R. I. B. The distribution of radioactivity. Nature, **169**, 350-352 (March 1, 1952).

Fendler, H. Altersbestimmung mit radioaktivem Kohlenstoff. Phys. Bl., 8, Heft 2, 73-77 (1952).

Landes, K. K. Our shrinking globe. Bull. Geol. Soc. Amer., **63**, No. 3, 225-240 (1952).

Libby, W. F. Radiocarbon dating. Chicago, University of Chicago Press, vii + 124 (1951). 23 cm.

McCrady, E. The use of lead isotope ratios in estimating the age of the earth. Trans. Amer. Geophys. Union, **33**, No. 2, 156-170 (1952).

Nadai, A. Stress and strain in the outer solid shell of the earth. Trans. Amer. Geophys. Union, **33**, No. 2, 247-276 (1952).

National Research Council, Division of Geology and Geography. Report of the Committee on the Measurement of Geologic Time. Washington, D.C., Nation. Acad. Sci., Pub. No. 212, 140 pp. (1952). 28 cm.

Rikitake, T. Electrical conductivity and temperature in the earth. Bull. Earthquake Res. Inst., Tokyo Univ., **30**, pt. 1, 13-24 (1952).

Sitter, L. U. de. Pliocene uplift of tertiary mountain chains. Amer. J. Sci., **250**, No. 4, 297-307 (1952).

Urey, H. C. On the early chemical history of the earth and the origin of life. Proc. Nat. Acad. Sci., **38**, No. 4, 351-363 (1952).

Willmore, P. L., A. L. Hales, and P. G. Gane. A seismic investigation of crustal structure in the western Transvaal. Bull. Seis. Soc. Amer., **42**, No. 1, 53-80 (1952).

F—*Miscellaneous*

International Meteorological Organization, Temporary Commission on the Liquidation of the Polar Year 1932-33. Bibliography for the Second International Polar Year 1932-33. Compiled by V. Laursen, Executive Officer of the Commission. Copenhagen, Hørsholm Bogtrykkeri, 253 pp. (1951). 24.5 cm.

International Union of Geodesy and Geophysics, Association of Terrestrial Magnetism and Electricity. Preliminary transactions of the Brussels meeting, August 21—September 1, 1951. Washington, D.C., 36 pp. (1952). 25 cm. [Contains summary of the proceedings of the Association, minutes of the meetings, approved budget for period 1951-53, resolutions, and committees.]

Maxwell, A. Possible identification of a solar *M*-region with a coronal region of intense radio emission. Observatory, **72**, No. 866, 22-26 (1952).

Sayers, N. D., and K. G. Emeléus. Experiments on production of auroral radiation. Proc. Phys. Soc., A, **65**, No. 387, 219-226 (1952).

Thiessen, G. Lichtelektrische Messung en des solaren Magnetfeldes. Zs. Astroph., **30**, Heft 3, 185-199 (1952).

Waldmeier, M. Die Sonnenkorona. I—Beobachtungen der Korona 1939-1949. Basel, Verlag Birkhäuser A.G., 270 pp. (1951). 24.5 cm. [Lehrbücher und Monographien aus dem gebiete der Exakten Wissenschaften, Astronom. Geophysik. Reihe, Band 4.]

NOTICE

When available, single unbound volumes can be supplied at $3.50 each and single numbers at $1 each, postpaid.

Charges for reprints and covers

Reprints can be supplied, but prices have increased considerably and costs depend on the number of articles per issue for which reprints are requested. It is no longer possible to publish a schedule of reprint charges, but if reprints are requested approximate estimates will be given when galley proofs are sent to authors. Reprints without covers are least expensive; standard covers (with title and author) can be supplied at an additional charge. Special printing on covers can also be supplied at further additional charge.

Fifty reprints, without covers, will be given to institutions paying the publication charge of $4.00 per page.

Alterations

Major alterations made by authors in proof will be charged at cost. Authors are requested, therefore, to make final revisions on their typewritten manuscripts.

Orders for back issues and reprints should be sent to Editorial Office, 5241 Broad Branch Road, N.W., Washington 15, D.C., U.S.A.

Subscriptions only are handled by The Johns Hopkins Press, Baltimore 18, Maryland, U.S.A.

CONTENTS—Concluded